AI-71-37

DEVELOPMENT OF A MOLTEN CARBONATE PROCESS FOR REMOVAL OF SULFUR DIOXIDE FROM POWER PLANT STACK GASES

PROGRESS REPORT NO. 4

AUGUST 1, 1969 TO MARCH 19, 1971

Atomics International
North American Rockwell

P.O. Box 309
Canoga Park, California 91304

AI-71-37

DEVELOPMENT OF A MOLTEN CARBONATE PROCESS FOR REMOVAL OF SULFUR DIOXIDE FROM POWER PLANT STACK GASES

PROGRESS REPORT NO. 4

August 1, 1969 to March 19, 1971

July 28, 1971

The work upon which this publication is based was performed by Atomics International, a Division of North American Rockwell Corporation, Canoga Park, California, pursuant to Contract No. CPA 70-78 with the U. S. Environmental Protection Agency. Patents covering the basic process have been issued to North American Rockwell Corporation.

Errata for AI-71-37

Page A-48, Figure 16

"d = 20 ft and d = 5 ft" on curves should read

D = 20 ft and D = 5 ft

"Expanded Bed Depth = 0. 4 d" in legend should read

Expanded Bed Depth = 0. 4 D.

Page A-49, Figure 17

"Expanded Bed Depth = 0. 4 d" in legend should read

Expanded Bed Depth = 0. 4 D.

Page A-54, Figure 18

"Kroft Furnace 600 psia Steam" on curve should read

Kraft Furnace 600 psia Steam

Units on k_{SKULL} in legend are

$Btu/ft^2\text{-}^\circ F\text{-}hr$

Page B-3, Line 16

"$K_2 = 1.24 \times 10^{-3}\ 3^{27,720/RT}$" should read

$K_2 = 1.24 \times 10^{-3}\ e^{27,720/RT}$

Report No. AI-71-37

NOTICE TO RECIPIENTS

This document contains inventive subject matter and may not be published, disseminated to others, or used for any purpose without prior approval from the Patent Branch of the Environmental Protection Agency and from the Patent Counsel of the Contractor.

TABLE OF CONTENTS

TABLE OF CONTENTS (Contd)

SUMMARY

This report presents the results of the process development work for the period August 1, 1969 to December 31, 1970. During this period, the following advances were made:

(1) Filtration Studies

Fly ash filtration tests were performed with a Croll-Reynolds filter cartridge having 25-micron spacings between the wire windings. The filter performed well, with an average removal efficiency of 93%. Data from the tests were used to obtain the relationship between throughput, pressure drop, and ash loading over the range of ash loadings from 0 to 1.24 lb ash/ft^2 filter area. This relationship was then used in a reevaluation of the filter requirements for an 800-Mw installation. The results showed that while Croll-Reynolds type cartridge filters could be used in a full-scale unit, there would be an economic advantage to using a continuous filter. However, this would probably require building up a thicker cake, through use of a filter aid or filter precoat material; tests of filter aids and precoats should be done.

(2) Mist Recovery Tests

Tests of wire-mesh mist eliminator pads were performed. Very high mist recovery efficiencies were obtained, but the tests were hampered by the lack of a source of large volumes of hot gas. Consequently, the tests were limited to lower gas velocities than desired (6.5 ft/sec maximum) and to short durations. These limitations made it impossible to obtain enough carryover to determine accurate mist eliminator efficiencies. Accurate data will have to be obtained from longer tests with larger equipment, such as in a pilot plant.

(3) Materials Studies

Five long-term dynamic corrosion tests and three thermal transport tests were completed. In the dynamic tests, stressed and unstressed specimens of Type 347 and Type 321 stainless steel were exposed at 932°F (500°C) to carbonate melts containing (1) 20% sulfide and 5% chloride (both steels); (2) 20% sulfite and 5% chloride (both steels); and (3) 40% sulfite and 5% chloride (Type 347 only). The tests were performed in rotating capsules which initially contained atmospheres of nitrogen, oxygen, and water vapor. Four of the tests attained the desired one-year lifetime; the fifth was terminated after 1580 hours when the temperature controller failed, allowing the temperature to exceed 1200°F (650°C). The results showed that

(a) Type 347 was superior to Type 321;

(b) Type 347 was satisfactory at 932°F in both the 20% sulfide and 20% sulfite melts, having a corrosion rate of about 1-3 mils/yr;

(c) There was no enhanced corrosion due to sensitization and no chloride stress corrosion cracking; and

(d) The Type 347 specimens in the 40% sulfite-5% chloride melt were severely corroded, probably due to overheating and thermal cycling when the controller malfunctioned.

In the one-year thermal transport tests, capsules containing stressed and unstressed test specimens in various melts were mounted in furnaces with one end maintained at 932°F (500°C) and the other end maintained at 797°F (425°C). The furnaces (and capsules) were inverted every 3-1/4 hours, causing the melt to flow from one temperature zone to the other, the purpose being to determine the extent to which thermal transport of alloy constituents would occur. Specimens of Type 347 and Type 321 were tested in melts of carbonate containing 20% sulfide and 10% chloride, and Type 347 specimens were tested in a melt of carbonate containing 20% sulfite and 10% chloride. The

results showed that no thermal transport occurred, and the corrosion rates were similar to those in the one-year dynamic tests. As a result of the dynamic and thermal transport tests, Type 347 stainless steel remains the construction material of choice for use in the low-temperature (below 950°F) part of the process. However, further testing should be done to define the upper temperature limit for this alloy.

A forced-circulation materials test loop design was completed and the procurement package for it was prepared. A revised design was also completed, in which a commercial pump is used and only Type 347 stainless steel is tested. This latter design should be built and put into operation, to study corrosion under flow conditions and to obtain experience with the pump, valves, controls, and instrumentation.

(4) Reducer Engineering Analysis

An engineering analysis of the two-zone reducer using petroleum coke was performed. The results showed that an alumina liner is needed to control corrosion and reduce heat losses. The controlling design considerations were found to be the maximum allowable air velocity in the oxidation region, and the reaction rate (and required residence time) in the reduction zone. The dimensions, heat losses and coke and air requirements for pilot-plant and full-sized reducers were calculated. Experimental data are needed to verify the design; this can be obtained by modeling the reducer hydraulics, studying the rate of internal circulation and testing methods for introducing the melt, coke, and air.

(5) Regenerator Engineering Analysis

An engineering analysis of the regenerator was completed. The results indicate that 9 theoretical plates will be required, and that melt cooling will be required at a tray above the middle and at the regenerator outlet. The actual tray location for cooling and the number of actual trays will have to be estimated, and then verified when tray efficiencies are measured experimentally in a pilot plant.

(6) Heat and Mass Balances

Based upon a flow diagram which included a two-zone reducer using petroleum coke, revised preliminary heat and mass balances were derived for an 800 Mw installation.

(7) Cooperation with Process Evaluator

Information and assistance were provided Singmaster & Breyer in their engineering evaluation of the Molten Carbonate Process. Data supplied included process flow diagrams, material and energy balances, equipment configuration, fly ash filtration data, and process economics. Singmaster & Breyer made a thorough evaluation of the process, pointing out potential problem areas and making valuable suggestions. They concluded that the process was feasible and that its development should continue, with a pilot plant and materials test loop as the next logical steps.

I. INTRODUCTION

The Atomics International Division of the North American Rockwell Corporation is developing a molten carbonate process to remove sulfur oxides from power plant gas streams under contract with the Air Pollution Control Office of the Environmental Protection Agency. Work was begun in June 1, 1967, under contract PH 86-67-128 and has proceeded since then. There have been three previous progress reports: the first covered the period from June 1, 1967, to February 28, 1968; the second covered the period from February 29, 1968, to October 27, 1968; and the third covered the period from October 28, 1968 to July 31, 1969. This report covers the period from August 1, 1969, to December 31, 1970; the work done was under contract CPA 70-78.

A. PROCESS DESCRIPTION

In the Molten Carbonate Process, a molten eutectic mixture of lithium, sodium, and potassium carbonates is used to scrub the power plant gas stream. The sulfur oxides in the gas stream react with the carbonates to form sulfites and sulfates, which remain dissolved in excess unreacted carbonate melt. The molten carbonate-sulfite-sulfate mixture is then regenerated chemically, converting the sulfite and sulfate back to carbonate and recovering the sulfur as hydrogen sulfide. The regenerated carbonate is recirculated to the scrubber to repeat the process cycle, and the hydrogen sulfide is converted to elemental sulfur in a Claus plant.

The regeneration of spent melt from the scrubber is done in two steps; first a reduction of the sulfite and sulfate to sulfide, followed by conversion of the sulfide to carbonate plus hydrogen sulfide. The reduction step is accomplished by reaction with a form of carbon, such as petroleum coke. The conversion of the sulfide to carbonate is accomplished by reacting the reduced melt with steam and carbon dioxide, liberating hydrogen sulfide.

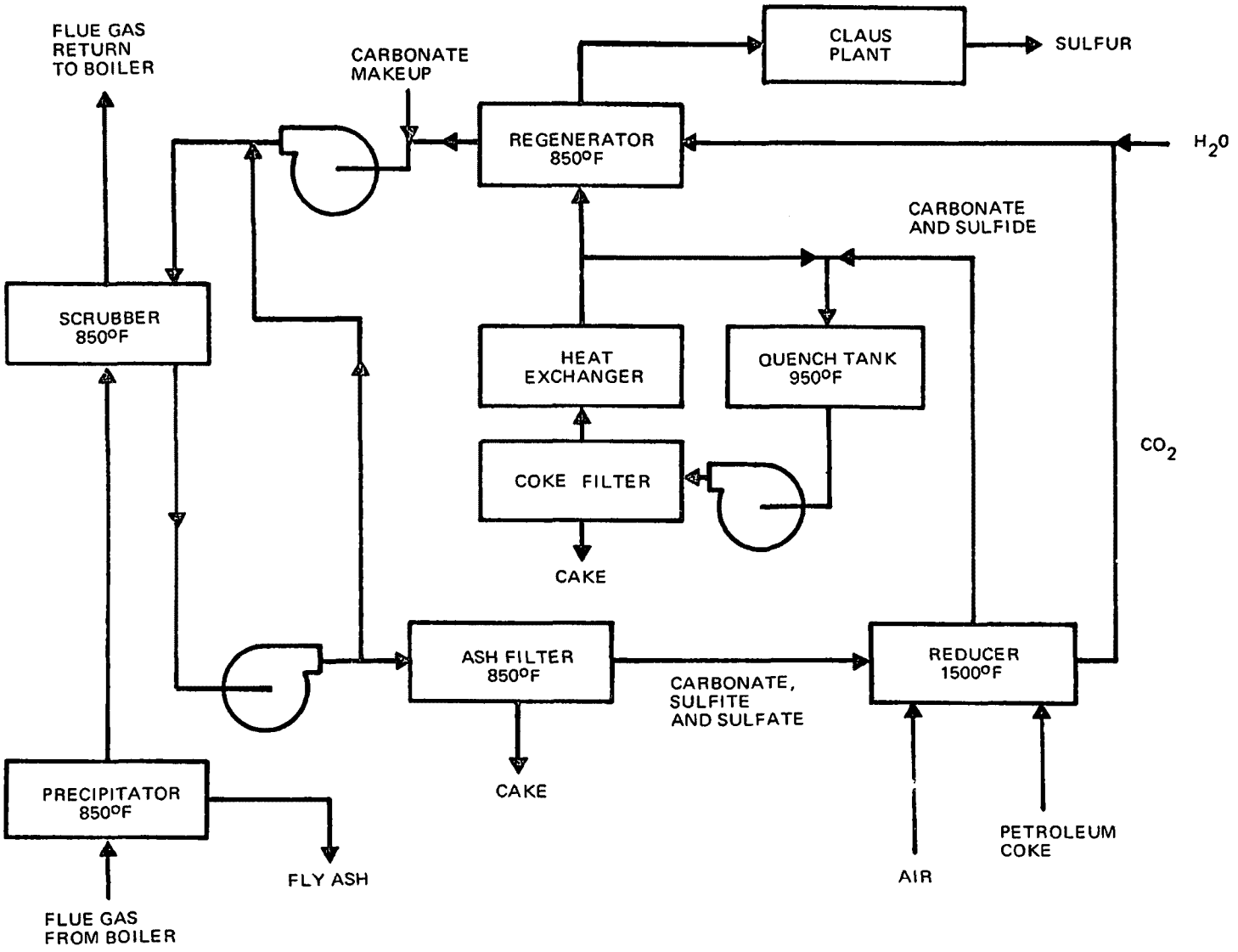

71-F4-7-16A

Figure 1. Molten Carbonate Process Flow Diagram

The alkali carbonate melt used in the process has the following advantageous features:

(1) It is a liquid, easy to handle, pump, and transport;

(2) It has a negligible vapor pressure, so that it is not lost by evaporation;

(3) It reacts rapidly with sulfur oxides, so that scrubbing contact time can be short;

(4) It has a high capacity for sulfur oxides, so that the amount of melt being circulated is relatively small; and

(5) The chemical affinity with sulfur oxides is so great that it can remove nearly all of the sulfur oxides from even very dilute gas streams.

Furthermore, its use in the scrubber does not cool off the gas stream or saturate it with water vapor.

These features make possible a process which can effectively treat large volumes of dilute flue gas, while requiring regeneration of relatively small volumes of material, and recovering the sulfur in elemental form.

The process flow diagram is shown in Figure 1. The process works as follows:

1) The gas to be treated is removed from the boiler at about 850°F and passed through a high temperature, high efficiency electrostatic precipitator where 99% or more of the fly ash is removed. The gas then passes through the scrubber, where the sulfur oxides are removed by contacting the gas stream with a spray of molten carbonate at 850°F. This gas-liquid contact removes 95% or more of the sulfur oxides and most of the remaining fly ash from the gas stream. The cleaned gases are then returned to the boiler for further heat recovery, and eventually pass out the stack.

2) The molten salt stream containing carbonate, sulfite, sulfate and fly ash from the scrubber is filtered to remove the fly ash. The fly ash filter cake is subsequently treated to recover the lithium carbonate it contains.

3) The filtered melt is fed into the reducer, and reacted with carbon. The melt temperature is raised from ~ 850°F to ~ 1500°F by heat from the indirect combustion of part of the carbon with air, and the sulfite and sulfate in the melt are reduced to sulfide in about 20 minutes.

4) The melt stream from the reducer is passed into a quench tank where its temperature is lowered from 1500°F to about 950°F by mixing with melt at 850°F. The effluent from the quench tank is pumped through a filter to remove residual coke from the reduction step, cooled further to 850°F in a heat exchanger and then passed on to the regenerator.

5) In the regenerator, the reduced melt is reacted with carbon dioxide (produced in the reduction step) and steam in a multi-stage, countercurrent tower. The sulfide in the melt is regenerated to carbonate, and the sulfur is released as hydrogen sulfide. The hydrogen sulfide is sent to a Claus plant, where it is converted to elemental sulfur.

6) The regenerated melt is recirculated to the scrubber, with the small losses in the purification system being made up by addition of fresh carbonate.

The status of development of the process is described briefly in the following section.

B. STATUS OF DEVELOPMENT OF THE PROCESS

The process development work done to date has consisted primarily of chemistry studies, bench-scale engineering tests, materials tests, test loop design, and process analysis. The chemistry of each step of the process has been studied separately, and kinetic and equilibrium data have been obtained. Bench-scale engineering tests of the scrubbing step (including mist elimination) and filtration step have also been carried out, and extensive corrosion testing has been done. The status of each process step and of the materials testing program are summarized below.

1. Scrubbing

In the scrubber, it is necessary to bring about good contact between the huge volumes of flue gas and the relatively small melt stream. Further, power plant integration requirements make it important to impose as small a pressure drop as possible on the gas stream. Because of this, a spray contactor has been selected as the most promising scrubber concept. The spray contactor requires spray nozzles, to break the melt up into small droplets for good gas-liquid contact, and a very efficient mist eliminator, to prevent the gas stream from carrying melt mist out of the scrubber.

In bench-scale tests, synthetic flue gas was scrubbed in a small (4-in. ID) spray chamber equipped with a single pneumatic nozzle, and removal efficiencies of greater than 95% were obtained at gas velocities of up to 25 ft/sec. Mist elimination tests were done with the same apparatus; they showed that wire mesh pads were quite effective in removing melt droplets from the gas. However, the tests were hampered by the lack of a source of large volumes of hot gas. This made it necessary to use such a small spray contactor, and also limited the mist eliminator tests at high velocities to very short runs. Consequently, it was difficult to separate out the wall effects in both the scrubbing and mist elimination tests, and it was impossible to obtain enough mist carryover to get accurate mist eliminator performance data. Also, the use of synthetic gas precluded any study of effects of fly ash or other fuel-derived impurities. Further testing of spray contactors, mist elimination and fly ash effects requires a side stream of flue gas from an operating power plant. Therefore, tests of the scrubber and mist eliminator must be a part of a pilot plant program.

2. Reduction

The melt produced in the scrubber is a mixture of alkali metal carbonate, sulfite and sulfate. However, when this mixture is heated to the reduction temperature, the sulfite rapidly disproportionates to form sulfate and sulfide.

Consequently, the reduction step actually involves the reduction of sulfate dissolved in a melt of carbonate and sulfide. To accomplish this effectively with carbon, the temperature must be raised from 850°F to about 1500°F and the endothermic heat of reaction (~ 40 kcal/g mole of sulfate) must be supplied. Because of materials limitations, the most feasible way to supply the heat of reaction is to generate the heat internally, by the indirect combustion of carbon with air. Generating the heat directly within the melt inside the reduction vessel eliminates the necessity for heat transfer surfaces operating at high temperatures in a corrosive environment.

The chemistry of the reduction step with simultaneous heat generation is quite complex. Both oxidation and reduction must occur in the same vessel, under conditions which yield the desired sulfide product and supply the sensible heat required to raise the incoming melt to the reduction temperature, the endothermic heat of reaction, and the heat losses from the reducer vessel. Tests done so far have demonstrated the feasibility of performing the reduction step with carbon (petroleum coke) while simultaneously generating the required heat internally by air oxidation. The reduction is rapid and is complete in 15 to 20 minutes at temperatures of 1450 to 1500°F, and yields a product containing essentially no sulfate as long as excess coke is present.

Analytical studies have indicated that the concept of a two-zone reduction vessel (oxidation and reductions zones separated by a ported barrier) with internal circulation shows the most promise. These same studies indicated that an alumina-brick-lined vessel is needed to minimize heat losses. However, the vessel configuration, dimensions, and locations of the inlet and exit ports as well as the methods to be used for introducing the air and carbon into the reduction vessel have not been fixed. Further work, including a laboratory program to model the reducer hydraulic processes, is needed to supply data on which to base the pilot plant reducer design.

3. Regeneration

In the regeneration step, the carbonate-sulfide melt from the reducer is reacted with a mixture of carbon dioxide and steam, converting the sulfide into carbonate plus gaseous hydrogen sulfide. The chemistry of this step has been studied extensively; the reaction is rapid, exothermic, and equilibrium-controlled. For complete regeneration, a multi-stage countercurrent contactor such as a tray column is required, with cooling provided to remove the heat of reaction.

The equilibrium and heat evolution data were measured experimentally, and used to calculate the number of theoretical stages required and the amount of heat evolved. To complete the design of a regenerator column, tray efficiency and heat transfer coefficient values are needed. However, it will be difficult to measure these parameters in the laboratory, and the values can be estimated well enough to permit the design of a pilot plant regenerator. The tray efficiency and heat transfer coefficient values for use in designing a full-scale unit can then be obtained accurately from the pilot plant tests.

4. Filtration

In laboratory fly ash filtration tests, cartridge filters with sintered metal, etched disc, and wire wound filter elements have all been tested successfully. The filters remove essentially all the ash from the melt, forming a filter cake which contains about 60% melt and 40% fly ash. Economic considerations make it necessary to remove the filter cake from the filter continuously and as "dry" as possible, for reprocessing to recover the lithium carbonate. The most effective way to recover a dry filter cake is to use a centrifugal basket filter, and remove the cake continuously with a plow or scraper. It is necessary to build up a filter cake at least 1/4 in. thick for this to work. However, fly ash forms a dense filter cake, so that a thick cake layer causes a high pressure drop. Improving the porosity of the cake by use of filter aid or filter

precoat material, such as fluidized petroleum coke, would ease the filtration problem considerably. A program to study filter aids and precoat materials should be carried out in conjunction with the pilot plant program.

5. Lithium Recovery System

The lithium recovery system must recover a large fraction of the lithium carbonate from the fly ash filter cake and return it to the process. An aqueous method has been developed and tested to separate the insoluble lithium carbonate from the soluble material (chlorides and the relatively inexpensive sodium and potassium carbonates). Laboratory tests have demonstrated that this method can recover most of the lithium carbonate from the filter cake. A program to complete the development of this process should be undertaken in conjunction with the pilot plant program. However, the work need not start until the pilot plant is in operation and producing filter cake.

6. Materials and Components

A test program to select materials of construction which resist corrosion by the process melts has been underway for over three years. At first, the common metals, alloys, and ceramics were given screening tests. Successful candidates were then subjected to long term tests, including one-year tests in rotating capsules. As a result, it was found that type 347 stainless steel was the best of the standard alloys for service below 1000°F.

After the preliminary selection of type 347 stainless steel, this alloy was subjected to further tests to study the effect of stress in the presence of chloride, oxygen, and water vapor, the effect of sensitization, and the rate at which the alloy constituents are leached out and transported under the influence of a temperature gradient. The results have been satisfactory, and type 347 stainless steel is presently the planned material of construction for all process equipment operating below 1000°F. However, further testing should be done, to study the suitability of this alloy when exposed to flowing melt under process

conditions. For such tests a forced-circulation test loop is needed. This loop will include a pump, valves, and flow meters in addition to corrosion test sections. The need for such a test loop was recognized early in the development program, and the design of a test loop was completed and the procurement package has been prepared. In addition, Atomics International has already purchased the pump and a NaK-filled differential pressure cell for a flowmeter, since these are long-lead-time items. The test loop should be built and operated as soon as possible, both to study corrosion under melt flow conditions, and to gain experience with the pump, valves, and instrumentation.

C. DEVELOPMENT PROGRAM DURING REPORT PERIOD

The development program for this report period concentrated on (1) obtaining additional data on the performance of filters to remove fly ash from the molten salt stream, (2) studying the effectiveness of mist elimination pads to remove entrained salt from the gas stream exiting from the scrubber, (3) continuing the materials test program, (4) completing the design of a materials test loop, (5) cooperating and assisting Singmaster & Breyer in their evaluation of the process, (6) completing preliminary engineering analyses of the two region molten carbonate reducer and the regenerator, and (7) revising the material and energy balances for 800 and 10 Mw plants. The results of the work on each of these topics are described in the following section of this report.

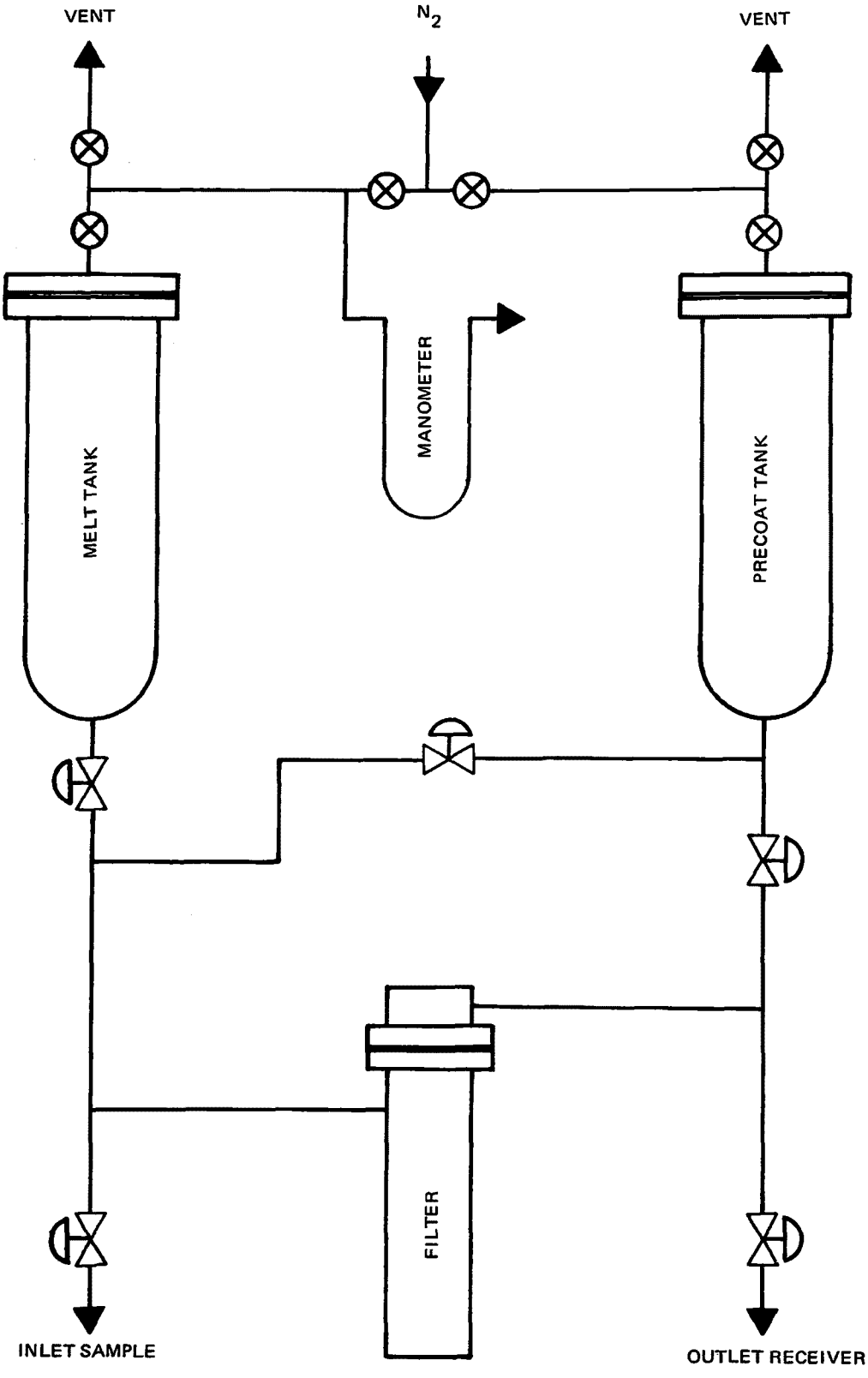

Figure 2. Filtration Test Stand

II. PROGRESS DURING REPORT PERIOD

A. FILTRATION STUDIES

1. Introduction

The flue gas which enters the scrubber contains any fly ash which passes through the electrostatic precipitator, plus other impurities such as chlorides. These impurities will be picked up by the molten carbonate and incorporated into the process melt. To keep them from accumulating and building up to a high level in the process stream, it is necessary that they be removed from the melt continuously. It has been demonstrated that fly ash can be removed by filtration, and that chloride, after reaching its solubility limit (effectively about 4 wt %), forms crystalline particles which should also be filterable.

2. Experimentation

As part of the continuing effort to develop an effective filter for the removal of fly ash from molten salts, additional tests were conducted with a Croll Reynolds 25 micron filter to study the effect of filter cake buildup on removal efficiency and pressure drop across the filter. The apparatus that was used for the tests is shown schematically in Figure 2. By applying pressure on the melt tank, the melt-ash suspension was caused to flow from the tank through the filter into containers. The flow rate was controlled by varying the pressure on the melt tank. Filtration efficiency was determined by analyzing inlet and outlet samples for ash content.

During the test, the filter was operated with an average melt throughput rate of ~ 150 g/min, until the pressure drop across the filter necessary to maintain the flow rate increased to 40 psi. A total of 26.6 kg of melt containing 1 wt % of Colorado Public Service fly ash was passed through the filter during the experiment. This corresponds to an ash loading of 0.609 g/cm^2 filter surface. The data from this test were compared with data for the 25 micron Croll Reynolds filter reported in Progress Report No. 3; the results are shown graphically in Figure 3.

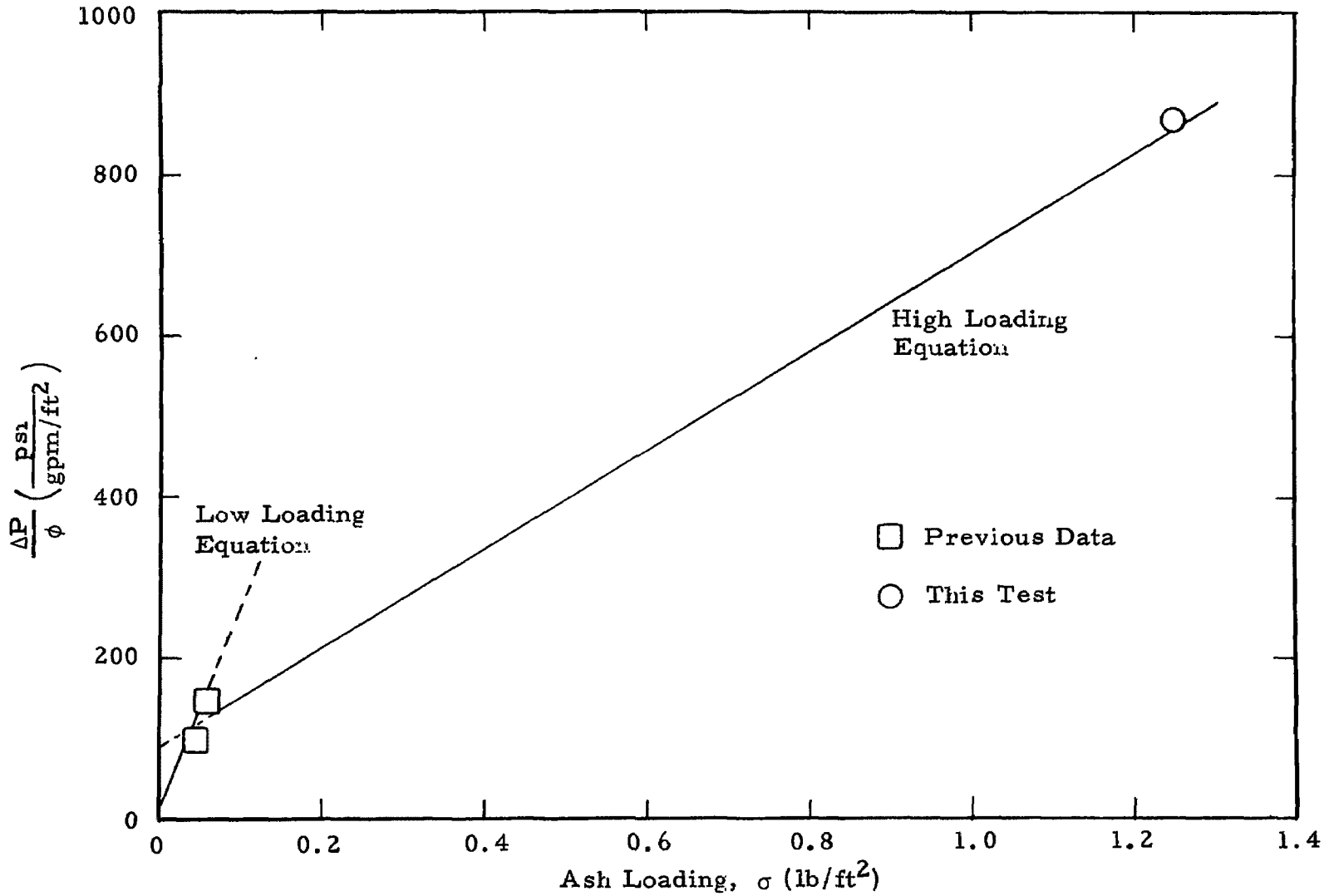

Figure 3. Experimental Measurement of Dependence of $\Delta P/\phi$ on Ash Loading for th 25-μ Croll-Reynolds Filter

Two equations were developed to fit the data for the Croll-Reynolds filter over the entire range of ash loadings:

$$\text{Low capacity range: } \frac{\Delta P}{\phi} = 16.3 + 2530\,\sigma \qquad 0 \le \sigma \le 0.067$$

$$\text{where} \qquad \sigma = \text{ash loading} \frac{\text{lb ash}}{\text{ft}^2 \text{ filter area}}$$

$$\text{and} \qquad \frac{\Delta P}{\phi} = \frac{\text{pressure drop}}{\text{unit flow rate}}, \frac{\text{psi}}{\text{gal./ft}^2 \text{ min}}$$

$$\text{High capacity range: } \frac{\Delta P}{\phi} = 88 + 610\,\sigma \qquad 0.067 \le \sigma \le 1.24$$

The buildup in filter cake appeared to have little effect on filter efficiency. This could possibly be explained by channeling. The average removal efficiency during the experiment was 93%. Attempts to preserve the filter cake on the filter while it was being removed from the filter housing were unsuccessful. This supports earlier observations that the filter cake can be removed from the filter body by simply draining the housing.

3. Evaluation

a. Fly Ash

The fly ash filter requirements were re-evaluated, based upon the above pressure drop data. The following criteria were used in the evaluation: (1) coal producing 10% fly ash, (2) all of the fly ash entering the absorber being removed by the molten carbonate spray, (3) 1 hour filtration time between filter cake removal and (4) a 50 psi pressure drop allowance across the filter. The calculations were made for a 99.5% and a 99.75% efficient electrostatic

precipitator and a 719 gpm and 180 gpm flow rate (the former reflecting a 3:1 recirculation rate around the scrubber and the latter reflecting a once-through stream). One additional estimate was prepared for a 99.9% efficient electrostatic precipitator. Table I shows the results of the calculations and the budgetary prices obtained from the Croll Reynolds Engineering Company. The prices were based on Type 347 stainless steel and were for both 70 micron and 25 micron elements. The 25 micron element cost is 50% higher, but has been shown to be more efficient in filtering the fly ash. The largest unit manufactured by Croll Reynolds has 1200 ft^2 of filter area. The quote was therefore based on multiple units where required. In most cases 100% standby capacity is furnished to provide 60 minutes of downtime to remove the filter cake and ready the unit for reuse. However, also shown for comparison are two cases of lower extra capacity for less downtime. The extra capactiy needs will depend on the cleaning time actually required and the excess capacity desired for non-normal operation.

b. Effects of Chlorides

In the Singmaster & Breyer evaluation (see Section G), it was assumed that a coal containing 0.04% chloride is burned, and that all of this chloride volatilizes, reacts with the carbonate melt in the scrubber, and then forms solid potassium chloride. The potassium chloride is then filtered out of the melt along with any fly ash which is picked up in the scrubber. These assumptions increase the filter duty markedly, since the amount of potassium chloride formed is approximately equal to the amount of fly ash picked up when a 99% efficient electrostatic precipitator is used. The actual fate of chloride in the process is not known. Tests have shown that if the chloride content of the melt builds up to about 4%, the melt is saturated and additional chloride forms a crystalline solid material which would be filtered out with the fly ash. However, potassium chloride will also be sublimed out of the melt during the reduction process. This may remove all or a large part of the chloride, so the assumption that all of it must be filtered out is probably quite conservative. The inclusion of chlorides in the filter duty

would change the filter requirement assumed in the process cost estimate given in Section E of Progress Report No. 3, either by increasing the cost or by decreasing the time of the filter cycle.

c. Costs

Based on the latest flow diagram for an 800 Mw installation where a 3:1 melt recirculation is used, the filter cost using 100% standby is $675,000. If only the stream going to the reducer is filtered or no recirculation is required, this cost is reduced to $300,000. However, if the fly ash filter must also remove chlorides, the cost will increase substantially, to ~$700,000 for the no recirculation case.

TABLE I

FILTRATION PRICES USING CROLL REYNOLDS FILTER
(800 Mw Plant)

gpm	Fly Ash Removal Efficiency	Required Filter Service		Model	Total Filter Surface Provided	Cycle Time (min)	Total Filter Cost ($K)	
		ft^2	No. of Filters				70 μ	25 μ
180	99.5	940	2	S72-940	1880	60	200	300
180	99.75	722	2	S60-722	1444	60	150	225
719	99.5	2310	6	S60-722	4332	56	450	675
			4	S66-770	3080	40	330	495
719	99.75	1900	4	S72-940	3760	60	400	600
			3	S72-940	2820	45	300	450
180	99.9	545	2			60		150*

*Estimated

d. Improved Filtration

On recommendation of Singmaster & Breyer (the process evaluators) we discussed ways to improve the filtration step with U. S. Filter Company. The

experimental results showing a 40 psi pressure drop with a 1/16 in. thick filter cake suggested that cake porosity be increased by use of a filter aid. The suggested filter would have 200 micron openings and use a 1/16 in. to 1/8 in. thick filter aid layer, operating on a one-hour cycle. Fluidized coke was suggested as a suitable filter aid. The estimated cost of a 940 ft^2 unit is $70,000. This is in line with the Croll Reynolds filter costs.

e. Conclusions

(1) Experiments should be conducted to determine the merits of using fluidized coke as a filter aid.

(2) Experiments should be conducted to determine the effects of chlorides on the performance requirements for the fly ash filter.

(3) The effect of recirculating melt containing fly ash through the scrubber should be determined.

(4) The basis for filter overdesign should be established (maximun fly ash burst).

(5) The minimum downtime between cleaning and the penalty in melt loss at every cleaning should be determined to find the optimum filtering time.

(6) There is an incentive to develop a continuous filter.

B. MIST RECOVERY TESTS

In the scrubbing step of the process, the melt will be sprayed into the gas stream being treated. It is very important that this melt be recovered, so that it is not carried away entrained in the gas. A highly efficient mist eliminator is needed for this. Wire mesh pads have been used for mist recovery with aqueous systems; their suitability for use with molten carbonate had to be studied. Therefore, a series of tests was conducted to investigate the effectiveness of woven wire mesh pads as a means of separating entrained salt from the gas stream.

The mist elimination test system that was utilized in these tests is shown schematically in Figure 4. In operation, melt is pressurized from the melt tank into a pneumatic nozzle where it is atomized by a jet of hot gas. The generated mist is picked up by the main gas stream and carried upward through two wire-mesh mist elimination pads. The gas then exits through a short constricting stack. Mist which passes through the first pad is collected on the second pad. The quantity of mist which passes through both pads will appear in an exit gas sample which is collected continuously during a test. During the first two tests, it was found that the quantity of material collected in the exit gas sample train was too small to be analyzed and this technique was abandoned in favor of weighing the pads prior to and following each test. The separation efficiency was then determined by changes in weight and by making a material balance around the system.

As a result of operating problems (discussed below) attendant with the equipment itself, only three tests were conducted. The conditions for the tests are given in Table II.

TABLE II

MIST ELIMINATION TEST CONDITIONS

Test No.	Melt Conditions			Gas Conditions			Linear Velocity Through Demister (ft/sec)
	Composition	Temp (^{o}F)	Flow Rate (lb/hr)	Composition	Temp (^{o}F)	Flow Rate (ACFH)	
1	M_2CO_3	900	20	Compressed Air	950	4720	6.5
2	M_2CO_3	1020	35.5	Compressed Air	930	4200	5.8
3	M_2CO_3	1100	36.3	Compressed Air	850	2410	3.3

In the first test, a large nozzle was used, with the apparatus arranged as shown in Figure 4. The test lasted for about 20 min, and then stopped when water from the compressed air line got through the water trap and cooled the nozzle below

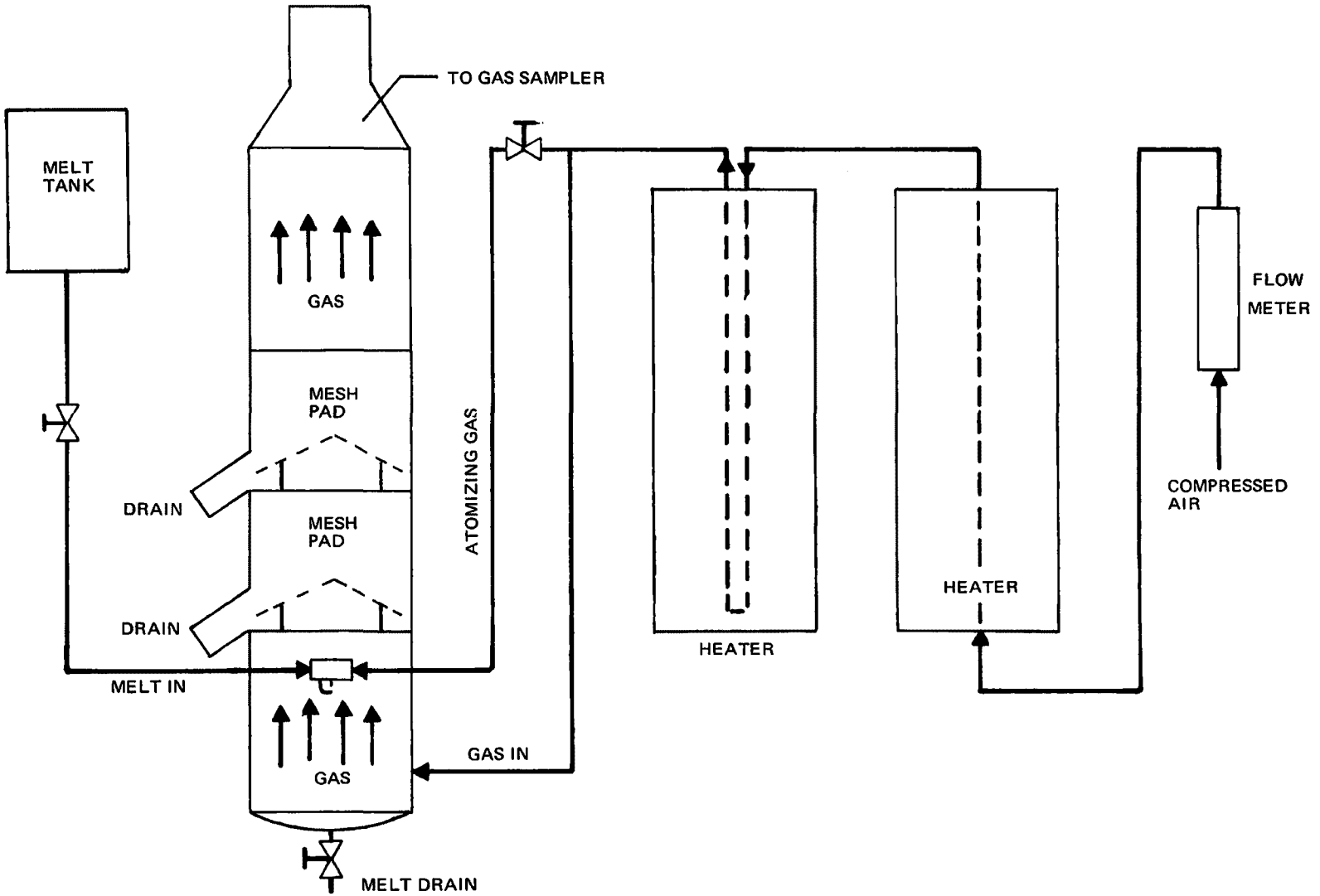

Figure 4. Mist Eliminator Test System

the melt freezing point, plugging it. During the test, no melt drained from either mist eliminator section, although faint traces of salt could be seen coming out with gas escaping from the lower section drain. The linear gas velocity through the mesh pads was about 6.5 ft/sec. At this velocity the overall pressure drop through the two mist eliminator sections was 1/8 in. of water at the start, rose to 3/8 in. while melt was spraying, and then fell back to 1/8 in. after the nozzle plugged. These values are quite low; the decrease after the nozzle plugged may indicate some mist was picked up, but that it dripped back into the spray chamber instead of draining into the circumferential weir.

During the test, the gas passing through the mist eliminator was continuously sampled and scrubbed with water. The resulting solutions were evaporated and analyzed for lithium, sodium and potassium using x-ray emission spectroscopy. However, there was such a small amount of material collected in the upper pad that the data were very inconsistent and scattered. Therefore, although the mist collection efficiency could not be determined accurately, mist carry-over was found to be very slight.

In the second test, the test system was modified to provide a separately-heated source of dry nitrogen for the atomizing nozzle, a smaller nozzle was used, and the upper pad was removed so that all of the mist passing through the first pad would appear in the exit gas. The exit gas was sampled by sucking it through a water bath at a controlled rate. During the test, melt did drain out of the lower section drain, showing that the nozzle was producing mist and that the mesh pad was removing it. However, analysis of the gas sample was inconclusive, due to the small quantities of collected material.

In the third test a clean weighed demister pad was installed downstream of the test demister. Based upon weight gain of the downstream demister during the test and the total salt passed through the nozzle, the test demister was 99.92% effective in preventing mist carry-over at a gas velocity of about 6 ft/sec. However, there was difficulty in attaining the desired gas temperature (850^{o}F) at the desired gas velocities. Consequently, modifications were instituted to double the heating capability of the gas system.

The mist eliminator test stand was modified to double the gas heater capacity, and tests were then attempted at high gas velocities (up to 25 ft/sec). The tests failed, due to the presence of large amounts of water in the compressed air supply. Vaporization of this water cooled the gas stream to below the melt freezing point. It is apparent that a different gas supply will be needed if high velocity tests are to be run for periods long enough to obtain accurate carryover data. Hot combustion gases from a burner should be suitable. However, incorporating a burner system into the mist eliminator test stand was not possible during the present report period, so the effort on mist elimination studies was suspended. The work done to date indicates that two wire mesh pads in series will remove all or nearly all of the fine mist produced by the aspirator nozzle at velocities of up to 6 ft/sec and probably higher. However, caution should be utilized in applying these results to a large scale plant due to inabilities to separate out the wall effects. Also, the use of a synthetic gas precludes the study of the effects of fly ash and/or other fuel derived impurities. Consequently, pilot plant tests are really needed to determine whether the removal efficiencies of large mesh pads will be high enough, under actual power plant conditions.

C. MATERIALS STUDIES

1. Introduction

A test program to find construction materials that are resistant to corrosion by the process melts has been underway for over three years. Initially, the more common metals, alloys, and ceramics were subjected to corrosion screening tests at 932°F (500°C). The results of the screening tests indicated that the austenitic stainless steels (preferably type 347) were suitable for service at 900-950°F, with some other alloys (e.g., Hastelloys G and X and Haynes 25) also suitable as alternates. These materials were then tested more extensively, in both static and dynamic (rotating capsule) tests. The results of many of these tests have been presented in the first three progress reports. During this report period, five one-year dynamic tests and three one-year thermal transport tests were completed; they are discussed in section 2

below. In addition, the design of a pumped corrosion test loop was completed. This test loop is needed to study the corrosion effects of circulating melt streams under process conditions. The design is presented and discussed in section 3 below.

2. Corrosion Tests

During the report period, five dynamic corrosion tests of type 347 and type 321 stainless steels were performed in rotating test vessels with the equipment and techniques described in Progress Report No. 1 (AI-68-104; PB 179-908). The test specimens were stressed (clamped horseshoe) and unstressed strips of type 347 and type 321 stainless steels exposed to carbonate melts containing

(1) 5% chloride and 20% sulfide (both steels);

(2) 5% chloride and 20% sulfite (both steels); and

(3) 5% chloride and 40% sulfite (type 347 only).

All of the test capsules initially had atmospheres of nitrogen, oxygen, and water vapor above the melt level; the tests were all conducted at 932°F (500°C) and were intended to last for one year (8760 hours).

In addition to the five dynamic tests, three thermal transport tests were conducted of both stressed and unstressed steel specimens and different melt mixtures; in each of these tests the test capsules were mounted in furnaces with one end of the vessel maintained at 932°F (500°C) and the other at 797°F (425°C). The furnaces (and vessels) were inverted every 3-1/4 hours, causing the melt to flow from one temperature zone to the other. The purpose of these "flip-flop" tests was to determine the extent to which thermal transport of alloy constituents occurs. The tests involved both type 347 and 321 specimens in melts of carbonate plus 10% chloride and 20% sulfide, and type 347 specimens in a melt of carbonate plus 10% chloride and 20% sulfite.

TABLE III

RESULTS OF ONE YEAR CORROSION TESTS

Test No.	Metal	Test Type	Melt (wt %)			Test Temp (°C)	Test Duration (hr)	Vessel Internal Pressure (psig)		Internal Atmosphere (vol %)								Corrosion Rate (mils/yr)[a]	Stress Relief (%)	Effect of Stress	Remarks
										Initial			Final								
			Cl^-	$SO_3^=$	$S^=$			Initial	Final	N_2	H_2O	O_2	N_2	O_2	H_2	H_2O	CO_2				
29	347	Flip Flop	5	0	20	425 500	8750	35	-10[b]	100	0	0	>99[b]	0	0	0	0	0.15 0.17	43 61	None None	Excellent Excellent
31	347	Flip Flop	5	20	0	425 500	8850	35	19	100	0	0	>99	0	0	0	0	0.3 4.5[d]	54 46	None None	SR Heavy corrosion at interface[c, d]
35	321	Flip Flop	5	0	20	425 500	8770	35	-10[b]	100	0	0	>99[b]	0	0	0	0	0.14 0.65	88 46	None None	Excellent Rusted-Cr depleted
40	347	Rotating	5	0	20	500	8860	35	-10[b]	72	26	2	93[b]	7	0	Yes[e]	0	1	50	None	SR
41	347	Rotating	5	20	0	500	8800	35	-10	72	26	2	94	6	0	0	0	3.3	60	None	SR, E
43	347	Rotating	5	40	0	500[c]	1580	35	0	72	26	2	>99	0	0	0	T	>29[f]	58	None	Pitting factor 4[f]
39	321	Rotating	5	0	20	500	8760	35	5	72	26	2	>99	0.2	T	Yes[e]	0	1	67	None	SR
42	321	Rotating	5	20	0	500	8810	35	2	72	26	2	>99	0[b]	0	0	0	>10	g	Unknown	Corroded into at interface

[a] Based on weight loss over entire specimen - localized corrosion may be greater

[b] Sample lines probably plugged with salt therefore this is probably pressure and analysis in lines and not in main vessel

[c] Thermal excursion to >650°C for 36 hr about 1/3 through test

[d] Corrosion not uniform but greater at interfacial area

[e] Water determined qualitatively

[f] Controller malfunction - wide thermal oscillation for several days

[g] Good spring back on part of stress samples left

T = Trace, SR - surface roughening or micropits, E = embittlement of wire used to tie specimens onto holders

All of the tests were concluded during the report period. Seven of the eight had attained the desired 1-year lifetime, while one of the dynamic tests was terminated after 1580 hours due to a controller malfunction which allowed the temperature to exceed 1200°F (650°C). The test conditions and results are summarized in Table III, and discussed below.

a. Gas Sample Analysis

The three flip-flop test vessels were originally filled to 35 psig with dry nitrogen. At the end of the test, one vessel contained nitrogen at 19 psig; the gas sample lines to the other two vessels were plugged so that the internal pressure could not be measured. The loss of nitrogen was probably via a line leak, too small for melt to escape through.

The five rotating test vessels were originally filled to 35 psig with a 72% nitrogen-26% steam-2% oxygen mixture. At the end of the tests, one of the gas sample lines was plugged. The other four vessels had all lost pressure, possibly due to leaks. However, there is also evidence that the oxygen and part of the steam were consumed during the tests, probably by reaction with the melt on the vessel walls. The only gas samples containing significant amounts of oxygen (tests 40 and 41) had negative pressures, and the oxygen probably came from a small amount of air leaking into the vessel during cooldown. Thus, in all these dynamic tests oxygen and probably steam were lost by reaction sometime during the test. These tests will be repeated later in a corrosion test loop with a constant composition of gas.

b. Metallurgical Examination

1) Dynamic Tests

Specimens from the one-year dynamic corrosion tests were mounted, vibrapolished and etched with 10% ammonium persulfate to determine if carbide precipitation took place. Both intergranular and intragranular carbide precipitation were found in the type 347 stainless steel specimens kept at 500°C (932°F) for one year; as expected, much less carbide precipitation was

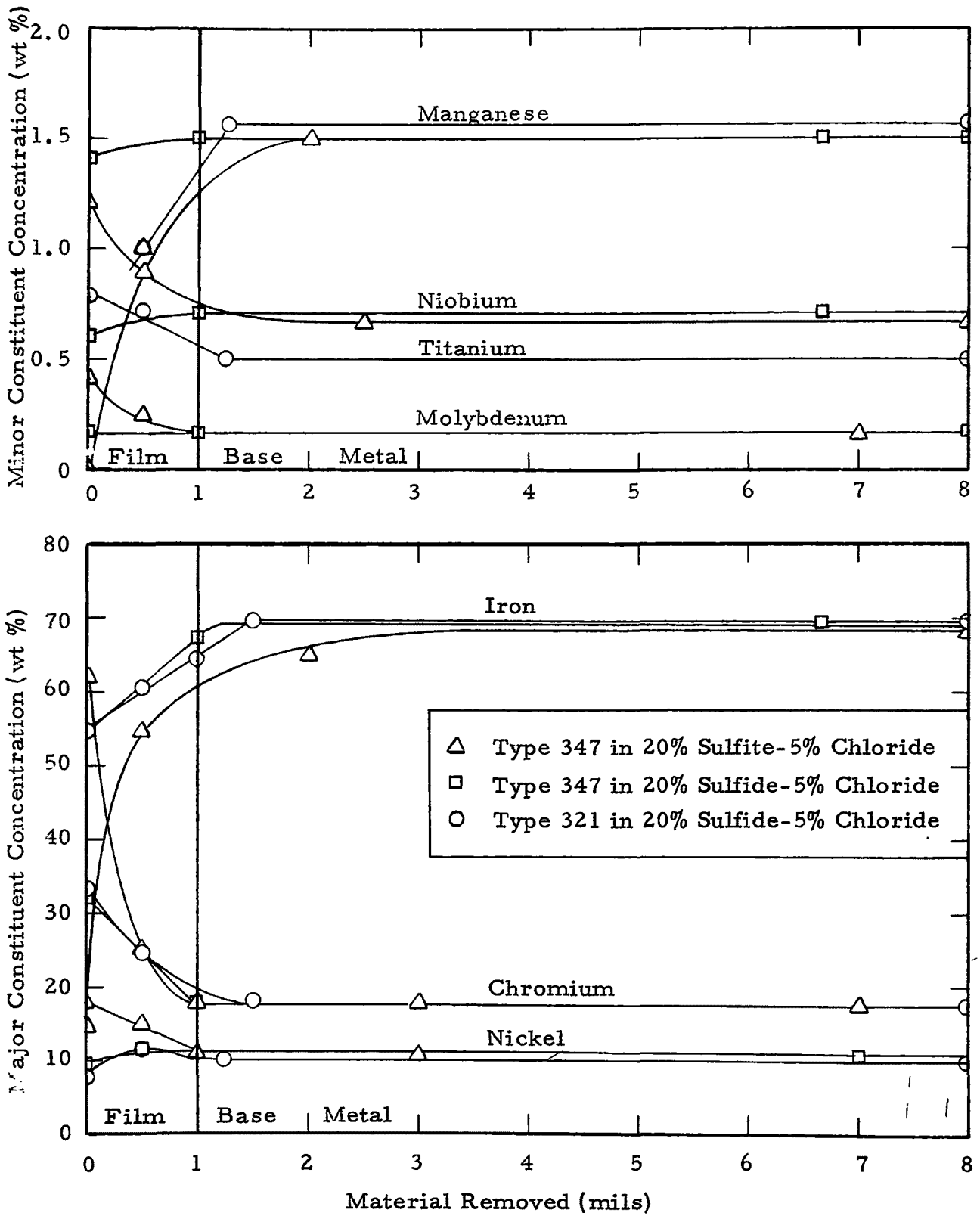

Figure 5. Concentration of Alloy Constituents in Film and Base Metal After 1 Year in a 75°C Melt Thermal Gradient (500°C to 425°C)

observed in the specimens kept at 425°C (797°F) for one year. Maximum sensitization due to chromium carbide precipitation in the grain boundaries always occurs in Type 347 stainless after about one year at 500°C. Enhanced intergranular corrosion, due to chromium depletion along the grain boundary when chromium carbide precipitation occurs, would be a serious problem. However, in the three samples examined little (if any) enhanced intergranular corrosion occurred. After one year at 500°C what appears to be intergranular corrosion was found to a depth of 1/2 to 1 mil; but this is the same depth of penetration which was found after 1500 hr at 500°C. Such intergranular corrosion thus does not appear to increase with time or sensitization, and therefore will probably not be significant in plant applications.

2) Flip-Flop Tests

In these tests metal specimens were exposed to carbonate melt containing 5% chloride and 20% sulfite for SS 347 and 5% chloride and 20% sulfide for SS 347 and SS 321. The melt flowed from a 500°C hot zone to a 425°C cold zone and vice versa at 200 min intervals. The purpose of these tests was to determine if alloying constituents of the metal (particularly chromium) would be transported from the hot zone to the cold zone. If this were to occur, enhanced corrosion with time could be expected and extended use of such an alloy would be questionable.

The test samples were analyzed metallographically to see if thermal transport occurred. Mounted specimens from the hot zone of the three flip-flop tests were repeatedly examined by x-ray fluorescence as the surfaces of the samples were ground away. In this manner the metallic composition of the specimen *vs* depth was determined. The results are shown in Figure 5. In the film on the metal surface, the chromium content was higher than in the base metal while iron was lower; this reflects the formation of the protective lithium chromite film. However, at one-half mil below the film-metal interface (i.e., into the metal), the concentrations of all major (Fe, Cr, and Ni) and minor (Mn and Nb for SS 347 and Mn and Ti for SS 321) constituents

were found to be the same as those for the bulk metal, in both alloys. Since little, if any, thermal transport of alloying constituents occurred, these austenitic stainless steels apparently are not susceptible to thermal transport of alloying components in chloride-sulfite (SS 347) or chloride-sulfide (SS 347 and SS 321) melts where 75°C (i.e., 500°C to 425°C) thermal gradients occur.

c. Corrosion Rates

Based on weight loss, the corrosion rates of type 347 stainless steel in the 5% chloride-20% sulfide melts were 0.15 mils/year at 425°C (797°F) and 0.17 to 1.0 mils/year at 500°C (932°F); the rates in 5% chloride-20% sulfite melt were 0.3 mils/year at 425°C and 3.3 to 4.5 mils/year at 500°C. For type 321 stainless steel, the rates in the 5% chloride-20% sulfide melts were 0.14 mils/year at 425°C and 0.65 to 1.0 mils/year at 500°C; in the 5% chloride-20% sulfite melt, the rate was greater than 10 mils/year. These results show that type 347 is more corrosion resistant than type 321 and that sulfite is more corrosive than sulfide.

The test of type 347 stainless steel in a 5% chloride-40% sulfite melt at 500°C (test 43) was terminated after 1580 hours due to a controller malfunction which allowed the temperature to rise to ~675°C for 36 hours. The specimens from this test showed corrosion rates of greater than 29 mils/year, with pitting also evident. The high corrosion rate and pitting were probably caused by the overheating and thermal cycling. Further testing is needed to verify this.

As a result of the tests, type 347 stainless steel appears to remain acceptable as a construction material. However, care will have to be used to prevent overheating; pitting was found when thermal excursions occurred (tests 31 and 43). Further testing is needed to determine the maximum temperature at which type 347 can be used, and also to study the effects of thermal cycling.

d) Stress Effects

No effects of stress were found. It appears as if sodium carbonate (a known inhibitor of aqueous chloride stress cracking) prevents stress cracks from developing. Corrosion is evidently due predominantly to the sulfur compounds in the melt.

3. Materials Test Loop

As was pointed out above, further testing should be conducted to verify the suitability of the chosen materials of construction when exposed to flowing melt under process conditions. For such tests, a forced circulation test loop is required. The need for such a loop was recognized early in the development program and the design of the test loop using an AEC pump (from Oak Ridge National Laboratory) with separate test legs of Type 347 and 321 stainless steel was completed and a procurement package prepared. The drawings are presented as follows:

P & I Diagram	Figure 6
Layout Drawing	Figure 7
Immersion Tank	Figure 8
Melt and Drain Tank	Figure 9

A revised version of the loop, using a commercial pump and providing only a single type 347 stainless steel leg, has also been designed. The revised P&I diagram is shown as Figure 10. The procurement package for this loop was also prepared.

D. REDUCER ENGINEERING ANALYSIS

A key component of the Molten Carbonate Process is the reducer, which provides for the reduction of the oxidized sulfur compounds formed in the scrubber. The melt exiting from the scrubber is a mixture of alkali metal carbonate, sulfite and sulfate. When this mixture is heated to the reduction temperature, the sulfite rapidly disproportionates to form sulfate and sulfide.

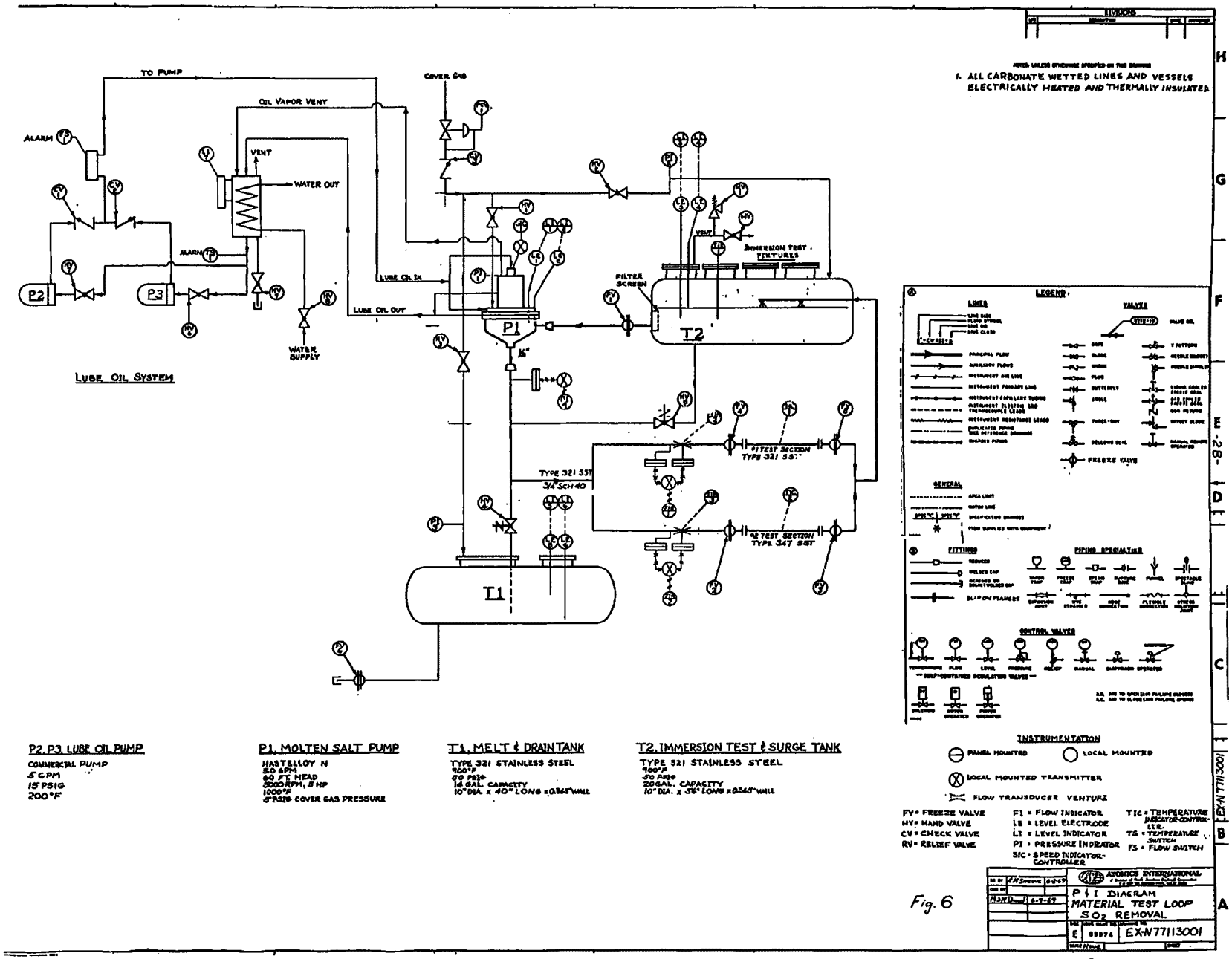

Fig. 6

Figure 6. P&I Diagram, Material Test Loop SO_2 Removal

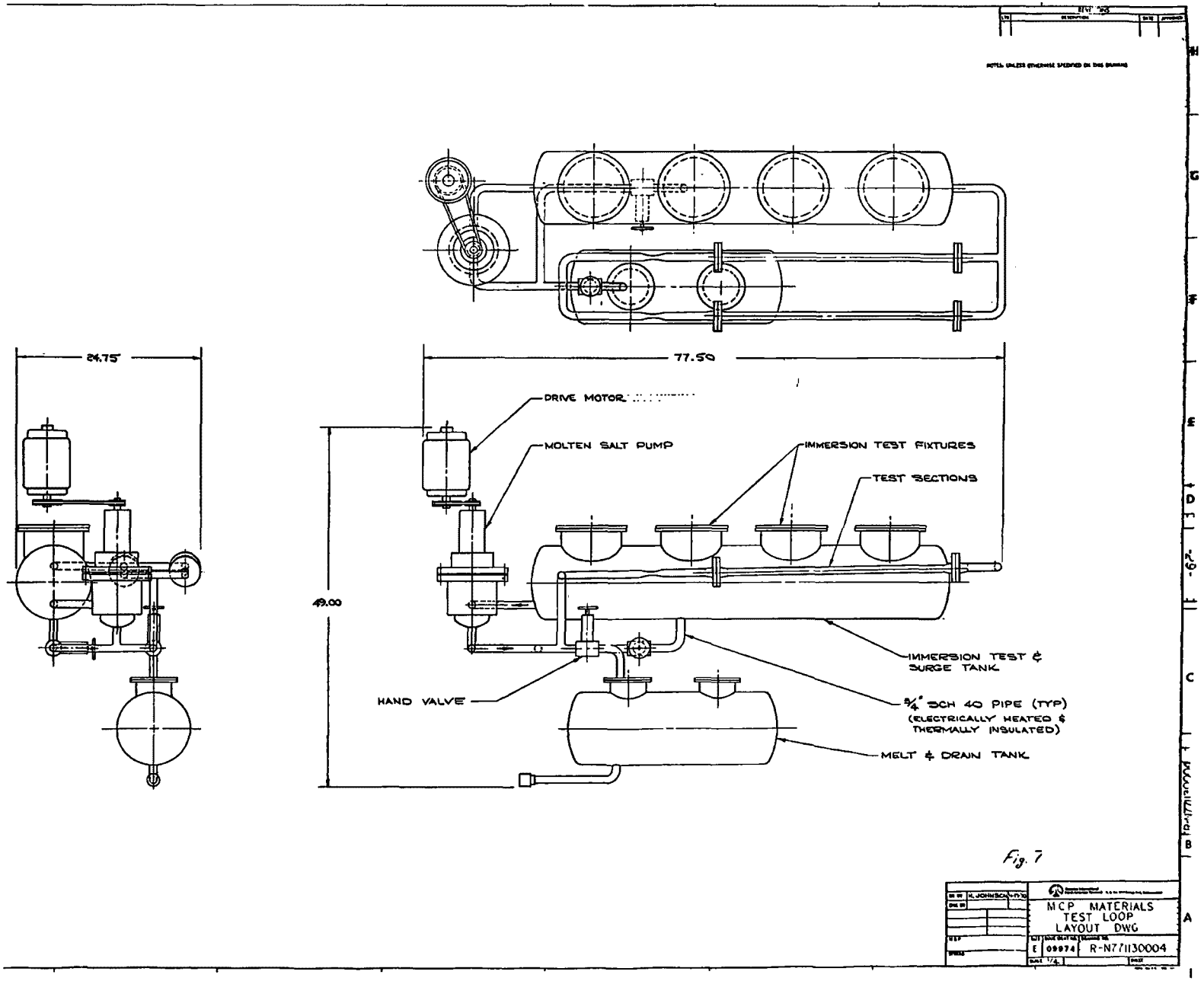

Figure 7. MCP Materials Test Loop Layout Drawing

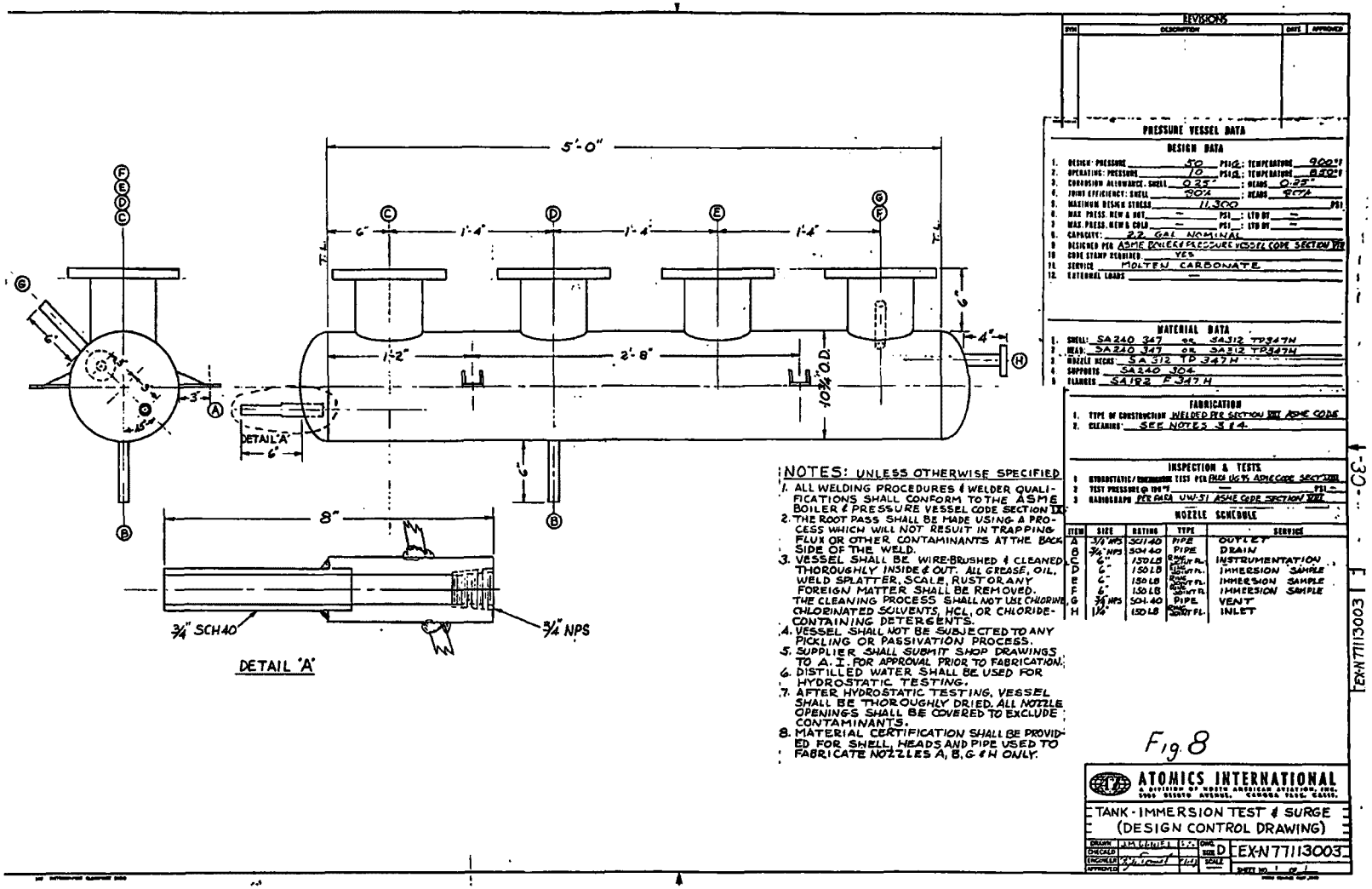

Fig. 8

Figure 8. Tank — Immersion Test and Surge
(Design Control Drawing)

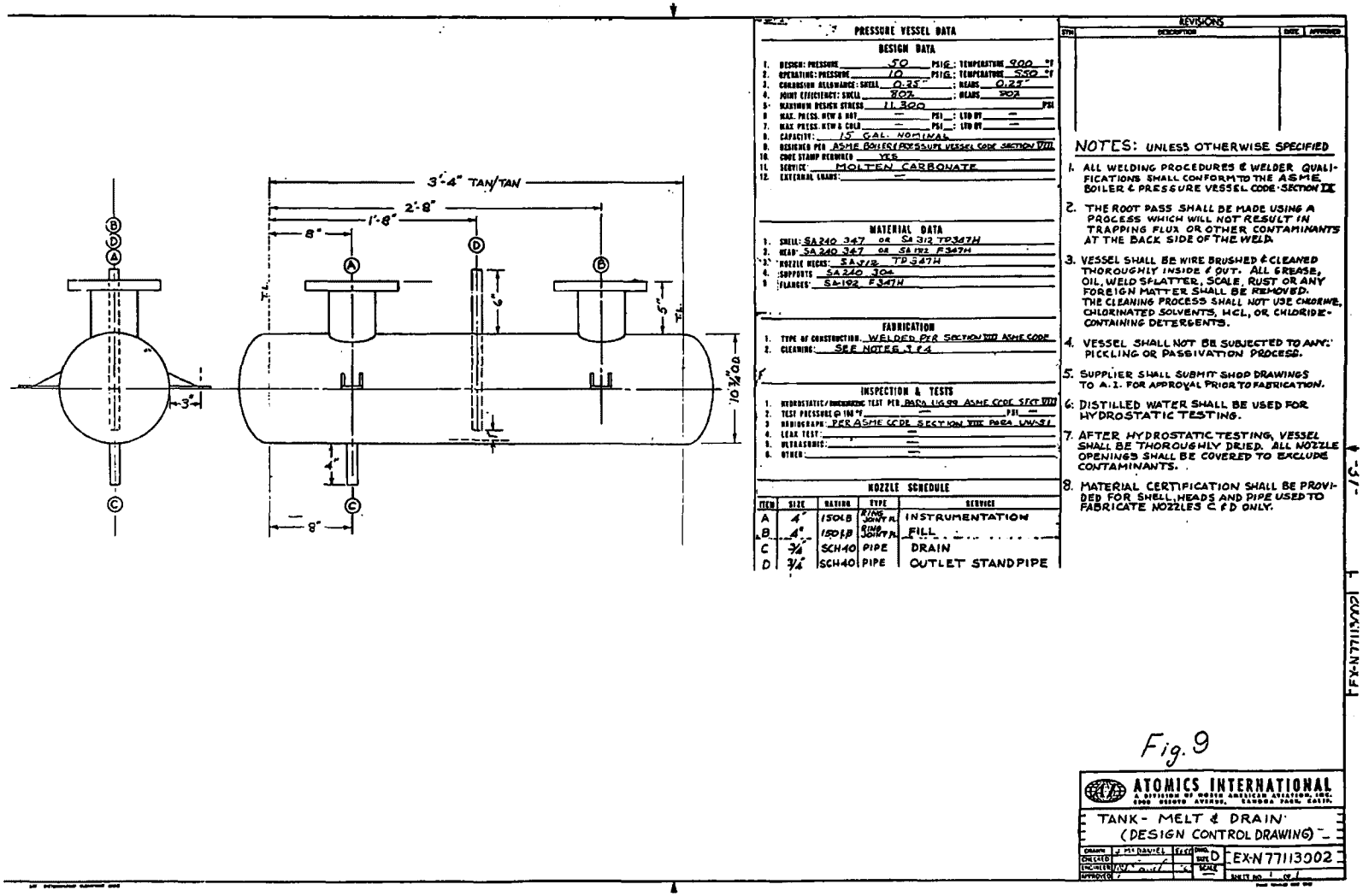

Figure 9. Tank — Melt and Drain
(Design Control Drawing)

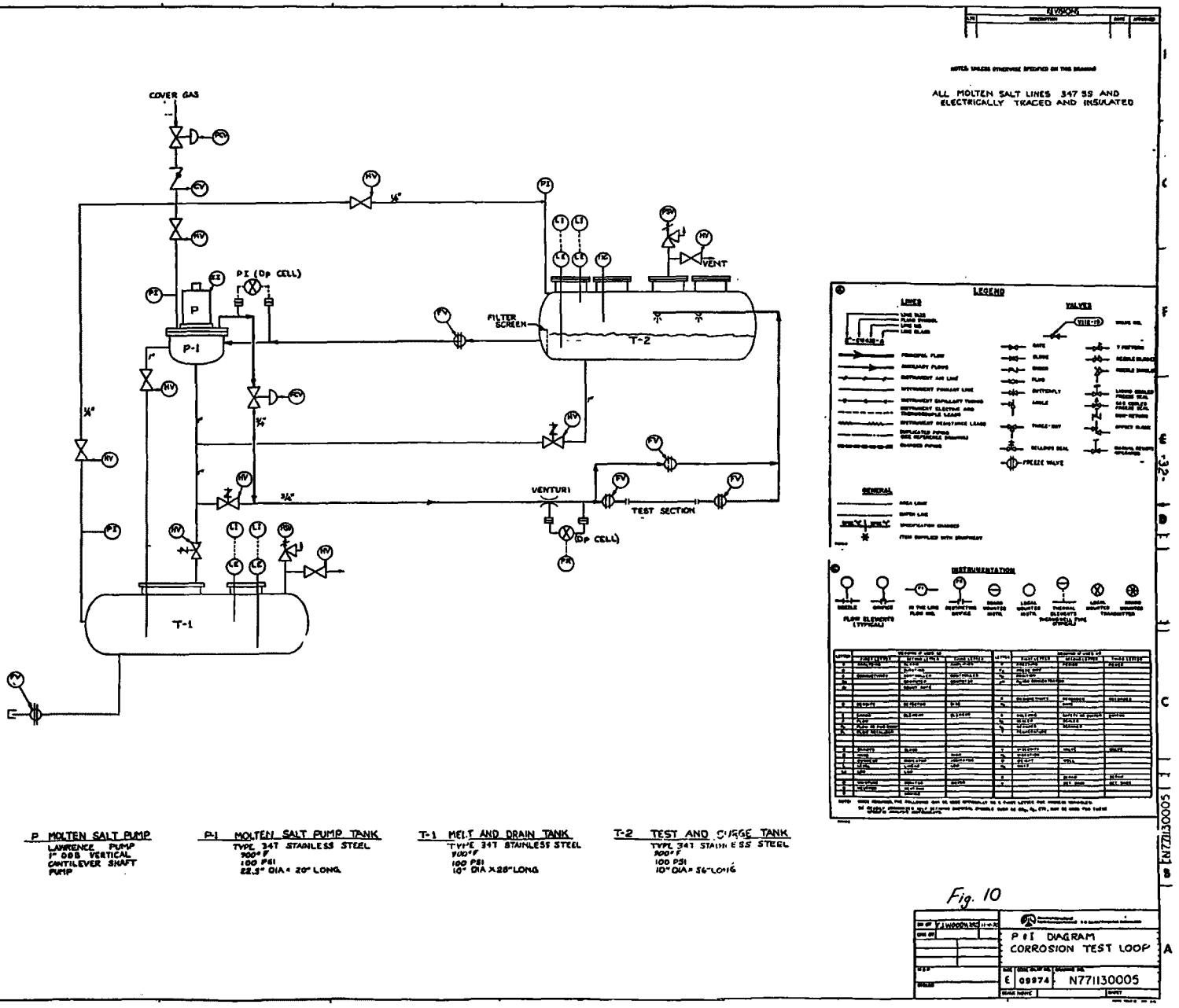

Fig. 10

Figure 10. P&I Diagram, Corrosion Test Loop

Consequently, the reduction step involves the reduction of alkali metal sulfates, dissolved in a melt of carbonate and sulfide. The sulfide reduction product is then subsequently regenerated into carbonate with the release of hydrogen sulfide. The reduction is carried out at a temperature of about 1500°F, using carbon in the form of petroleum coke as the reducing agent,and providing the heat required for the reduction internally through the indirect oxidation of excess coke with air.

Analytical studies have indicated that the concept of a two-zone reduction vessel (oxidation and reduction zones separated by a ported barrier) with internal circulation shows the most promise. In this concept, shown schematically in Figure 11, the reducer vessel will be divided into two zones separated by a ceramic baffle. The melt and coke will enter at the top of the oxidation zone or at the top of the reduction zone. Air will be blown into the bottom of the oxidation zone. The air will oxidize the sulfide in the melt, generating heat, and the unreacted nitrogen (plus some carbon dioxide from reduction) will bubble up through the melt, causing a convective circulation. The circulation will carry hot melt over the baffle into the reduction zone, where most of the reduction will take place, absorbing heat and releasing carbon dioxide. Part of the reduced melt will be removed at the bottom of the reduction zone, and the rest will be recirculated into the oxidation zone to be reoxidized, supplying more heat. An extension of the baffle through the gas space to the top of the vessel will separate the two gas streams, making it possible to use the relatively nitrogen-free carbon dioxide from the reduction zone in the regenerator.

An engineering analysis of this reducer concept was performed and is presented in detail in Appendix A. A summary and the main conclusions of this analytical study are presented below.

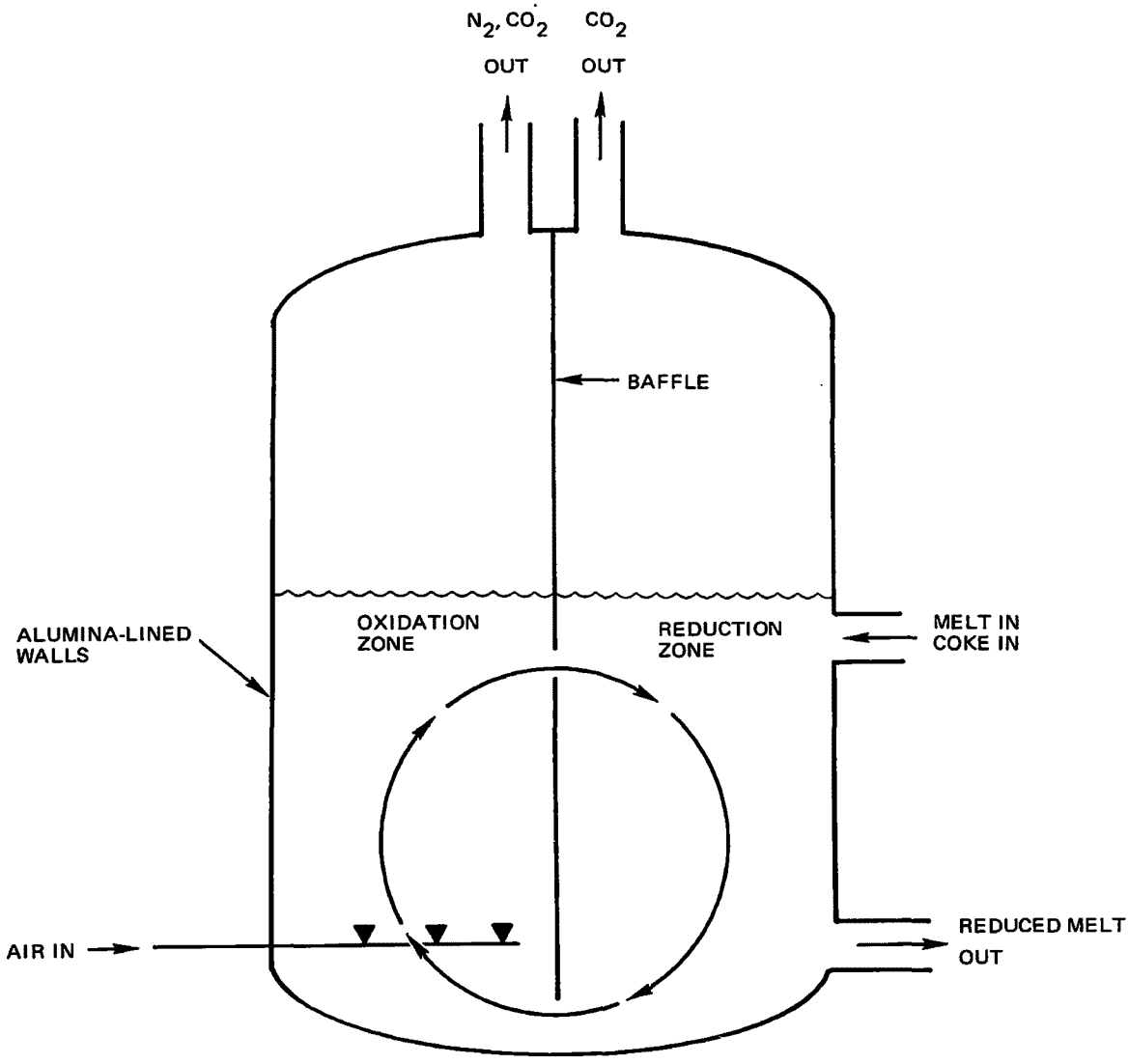

Figure 11. Two-Zone Reducer Vessel Concept

1. The heat loss from the melt bed must be minimized in order to minimize the coke and air requirements of the reducer and its physical dimensions.

2. The coke utilization in the reducer must be maximized in order to minimize the melt recovery and make-up requirement resulting from the melt losses associated with filtration of the unreacted coke.

3. The use of a frozen melt skull (cold wall) reducer vessel does not appear as economical as the use of an alumina-lined, internally-insulated vessel, because of the inherently high heat losses associated with maintaining the frozen skull.

4. The concentration of sulfur compounds in the carbonate melt must be as high as feasible, subject to solubility limitations, to minimize melt flow rate and preheat requirements.

5. Increasing the rate of the reduction reaction will result in a more significant reducer design improvement than increasing the superficial air velocity in the oxidation zone.

6. The internal melt recirculation between the oxidation and reduction zones of the reducer can be controlled through proper sizing of the orifices in the baffle between the two zones.

7. For the case of the alumina-lined vessel, accurate knowledge of the melt wall interfacial heat transfer coefficient is not essential for design of the pilot plant reducer.

Typical dimensions were determined for a vertically oriented two-zone alumina-lined, internally-insulated reducer as a function of processing capacity and heat loss. The controlling contraints in the design were found to be the maximum allowable superficial air velocity in the oxidation zone and the reaction rate (hence the required residence time of the melt) in the reduction zone.

Table IV gives the dimensions, and coke and air requirements for a 5 Mw pilot plant reducer and a 267 Mw reducer (one of the units proposed for an 800 Mw power plant). The calculations assumed a residence time of 15 min in the reduction zone, a superficial gas velocity of 3 ft/sec in the oxidation zone, 30 % mole fraction of sulfur compounds in the melt, and negligible heat losses.

TABLE IV

MOLTEN CARBONATE REDUCER CHARACTERISTICS

Plant Size (Mw)	Reducer ID (ft)	Expanded Bed Height (ft)	Coke Requirements (lb/hr)	Air Requirements (SCFM)
5	3.7	3	130	120
267	19.6	8	7000	6500

E. REGENERATOR ENGINEERING ANALYSIS

In the regeneration step, the carbonate-sulfide melt from the reducer is reacted with a carbon dioxide-steam mixture, which converts the sulfide into carbonate plus gaseous hydrogen sulfide. An analytical study of the regeneration step was conducted to determine the hydrogen sulfide concentrations achievable in the product gas and to establish the operating conditions required to achieve these concentrations. Specific emphasis was given to the constraints imposed by the thermodynamic equilibrium and heat generation of the reaction, by sulfide solubility considerations and by the composition of the available regeneration feed gas. The results of this study are presented in Appendix B. The conclusions are summarized below:

1. The operating parameters of the regenerator must be optimized to satisfy the following constraints:
   a. A thermodynamic equilibrium strongly favored by low temperatures
   b. A highly exothermic heat of reaction
   c. A solubility of sulfide in the carbonate melt which increases significantly with increasing temperature.

2. The regeneration equilibrium is strongly favored by a high steam concentration in the feed gas, and to a lesser extent by increased total pressure and carbon dioxide concentration.

3. The maximum hydrogen sulfide concentration attainable in the regeneration off-gas is practically independent of the sulfide concentration in the feed melt stream from the reducer.

4. As a result of potential solubility limitations, the operating temperature of the regenerator may be determined by the sulfide concentration in the melt feed stream from the reducer.

5. Approximately nine theoretical plates are required to regenerate 95% of the combined sulfide (15 mol %) at the temperature range of 950 to 1000°F with a feed gas containing 20 mol % carbon dioxide and 40 mol % steam. The corresponding hydrogen sulfide concentration is approximately 14 mol %.

6. The required number of theoretical plates, and the maximum attainable hydrogen sulfide concentration in the off-gas, are controlled by a pinch point between the operating line and the equilibrium line at the maximum allowable operating temperature of the regeneration step. Intercooling reduces the pinch point limitation and allows the reaction to proceed. A single cooling stage, cooling the melt taken off a plate slightly above the middle of the regenerator from 1000° down to 900°F, appears to be adequate.

F. HEAT AND MASS BALANCES

Based upon a revised flow diagram, preliminary heat and mass balances were derived for the Molten Carbonate Process installed on an 800 Mw power plant. The results are given in Figures 12 and 13. (The data for a 10 Mw installation can be obtained by scaling down the data for the 800 Mw installation.)

The following bases were used in these calculations.*

*This heat and mass balance work was done prior to the detailed reducer analysis of Appendix A. Although the two studies are essentially in agreement, there are some minor inconsistencies.

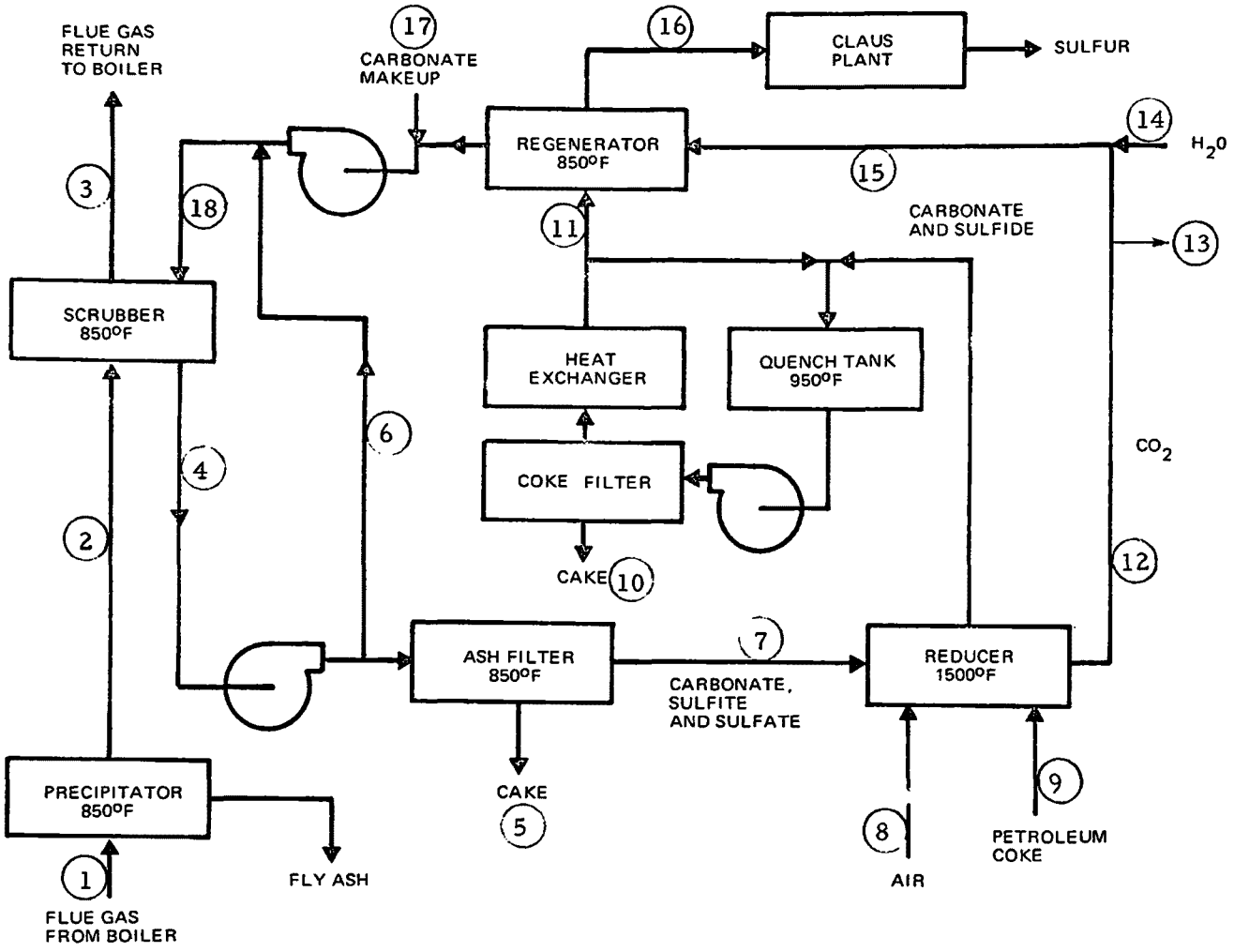

71-F4-7-16A

Component	1	2	3	8	12	13	14	15	16
N_2	177,000		177,000	2592	2592	1709		883	883
CO_2	32,800		33,300		1582	1042		540	27
H_2O	19,700		19,700	69	69	46	517	540	27
O_2	7,900		7,800	688					
SO_2	450		22.5		2	1.3		0.7	
SO_3	50		2.5						
H_2S	0		0						512
Ash, lb	45,000	225	0						

Component	5	9	10	17
Ash, lb	225	149	149	
Carbon, lb		19,100	566	
Sulfur, lb		1,280		
Melt, lb	450		715	1200

Component	4	6	7	11	18
M_2CO_3	4525	3394	1132	1094	5000
M_2SO_3	1316	888	296		888
M_2SO_4		660	220	22	682
M_2S		25	8	540	52

Figure 12. Molten Carbonate Process Mass Balances
Hourly Basis, 800-Mwe Plant
Units: lb-moles Unless Noted

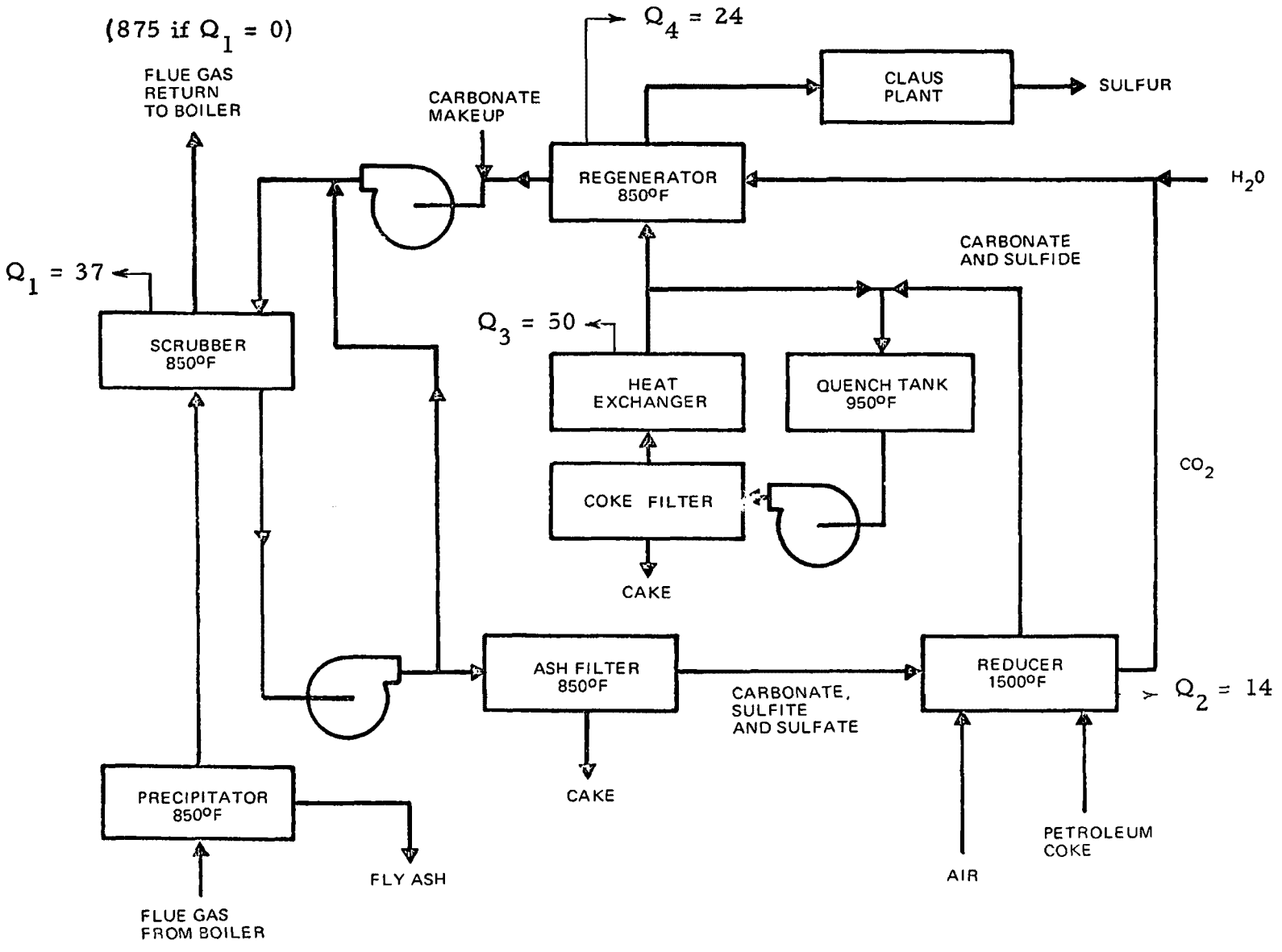

71-F4-7-16A

Figure 13. Molten Carbonate Process Heat Balances
800-Mwe Plant
Units: 10^6 Btu/hour

1. Mass Balance

The mass balance was based on a sulfur input into the absorber of 500 lb moles/hr for the 800 MW plant, exclusive of the sulfur introduced by the fluid coke (6.25 lb moles/hr for the 10 MW plant). This would be the case for a power plant operating under the following assumed conditions:

1) Coal characteristics

Analysis:

C	= 70.0%
H	= 4.8%
O	= 5.8%
S	= 3.0%
N	= 1.4%
Ash	= 10.0%
Moisture	= 5.0%
	100.0%

Heating value: 12,800 Btu/lb

2) Plant heat rate = 9000 Btu/kwh (~38% plant efficiency)

3) Fraction of coal sulfur appearing as SO_x in flue gas = 95%

4) Combustion carried out with 20% excess air (containing 0.013 lb H_2O/lb dry air, which corresponds to 60% relative humidity at 80°F). This assumption, together with the previous ones, yields a flue gas containing 0.21% SO_x. For the calculation it was assumed that 10% of the SO_x was SO_3 and the remainder SO_2. The 10% SO_3 value is high, since most reported values are less than 5%. It was, however, selected as a conservative upper bound value intended also to take into account the possible oxidation of a small fraction of the recycled sulfite in the scrubber.

5) Fly ash content of flue gas = 80% of ash originally in the coal. It was assumed that 99.5% of this fly ash carried by the flue gas is removed in a high temperature electrostatic precipitator prior to entering the absorber.

6) Fluid Coke Composition

C	= 90%
S	= 6%
Ash	= 0.7%

7) Stoichiometry

a. $\frac{\text{Scrubber inlet } M_2CO_3}{\text{Scrubber inlet } SO_x} = 10 \text{ (mole ratio)}$

Even with this rather high ratio, the resulting liquid-to-gas ratio in the absorber is only 0.0278 on a mole basis and 0.102 on a weight basis.

b. $\frac{\text{Carbon feed (in fluid coke)}}{\text{Carbon required for } M_2SO_4 \text{ reduction}} = 1.8$

This ratio was determined on the basis of the heat balance around the reducer, taking into account the heat of combustion needed to provide for the requirements of the endothermic reduction reaction, and the preheat of the melt, the coke and the air to 1500°F. It allows for only relatively small heat losses from the reducer.

8) Extent of Completion of Reactions

95% completion was assumed for the absorption, reduction, regeneration, and sulfur-from-coke recovery reactions.

It was also assumed that any M_2S recycled to the absorber would be completely oxidized to M_2SO_4. Recycled M_2SO_3 was assumed to go through the absorber without oxidation (assumption 4 was intended to take into account any small amounts of M_2SO_3 which might be oxidized).

10% disproportionation of the M_2SO_3 was assumed to take place downstream of the absorber prior to introduction into the reducer.

9) Minimum carbonate concentration in melt = 66 mole % which occurs just downstream of the reducer.

10) Filter losses and make-up

The weight of melt removed from the system in the fly ash filter downstream of the absorber amounts to twice the weight of the fly ash removed by the filter.

The weight of melt removed from the system in the coke filter downstream of the reducer is equal to the weight of unburnt carbon plus ash. The amount of unburnt carbon from the reducer was assumed to be that left over

from the stoichiometric combustion with the air supplied to the reducer and the 95% efficient reduction of the M_2SO_4 and the sulfur from the coke (this amounted to about 3% unburnt carbon).

The overall material balance made no attempt to correct the system flow rates shown for filter losses, except for indicating an equivalent salt make-up stream upstream of the absorber.

2. Heat Balance

a. Heats of Reaction

The heat of reaction data were obtained from available heats of formation. While they are subject to appreciable uncertainties, they form an internally consistent set of values. All the heats were taken at 850°F, except for that of the M_2SO_4 reduction which was taken at 1500°F.

The reaction considered for each component, and the heat of reaction values used are presented in the following paragraphs. The percentage contribution of each reaction to the total heat release of the component is also shown.

(1) Absorber

$$SO_2(g) + M_2CO_3(\ell) \longrightarrow M_2SO_3(\ell) + CO_2(g)$$

-12.8 Kcal/gm mole = -22,900 Btu/lb mole 26.8%

$$SO_3(g) + M_2CO_3(\ell) \longrightarrow M_2SO_4(\ell) + CO_2(g)$$

-59.7 Kcal/gm mole = -107,400 Btu/lb mole 13.9%

$$M_2S(\ell) + 2O_2(g) \longrightarrow M_2SO_4(\ell)$$

-233.8 Kcal/gm mole = -420,000 Btu/lb mole 59.3%

(2) Initial Disproportionation Downstream of Absorber

$$M_2SO_3(\ell) \longrightarrow \frac{1}{4} M_2S(\ell) + \frac{3}{4} M_2SO_4(\ell)$$

-11.9 Kcal/gm mole = -21,400 Btu/lb mole

(3) Reducer

$$M_2SO_3(\ell) \longrightarrow \frac{1}{4} M_2S(\ell) + \frac{3}{4} M_2SO_4(\ell)$$

11.9 Kcal/gm mole = -21,400 Btu/lb mole 7.1%

$$M_2SO_4(\ell) + 2C(s) \longrightarrow M_2S(\ell) + 2CO_2(g)$$

+41.9 Kcal/gm mole = +75,500 Btu/lb mole -35.5%

$$S(s) + O_2(g) + M_2CO_3(\ell) + \frac{3}{2} C(s) \longrightarrow M_2S(\ell) + \frac{5}{2} CO_2(g)$$

-64.5 Kcal/gm mole = -116,100 Btu/lb mole 4.9%

$$S(s) + O_2(g) \longrightarrow SO_2(g)$$

-74.1 Kcal/gm mole = -133,400 Btu/lb mole 0.3%

$$C(s) + O_2(g) \longrightarrow CO_2(g)$$

-94.2 Kcal/gm mole = -169,500 Btu/lb mole 123.2%

(4) Regenerator

$$M_2S(\ell) + CO_2(g) + H_2O(g) \longrightarrow H_2S(g) + M_2CO_2(\ell)$$

-25.8 Kcal/gm mole = -46,400 Btu/lb mole

b. Sensible Heat Requirements of Reducer

The sensible heat requirements of the reducer were assumed to be those necessary to preheat the melt from 850 to 1500°F, the coke from 600 to 1500°F and the air from 600 to 1500°F (it was assumed that both coke and air would be preheated to 600°F outside of the reducer).

The sensible heat requirements were

Melt	43.4 x 650 =	28,200 Btu/lb mole	52.4%
Coke	4.8 x 900 =	4,320 Btu/lb mole (C+S)	7.9%
Air	7.0 x 900 =	6,300 Btu/lb mole	23.7%
			84.0%

These percentages represent fractions of the net heat generation by chemical reaction in the reducer. They show that with a carbon stoichiometry ratio of 1.8 approximately 16% of the total net heat release is left over for heat losses.

G. COOPERATION WITH PROCESS EVALUATOR

1. Introduction

During the report period, the Molten Carbonate Process was evaluated by Singmaster and Breyer, under NAPCA Contract No. CPA 70-76. The purpose of this evaluation was to review and evaluate the Molten Carbonate Process for removal of SO_2 from coal-burning power plant stack gases and from copper smelter gaseous effluents, and then to advise NAPCA on the continued course of action regarding the process. During the report period, Atomics International worked closely with Singmaster and Breyer, supplying assistance and data where requested. Information transmitted included process flow diagrams, material and energy balances, equipment configurations and selection, fly ash and chloride filtration data, and process economics.

2. Conclusions and Recommendations

Singmaster and Breyer concluded that the Molten Carbonate Process is technically feasible, and that it should be tested in a pilot plant program. Their report includes the following statement:

> "The process appears to be feasible; however certain problem areas have been uncovered which should be defined in a thoughtful pilot program where corrective measures can be tested. A complete technical and economic evaluation of the process can only be performed after the pilot program is completed.
>
> "It is therefore recommended that development and evaluation of the process be continued. We believe that a pilot plant is the next logical step in this development. Operation of a materials test loop can either precede the pilot plant or be carried out as a study parallel to the pilot plant program, depending on time and funds available to the program."

Singmaster and Breyer made a very thorough evaluation of the process, pointing out many potential problem areas and making valuable suggestions about their investigation. Nearly all of these investigations will require the pilot plant for their implementation. However, Singmaster and Breyer also made several recommendations which can be carried out separately

starting before the pilot plant program. As quoted above, the materials test loop should be built and operated. Also, Singmaster & Breyer recommended that additional work be done on the two-zone reducer concept, to insure its operability, study its mechanical and hydraulic design, and determine the best way to introduce coke into the reactor. Much of this work can be done in a laboratory program, which can be completed in time to supply design data for the pilot plant reducer. A third recommendation was that more filtration work be done, directed toward increasing the filter cake thickness without excessive pressure drop. This work also lends itself to a laboratory study, utilizing the filtration test equipment available from the previous filtration studies.

3. Process Economics

In their study, Singmaster & Breyer made estimates of the capital requirements and operating costs for the Molten Carbonate Process treating flue gases from power plants and copper smelters. The base case selected was the removal of 95% of the sulfur oxides from the flue gas emitted by an 800 Mw power plant burning coal containing 3% sulfur, 0.04% chloride, and 10% ash, and operating with a 70% plant factor. For this case, they estimated the capital requirement to be $13,448,000 ($16.81/kw) and the total annual operating cost (including 14% capital charges) to be $4,703,000 (0.95 mills/kwh). These costs did not include the cost of the Claus sulfur plant, nor did they include any credit for the by-product sulfur or for reduced costs of high-sulfur fuel.

It is difficult to compare the above estimates with those for other flue gas desulfurization processes, because most other processes have not had the benefit of a thorough, independent evaluation. However, the costs are believed to be lower than those for any other process which recovers elemental sulfur. Also, the operating costs are competitive with the cost penalties for low-sulfur or desulfurized fuels.

III. FUTURE WORK

The process development work done to date has been successful, in that it has defined a feasible process and developed each step of the process through the laboratory bench-scale phase. The process as developed also appears economically attractive, as was shown by the independent Singmaster & Breyer evaluation. Thus continued development of the process is warranted.

The goal of the process development program must be to make available an efficient, relatively inexpensive stack gas treatment system. For this system to be accepted by the utility industry, it will have to be demonstrated on a full-scale basis, with a unit capable of treating all the flue gas from a large (800 Mw or more) power plant. To achieve this amount of scale-up will require two steps: first a pilot plant, of about 10 Mw capacity, followed by a demonstration unit of about 200 Mw capacity. The 200-Mw demonstration unit, when successfully developed, can then be used as a module in constructing large units.

The key item in the development effort now is the pilot plant. The pilot plant is needed to test the operability of the process cycle under realistic conditions, to develop and test engineering solutions to process problems as they arise, and to obtain the scale-up and cost data needed to develop the demonstration unit. The need for large amounts of real flue gas for accurate and reliable scrubber and mist recovery tests makes it necessary to build the pilot plant to treat a side stream of flue gas from an operating power plant. The use of power plant flue gas is also required to study the effect of fuel-derived impurities (ash, chlorides, and anything else) on the process. A program to design, build, and operate a pilot plant at a power plant site should be initiated as soon as possible, and carried out to completion.

The pilot plant program should also be supported by a parallel technology development effort, to carry out those studies suggested by Singmaster & Breyer, which can be performed in the laboratory. This effort should include

(1) the construction and operation of the materials test loop, (2) studies to improve the filtration characteristics of fly ash and other impurities, and (3) analytical and experimental studies of the chemistry and hydraulics of the two-zone reducer.

A pilot plant program and parallel technology development program will be proposed to APCO in the near future.

APPENDIX A

PRELIMINARY PROCESS ANALYSIS OF TWO REGION MOLTEN CARBONATE REDUCER

CONTENTS

CONTENTS (Continued)

TABLES

FIGURES

FIGURES (Continued)

NOMENCLATURE

A	Constant used in heat balance. Defined in Figure 3
A_{cs}	Cross-sectional area of reducer, ft^2
A_{ht}	Heat transfer area of reducer walls in contact with melt bed (including side walls and bottom of reducer vessel), plus "effective" free surface of melt, ft^2
A_o	Normalized cross-sectional area of oxidation region of reducer, ft^2 per lb mole/hr SO_x
A_{or}	Cross-sectional area of orifice in baffle between oxidation and reduction regions of reducer, ft^2
A_r	Normalized cross-sectional area of reduction region of reducer, ft^2 per lb mole/hr SO_x
$A_{r_{Gas\ Velocity}}$	Normalized cross-sectional area of reduction region of reducer based on superficial gas velocity limitation, ft^2 per lb mole/hr SO_x
A_t	Normalized cross-sectional area of reducer, ft^2 per lb mole/hr SO_x
a	Mole fraction of sulfur compounds in form of sulfite in melt leaving scrubber. Assumed equal to 0.67 for most of the numerical calculations of this study
$1-a$	Mole fraction of sulfur compounds in form of sulfate in melt leaving scrubber. Assumed equal to 0.33 for most of the numerical calculations of this study. Also written $\left[SO_4^{=}\right]$ and $\frac{\left[SO_4^{=}\right]}{\left[SO_3^{=}\right] + \left[SO_4^{=}\right]}$ or $\frac{\left[M_2SO_4\right]}{\left[M_2SO_3\right] + \left[M_2SO_4\right]}$ at various places in the report.
a^*	$= \frac{1}{1 + \frac{1-e}{4e}\ a}$
B	Constant used in heat balance. Defined in Figure 3.
b	$= \frac{A_o d}{V_r}$ for vertical cylinder reducer geometry
	$= \frac{A_o D}{4V_r}$ for horizontal cylinder reducer geometry
C	Normalized carbon feed rate into reducer, lb mole/hr per lb mole/hr SO_x

C_o — Normalized carbon utilization rate (carbon reacted) in reducer = $(1-\lambda)$ C, lb mole/hr per lb mole/hr SO_x

c — Orifice discharge coefficient. Assumed equal to 0.61

c_p — Specific heat, Btu/lb mole °F

c_{p_A} — Enthalpy increase of reducer air feed from 600 to 1500 °F = 33,900 Btu/lb mole of contained oxygen

c_{p_C} — Enthalpy increase of reducer coke feed from 60 to 1500 °F = 6,500 Btu/lb mole of contained carbon

c_{p_M} — Enthalpy increase of reducer melt feed from 850 to 1500 °F = 28,300 Btu/lb mole of melt

D — Internal diameter of reducer, ft

d — Depth of expanded reducer melt bed, ft

E — Constant used in heat balance. Defined in Figure 3.

e — Reaction completion efficiency. Assumed to be 0.95.

F_1 — $= 1 + \frac{0.4685}{[S]} + 1.5867 \left(\frac{Q_L}{10^5}\right)$

F_2 — $= 1 + \frac{0.4685}{[S]} + 1.0064 \left(\frac{Q_L}{10^5}\right)$

F_3 — $= 1 + \frac{0.4685 + 0.5484 \times 10^{-3} \Delta T}{[S]} + 1.0064 \left(\frac{Q_L}{10^5}\right)$

$= 1 + \frac{0.6330}{[S]} + 1.0064 \left(\frac{Q_L}{10^5}\right)$ when $\Delta T = 300$ °F

f — Fraction of scrubber outlet melt stream fed into reduction-regeneration system. 1 - f = fraction recycled directly back to scrubber

g — Mole fraction SO_3 in SO_x in feed gas to scrubber

$\left(g = \frac{[SO_3]}{[SO_2] + [SO_3]} \right)$ Also used in Section VIII for the conversion factor 32.2 ft/sec^2

h — Melt film heat transfer coefficient at surface of reducer vessel walls, Btu/ft^2 hr °F

j	Distance from axis or midplane of reducer vessel to separation baffle, ft
K	Constant used in heat balance. Defined in Figure 3
k	Thermal conductivity, Btu/ft hr °F
$k_{alumina}$	Thermal conductivity of alumina liner, Btu/ft hr °F
k_{melt}	Thermal conductivity of melt, Btu/ft hr °F
k_{skull}	Thermal conductivity of frozen melt skull, Btu/ft hr °F
L	Length of reducer (horizontal cylinder geometry), ft
L_o	Length of oxidation region of reducer (horizontal cylinder geometry), ft
L_r	Length of reduction region of reducer (horizontal cylinder geometry), ft
M	Symbol used to represent the alkali metals (Li, Na, K) in the chemical formulae of the salts contained in the melt
m	Sulfur to carbon atom ratio in coke. Assumed to be 0.025
N	Processing capacity of molten carbonate system, lb moles/hr SO_x entering the scrubber in the flue or other waste gases being treated
n	Hydrogen to carbon atom ratio in coke. Assumed to be 0.24. For purposes of the heat balance, however, n is considered equal to 0 if it is assumed that the hydrogen in the coke does not contribute to the reduction reactions.
O_2	Normalized oxygen feed rate into reducer, lb moles/hr per lb mole/hr SO_x
p	Fraction of sulfite in melt leaving scrubber which disproportionates to sulfide and sulfate prior to entering the reducer. Assumed to be 0.10
Q_L	Normalized heat loss from reducer melt bed, Btu/hr per lb mole/hr SO_x
Q_{L_o}	Normalized heat loss from oxidation region of reducer melt bed, Btu/hr per lb mole/hr SO_x
Q_T	Normalized heat transport from oxidation into reduction region of reducer, Btu/hr per lb mole/hr SO_x
(Q/A)	Heat flux at reducer walls in contact with melt, Btu/ft^2 hr

q	Proportionality factor = total ΔP/orifice ΔP, for melt recirculation. Assumed equal to 1.20.
r	Frozen melt skull temperature parameter = $\frac{T_{MP} - T_{heat\ sink}}{T_{melt} - T_{MP}}$
$[S]$	Mole fraction of sulfur compounds in melt leaving scrubber. Mole fractions of 0.15 and 0.30 were considered in this study.
SCFM	Standard cubic feet per minute taken at 60 °F.
T	Temperature, °F
T_{melt}	Temperature of melt, °F
T_{MP}	Melting point (freezing point) temperature of melt, °F. Assumed to be 750 °F.
$T_{heat\ sink}$	Temperature of heat sink (water, air) into which the heat loss from the reducer is discharged, °F
$T_{outer\ alumina}$	Temperature at outer (cold) surface of alumina liner, °F
T_{skull}	Temperature at outer (cold) surface of frozen melt skull, °F
t	Liner or skull thickness, ft
$t_{alumina}$	Thickness of alumina liner, ft
t_{skull}	Thickness of frozen melt skull, ft
U	Overall heat transfer coefficient from outer surface of frozen skull or alumina liner to heat sink, Btu/ft^2 hr °F
ι	Coke sulfur which is not recovered in reducer melt = $mC_o(1-e)$, lb moles per lb mole SO_x (= $C_o/800$ for the above listed values of m and e)
V	Volumetric recirculation rate of melt between the oxidation and reduction regions of the reducer, ft^3/hr
V_r	Normalized volume of melt bed in reduction region of reducer, ft^3 per lb mole/hr SO_x
v	Superficial air velocity in oxidation region of reducer, ft/sec. Values of 3 and 5 ft/sec were considered in this study
α	= arc cos $(1 - \frac{2d}{D})$
β	Coefficient of volumetric expansion, $(°F)^{-1}$

γ	$= \arcsin 2\delta = \arcsin \frac{2j}{D}$
δ	Separation baffle location parameter = j/D or j/L, as may be appropriate
ΔH	Enthalpy of reaction, Btu/lb mole. Subscripts and values for the various reactions defined in Section III-4
ΔP	Melt recirculation pressure drop, lb/ft^2
ΔT	Temperature differential between top and bottom of melt bed, °F. Assumed to be 300 °F
Δt	Temperature difference between bulk melt and reducer wall surface in contact with the melt, °F
ϵ	Ratio of radiation heat flux at free surface of melt to convection heat flux at reducer vessel walls in contact with the melt
θ	Melt residence time in reduction region of reducer, minutes. Values of 15 and 30 minutes were considered in this study
λ	Fraction unreacted coke (or carbon). Assumed to be 0.05
μ	Viscosity, lb/hr ft
ρ	Density, lb/ft^3
ρ_o	Effective average density of expanded melt bed in oxidation region of reducer, lb/ft^3
ρ_r	Effective average density of expanded melt bed in reduction region of reducer, lb/ft^3
ρ_{T_o}	Density of unexpanded melt at average temperature of oxidation region of reducer, lb/ft^3
ρ_{T_r}	Density of unexpanded melt at average temperature of reduction region of reducer, lb/ft^3

SUMMARY

Regeneration of the process melt in the Molten Carbonate Process for the removal of sulfur oxides from stack gases requires the reduction of the oxidized sulfur conpounds absorbed in the carbonate melt. This reduction is carried out at temperatures of around 1500°F using carbon in the form of coke as both the reducing agent and the fuel to supply the heat required by the reduction process.

As presently conceived, the design of the reducer is based on a separation of the reduction and heat generation (oxidation) functions. The reducer is divided into an oxidation region and a reduction region separated by a vertical baffle with internal melt recirculation between the two regions. The design of such a reducer requires a knowledge of reaction thermodynamics and kinetics, and multiphase system hydraulics and heat transfer. Most of this information must be obtained from laboratory and pilot plant tests. The purpose of this study was to develop the analytical techniques required for the process design of such a reducer and to provide preliminary data on the raw material requirements and physical dimensions of the reducer on the basis of presently available technical information.

Analytical techniques were developed for the process design of a two region molten carbonate reducer utilizing either a vertical or a horizontal cylinder vessel geometry. Most of the process analysis itself was conducted on the vertical cylinder geometry.

It was concluded that:

1) The heat loss from the melt bed must be minimized in order to minimize the coke and air requirements of the reducer and its physical dimensions.

2) The steady state sulfur compound concentration in the carbonate melt must be as high as feasible subject to solubility limitations, thus minimizing melt flow rate and melt preheat requirements.

3) The sulfate to sulfite ratio of the sulfur compounds in the melt leaving the scrubber must be minimized in order to minimze the coke consumption of the reducer.

4) The coke utilization in the reducer must be maximized in order to minimize the melt recovery and make-up requirement resulting from the melt loss associated with the filtration of the unreacted coke.

The controlling constraints in the design of the reducer are the maximum allowable superficial air velocity in the oxidation region and the minimum required residence time of the melt in the reduction region. A decrease in reduction region residence time from 30 to 15 minutes results in a more significant reducer design improvement than an increase in superficial air velocity from 3 to 5 ft/sec.

Typical reducer dimensions were determined as a function of processing capacity and heat loss. Coke and air requirements were estimated as a function of heat loss. For a sulfur compound mole fraction in the melt of 0.30, one-third of which is sulfate, the coke and air requirements of a reducer with a negligible heat loss amount to approximately 1.30 lb and 73 scf, respectively, per lb of sulfur fed into the scrubber.

The heat loss from the melt bed in the reducer can be minimized through use of an alumina-lined internally insulated (hot wall) reducer design. If it is air-cooled, the outside wall of the reducer vessel in this design cannot be insulated and operates at a temperature of around 500°F. Water cooling surrounded by insulation would allow operation of the outside of the reducer at a lower temperature.

Because of its inherently high heat loss a frozen melt skull (cold wall) reducer design does not appear attractive when a low melting point carbonate mixture such as the lithium-sodium-potassium carbonate eutectic is used as the carrier melt.

Internal melt recirculation between the oxidation and reduction regions of the reducer can be controlled through sizing of the orifices in the baffle between the two regions. These orifices must be small enough to assure satisfaction of the minimum residence time requirement in the reduction region and large enough to allow sufficient flow to transport the required heat without exceeding melt bed temperature rise limitations.

The results obtained are based on the technical information presently available and on various assumptions and approximations which had to be made in lieu of experimental data. They are therefore preliminary and must be confirmed through a development program. They are, however, believed to provide a sound basis for the conceptual design of a molten carbonate reducer and the planning of the required experimental program.

I. INTRODUCTION

A key component of the Atomics International Molten Carbonate Process for the removal of sulfur oxides from flue and other waste gases is the reducer which provides for the reduction of the oxidized sulfur compounds absorbed in the carbonate melt. The sulfites and sulfates are reduced to sulfides which can then be regenerated into carbonates with release of hydrogen sulfide for the recovery of sulfur. The reduction is carried out at a temperature of about 1500 °F using carbon in the form of petroleum coke as the reducing agent and providing the heat required for this reduction through the indirect oxidation of excess coke with air.

The molten carbonate reducer technology is somewhat related to the Kraft[9] furnace technology in the paper industry. It is nevertheless sufficiently different and novel to require the development of a strong analytical and experimental technology base. It is the purpose of this study to provide a preliminary process analysis of the molten carbonate reducer concept on the basis of the technical information presently available and thus lay a foundation for both the conceptual design of such a reducer and the experimental program required to establish its technology.

II. REDUCER DESIGN CONCEPT DESCRIPTION

The Molten Carbonate Process provides for recovery of the sulfur from the waste gases treated in the form of hydrogen sulfide which can be used for conversion either to elemental sulfur or to sulfuric acid. The sulfur oxides, however, are absorbed in the carbonate melt in the form of alkali metal sulfites and sulfates which require reduction to sulfides prior to recovery of hydrogen sulfide and regeneration of the carbonate melt. It is the function of the reducer to provide the environment required to perform this reduction. It is to be noted that such a reducer may be applicable not only to the molten carbonate process, but to other sulfur oxide recovery processes based on the use of carbonates as the reactive species of the scrubbing medium.

The sulfites disproportionate rapidly into sulfides and sulfates at the operating temperature of the reducer:

$$M_2SO_3 \rightarrow 1/4\ M_2S + 3/4\ M_2SO_4$$

The function of the reducer, therefore, is to provide for the reduction of the alkali metal sulfates in the melt to alkali metal sulfides. The present concept is based on the use of carbon as the reducing agent. This carbon is provided in the form of a petroleum coke, such as fluid coke, though other carbonaceous materials can be used if so desired.

The overall reduction reaction can be written as follows:

$$M_2SO_4 + 2\ C \rightarrow M_2S + 2\ CO_2$$

The kinetics of this reaction are such that temperatures of about 1500 °F are required to allow it to proceed at a practically acceptable rate. Moreover the reaction is endothermic, absorbing approximately 75,000 Btu per lb mole of sulfate reduced.

The reducer must provide the high temperature, the heat of reaction, and the residence time required to carry out the reduction. Provision of excess coke and partial combustion of this coke with air are used to preheat the reactants to the reaction temperature and generate the heat needed for the reaction, and to compensate for whatever heat losses may take place. The reducer thus becomes both a reduction and an oxidation unit.

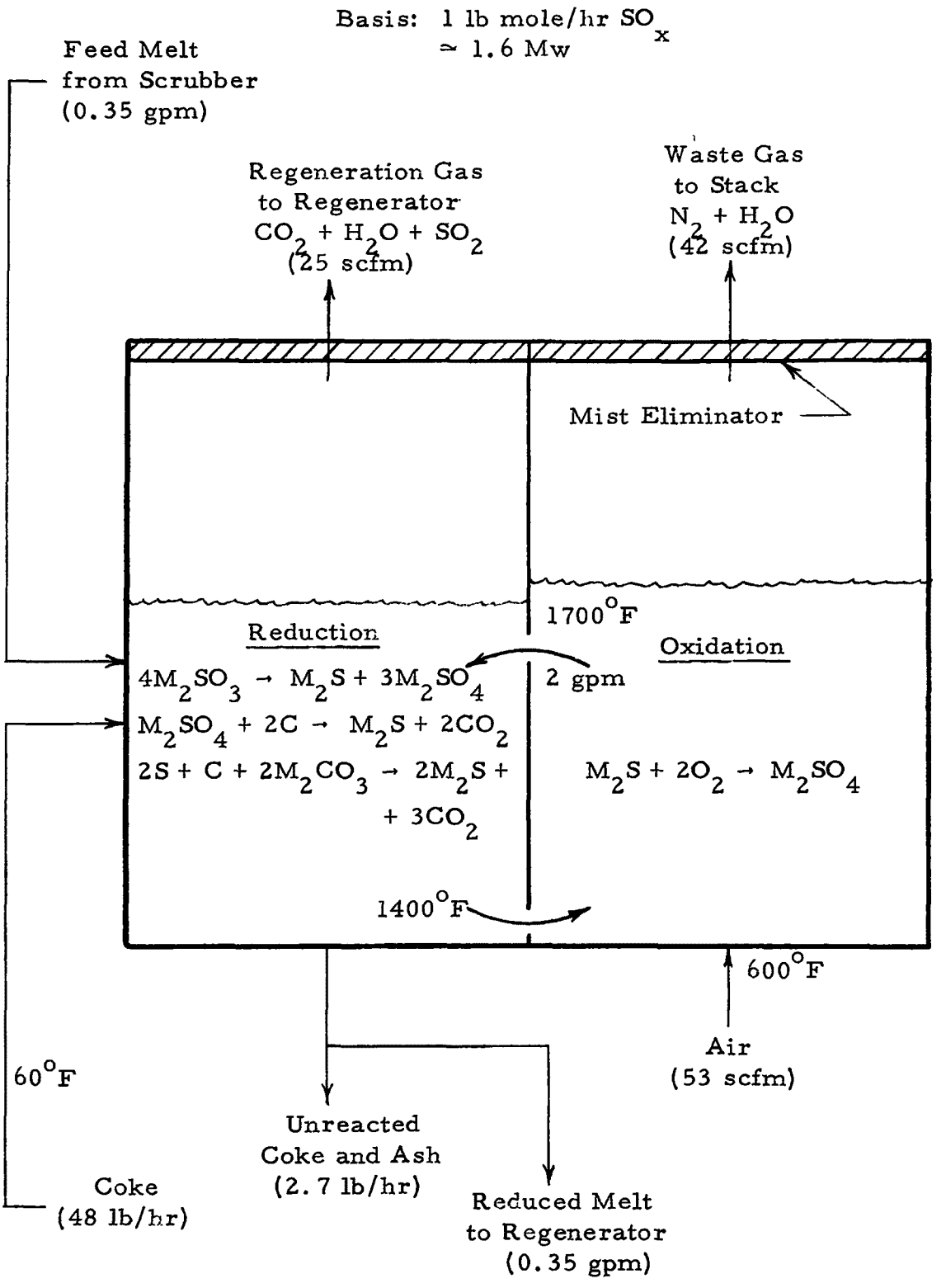

Figure 1. Schematic Diagram of Typical Molten Carbonate Reducer

The design of a reducer to allow performance of the reduction and the oxidation functions within a single region would be expected to minimize the overall size of the equipment required. Such a design, however, does not appear to be practical at this time on the basis of our present knowledge of the reactions involved, the reaction kinetics, and the required distribution and circulation of reactants within the reacting mass. A design concept was therefore selected which would provide for the separation of the reduction and oxidation functions, and thus prevent the occurrence of competitive reduction and oxidation reactions within a single highly turbulent region. Such a concept allows for a considerable simplification of the analysis of the process and a more reliable evaluation of the reducer design on the basis of presently existing experimental information. This concept, however, results in increased equipment size as compared with a hypothetical single region reducer.

Figure 1 shows a schematic diagram of a typical two-region molten carbonate reducer. The reducer consists of a reduction region and an oxidation region, with a vertical separation barrier between them. This barrier is provided with openings both just below the free surface of the melt and near the bottom of the reducer vessel to allow natural convection circulation between the two regions. The heat required for the endothermic reduction reaction and for preheating the molten salt melt and the coke and compensating for heat losses is generated in the oxidation region and carried into the reduction region by natural convection circulation of the hot melt.

Both the feed melt from the scrubber and the coke are schematically shown as being introduced into the top of the reduction region. Some of the melt may also be introduced at the top of the oxidation region and the coke may actually be brought in with the feed air stream into the oxidation region. Actual locations of the feed stream inlets and methods of distributing the inlet flows will have to be established from information to be obtained from the operation of an experimental test reducer. The melt and coke come into contact with the oxidized recirculating "high" temperature melt, are heated to reaction temperature, and react to form a reduced melt, leaving a small amount of unreacted coke and ash. The temperature of the melt decreases as the reaction proceeds. A product stream of reduced melt and unreacted coke and ash is withdrawn from the bottom of the reduction region. The remainder of the reduced stream is recirculated to the oxidation region.

In the oxidation region preheated air comes into contact with the recirculated "low" temperature reduced melt stream. Part of the sulfide in this stream is oxidized to sulfate, generating heat and raising the melt to the "high" temperature again. The required heat is then transferred to the reduction region by the recirculated "hot" melt.

The reduction and oxidation functions are thus carried out completely separately and the combustion of the excess coke is carried out through the intermediate oxidation and reduction of recirculated excess sulfide-sulfate.

This separation of functions allows the separation of the off-gases from the reducer, thus producing a high concentration carbon dioxide stream for use in the regeneration reaction with only a minimum dilution by nitrogen. Some carryover of CO_2 from the reduction to the oxidation region may, however, occur through release of CO_2 from the molten carbonates in the oxidation region and recombination of CO_2 with the oxides thus formed in the reduction region.

The flow rates shown in Figure 1 are normalized to the treatment of gases carrying 1 lb mole of SO_x per hour (approximately equivalent to 1.6 Mw electric power generation in a power plant buring 3 wt % sulfur coal). They are typical but obviously vary with variations in the operating parameters of the process, as shown in the study described in this report.

A key problem of the molten carbonate reducer concept is the selection of structural or liner materials which come in contact with the melt at the operating temperatures of the reducer. On the basis of presently available materials compatibility data, two design concepts were selected for analysis and evaluation. One of these is the so-called frozen skull concept, similar to the designs used in the Kraft furnaces in the paper industry.[9] This concept relies on a film of frozen melt at the inner surface of a steel vessel to provide the necessary protection of the steel from corrosion by the melt. The frozen skull is formed by cooling the walls of the vessel. The temperature at its surface in contact with the melt is the freezing temperature of the melt (approximately 750 °F) and its thickness is determined by the amount of heat which must be removed in order to maintain this temperature.

The second design concept makes use of a ceramic liner on the inside of a steel vessel. The ceramic presently under consideration is alumina. The alumina is compatible with the high temperature melt and provides both for physical protection and thermal insulation of the steel. Since the alumina is compatible with the melt, its surface temperature in contact with the melt can be maintained relatively close to that of the melt (1300-1450 °F) to minimize heat losses.

The two reducer design concepts selected can therefore be characterized as follows:

1. Frozen Melt Skull: A cold wall concept with relatively high heat loss.
2. Alumina-Liner: A hot wall concept with relatively low heat loss.

The present study has been directed toward the analysis and evaluation of a two region molten carbonate reducer using either a frozen melt skull (cold wall) or an alumina liner (hot wall) for corrosion protection of the steel shell of the reducer vessel.

III. BASIS OF STUDY

1. Composition and Physical Properties of Melt

Molten carbonate make-up: Eutectic mixture of lithium, sodium, and potassium carbonates of the following composition[1]:

Li_2CO_3	43.5 mole %	(32 wt %)
Na_2CO_3	31.5 mole %	(33 wt %)
K_2CO_3	25.0 mole %	(35 wt %)

Sulfur compound concentration in melt feed to reducer: Two cases were considered:

$$[S] = 0.15 \text{ and } 0.30 \text{ (mole fraction)}$$

Extent of oxidation of sulfur compounds in melt leaving the scrubber (prior to any disproportionation):

$$\frac{[M_2SO_4]}{[M_2SO_3] + [M_2SO_4]} = 1 - a = 0.33 \text{ (mole fraction)}$$

Extent of disproportionation of sulfite into sulfide and sulfate in melt upstream of reducer inlet:

$$\frac{4[M_2S]}{[M_2SO_3] + 4[M_2S]} = p = 0.10 \text{ (mole fraction)}$$

Physical properties of melt (assumed to be approximately equal to those of the alkali metal carbonate eutectic melt at the same temperature):

Density: $\rho = 147.60 - 18.87 \times 10^{-3}\ T$, lb/ft^3, with T in °R[1]

Specific volume of expanded bed $\tilde{=}$ 1.6 ft^3/lb mole of melt (equivalent to approximately 75% bed expansion due to coke addition and gas flow without attempt at differentiation between the melt in the oxidation region and that in the reduction region).

Viscosity: $\mu = 11.253 \times 10^{-3}\ e^{9965/T}$, lb/hr ft, with T in °R[1]

Specific heat: $c_p = 28.41 + 9.20 \times 10^{-3}$ T, Btu/lb mole °F, with T in °R[1]

Enthalpy increase of melt from 850 to 1500 °F: c_{p_M} = 23,800 Btu/lb mole (average specific heat = 43.5 Btu/lb mole °F)

Thermal conductivity: k = 0.5 Btu/ft hr °F, estimated (same value assumed for frozen melt skull)

Nominal freezing point temperature = 750 °F

2. Composition and Heat Capacity of Coke

Composition of typical high sulfur fluid coke:

C	90.0 wt %	
H	1.8 wt %	——→ n = 0.24 atoms H/atom C
S	6.0 wt %	——→ m = 0.025 atoms S/atom C
O + N	1.5 wt %	
Ash	0.7 wt %	

Present indications are that the hydrogen in the coke does not contribute to the reduction of the sulfate in the reducer. The overall heat balance of the reducer melt bed, therefore, did not take credit for any contribution from the heat of oxidation of the hydrogen, and was thus based on the use of a value of n = 0. In reality it is expected that some of the hydrogen will be oxidized within the melt, thus contributing to some extent to the heat balance of the bed.

The specific heat of the coke was assumed to be approximately equal to that of graphite, with values ranging from 0.142 Btu/lb °F at 0 °F to 0.435 Btu/lb °F at 1500 °F[2]. Numerical integration between 60 and 1500 °F yields an enthalpy increase of 487 Btu/lb over this temperature range (average specific heat = 0.338 Btu/lb °F).

On a mole basis the enthalpy increase of the coke from 60 to 1500 °F amounts to:

$$c_{p_C} = 6500 \text{ Btu/lb mole of contained carbon}$$

3. Composition and Heat Capacity of Air

Composition of air (lb moles/lb mole contained oxygen):

O_2	1
N_2	3.77
H_2O	0.10
Air	4.87

The assumed water content corresponds to 0.013 lb of water vapor per lb of dry air, or a relative humidity of 60% at 80 °F.

The enthalpy increase of the air from 600 to 1500 °F was estimated from the data of reference (3), yielding a value of 6960 Btu/lb mole of air (average specific heat = 7.73 Btu/lb mole °F). Per mole of oxygen, the enthalpy increase of the air from 600 to 1500 °F amounts to:

$$c_{p_A} = 33,900 \text{ Btu/lb mole of contained oxygen}$$

4. Heats of Reaction

The following values were used for the heats of reaction of the various reactions involved at the operating temperatures of the reducer[4][5]:

$$M_2SO_3\ (\ell) \longrightarrow 1/4\ M_2S\ (\ell) + 3/4\ M_2\ SO_4\ (\ell) \qquad (1)$$

$$\Delta H_{Disp} = 21,400 \text{ Btu/lb mole}$$

$$M_2SO_4(\ell) + 2\ C\ (s) \longrightarrow M_2S\ (\ell) + 2\ CO_2\ (g) \qquad (2)$$

$$\Delta H_{SO_4^{=} \rightarrow S^{=}} = +75,500 \text{ Btu/lb mole}$$

$$M_2S(\ell) + 2\ O_2(g) \longrightarrow M_2\ SO_4(\ell) \qquad (3)$$

$$\Delta H_{S^{=} \rightarrow SO_4^{=}} = -415,200 \text{ Btu/lb mole}$$

$$C(s) + O_2\ (g) \longrightarrow CO_2(g) \qquad (4)$$

$$\Delta H_{CO_2} = -169,500 \text{ Btu/lb mole}$$

$$H_2(g) + 1/2\ O_2(g) \longrightarrow H_2O(g) \qquad (5)$$

$$\Delta H_{H_2O} = -106,900 \text{ Btu/lb mole}$$

$$S(s) + O_2\ (g) \longrightarrow SO_2(g) \qquad (6)$$

$$\Delta H_{SO_2} = -133,400 \text{ Btu/lb mole}$$

$$S(s) + 1/2\ C(s) + M_2CO_3(\ell) \longrightarrow M_2S(\ell) + 3/2\ CO_2(g) \qquad (7)$$

$$\Delta H_{S \longrightarrow S^=} = +53,400 \text{ Btu/lb mole}$$

A recent reevaluation of the data used for the heats of reaction at 1500 °F for reactions (4) and (7) indicates that -169,900 and +43,200 Btu/lb mole, respectively, would have been more accurate values. The effect of this difference on the present calculations is negligible.

It is to be noted that the above listed values of the heats of reaction for reactions (1), (2), (3), and (7) are actually the values for these reactions with sodium salts. They were assumed to provide close enough approximations for the heats of reaction with the lithium and potassium salts to allow their use in this reducer study.

5. Reaction Completion Efficiencies

Assumed to be 95% for each step of the molten carbonate process, with one exception: complete consumption of the oxygen provided was assumed in the oxidation region of the reducer.

Coke loss as unreacted coke was assumed to be 5%, allowing usage of 95% of the coke feed material.

6. Reducer Design Parameters

Feed temperatures:

Melt	850 °F
Coke	60 °F
Air	600 °F

Reducer operating temperature = 1400 to 1700 °F, with a temperature rise of 300 °F in the oxidation region and a corresponding temperature drop in the reduction region. A smaller temperature gradient would have required a higher melt recirculation rate and therefore resulted in a larger size reducer. A larger gradient would have raised the oxidized melt temperature to an undesirably high level.

Superficial gas velocity $\leq$ 3 ft/sec, a controlling factor in the oxidation region, but not in the reduction region, since the amount of gas generated in the reduction region is much smaller than the amount of air used in the oxidation region. While most of the analysis was based on a velocity of 3 ft/sec, one set of calculations was performed for a velocity of 5 ft/sec to determine the effect of this parameter on reducer design.

Melt bed expansion due to gas flow and coke addition = 75 volume %[6]. No attempt was made to differentiate between the oxidation and reduction regions (except in the melt recirculation calculations of Section VIII).

Melt residence time in reduction region $\geq$ 15 minutes[7]. The residence time in the oxidation region is not a controlling factor since the oxidation of sulfide to sulfate is rapid at reducer operating temperatures. While most of the analysis was based on a residence time of 15 minutes, one set of calculations was performed for a residence time of 30 minutes to determine the effect of this parameter on reducer design.

7. Reducer Design Concepts

Two-region reducer with separate oxidation and reduction regions.

Reducer wall corrosion protection provided by either frozen melt skull (cold wall) or alumina liner (hot wall).

Reducer geometry: Vertical cylinder. Process design equations were also developed for a horizontal cylinder geometry both with the separation baffle perpendicular to the axis of the cylinder and the separation baffle parallel to the axis of the cylinder. Within the scope of this work only one set of calculations was performed on a horizontal cylinder geometry for comparison purposes.

8. Reducer Processing Capacity

The mass and heat balance analysis was performed on a normalized basis of treatment in the molten carbonate scrubber of a waste gas feed stream carrying 1 lb mole per hour of sulfur oxides (SO_2 and SO_3).

The physical dimension and heat loss optimization was then conducted as a function of reducer unit capacity over a range of 0 to 200 lb moles of sulfur oxides per hour in the waste gas feed stream to the molten carbonate process system. Special emphasis was placed on capacities of 3.125 and 166.7 lb moles of sulfur oxides per hour. For power plants burning 3 wt % sulfur 12,800 Btu/lb coal with a heat rate of 9000 Btu/Kwh these capacities are equivalent to those of a 5 Mw pilot plant size unit and a 267 Mw (one of three units of an 800 Mw plant) full scale unit, respectively.

IV. REDUCER MASS BALANCE

A mass balance was performed around the whole molten carbonate process system on a normalized basis of 1 lb mole per hour of sulfur oxides contained in the feed waste gas stream entering the system. The reaction completion efficiencies were assumed to be as described in Section III. The mass balance around the reducer is shown in Figure 2.

The key independent variable in this mass balance is C_o, the carbon requirement, expressed in lb moles of carbon which do react in the reducer per lb mole of sulfur oxides contained in the feed waste gas stream to the scrubber. C_o is determined by a heat balance around the melt bed in the reducer, as described in Section V. The actual carbon usage amounts to $C_o/1-\lambda$ when one takes into account the fraction, λ, of the carbon feed which is discharged unreacted from the reducer.

All other parameters are determined by the composition of the feed streams and the extent of the chemical reactions which take place upstream of the reducer (partial oxidation of sulfite to sulfate, partial disproportionation of the sulfite).

If one assumes that a mole fraction, g, of the sulfur oxides in the feed gas to the scrubber is in the form of SO_3, that no further oxidation of SO_2 to SO_3 or sulfite to sulfate takes place in the scrubber, and that all the sulfide in the melt feed to the scrubber is oxidized to sulfate, the parameter a can be expressed as follows:

$$a = \left\{ \frac{[M_2SO_4]}{[M_2SO_3] + [M_2SO_4]} \right\}_{\text{scrubber outlet}} = \frac{\frac{1}{1+u}\,\frac{g}{e^2}}{1 + p\,\frac{1-f}{f} - \frac{1-g}{1+u}\,\frac{e(1-e)}{4}}$$

The parameter a decreases, and therefore the sulfate fraction in the melt at the outlet from the scrubber increases with increasing concentration of SO_3 in the feed gas, g, decreasing reaction completion efficiency, e, increasing disproportionation upstream of the reducer (actually upstream of the branching off of the scrubber recycle melt stream from the reducer melt stream), p, and increasing ratio of scrubber recycle to reducer melt flow, $\frac{1-f}{f}$.

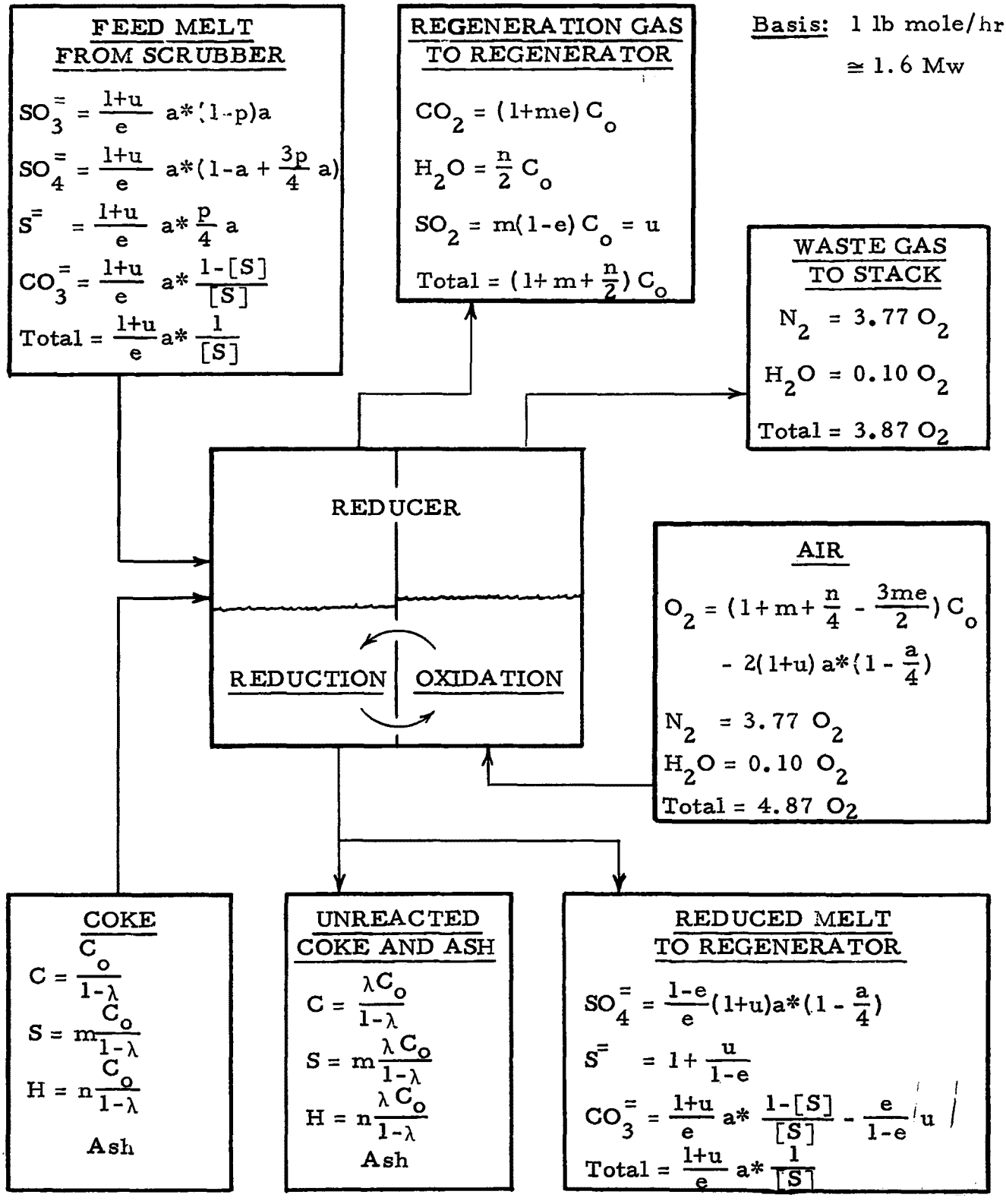

Figure 2. Molten Carbonate Reducer Mass Balance

The parameter u is given by the relationship:

$$u = m\,(1\text{-}e)\,C_o$$

It represents that sulfur in the reacted coke which is not reduced to sulfide in the reducer and is assumed to become converted to SO_2. It is a very small quantity, amounting to $C_o/800$ at the selected values of e = 0.95 and m = 0.025.

The parameter a* is a reaction efficiency adjustment factor:

$$a^* = \frac{1}{1 + \frac{1\text{-}e}{4\ e}\ a}, \text{ which for } e = 0.95 \text{ gives } a^* = \frac{1}{1 + \frac{a}{76}}, \text{ and}$$

is therefore generally almost equal to unity.

It is to be noted that, as expected, the controlling parameter determining the net melt flow rate into and out of the reducer is the maximum allowable sulfur compound concentration in the melt, $[S]$. At sulfur compound concentrations of 15 and 30 mole %, the melt flow rates into and out of the reducer will be approximately 7.0 and 3.5 lb moles, respectively, per lb mole of SO_x in the feed gas to the scrubber, corresponding to about 0.70 and 0.35 gpm (at 850 °F) per lb mole/hour of SO_x in the feed gas.

V. REDUCER HEAT BALANCE

The reducer must provide the heat necessary to heat the various feed streams to the reaction temperatures, to furnish the endothermic heat of reaction, and to compensate for the heat losses to the walls of the reducer vessel. The heat is generated by the oxidation of the carbon in the excess coke used for this purpose. The heat balance around the reducer, therefore, determines the amount of coke required, and hence the parameter, C_o, lb moles of carbon which react in the reducer per lb mole of sulfur oxides in the feed waste gas to the scrubber, in the mass balance described in Section IV. The heat balance also determines the amount of air required to oxidize the excess carbon and the amount of melt which must be recirculated between the oxidation and reduction regions to transport the required heat from the former to the latter. It therefore determines the physical size requirements of the reducer.

It is important to note that for purposes of the present analysis, heat balance around the reducer and heat loss from the reducer are defined as heat balance around the bed of melt in the reducer and heat loss from this bed, since all the chemical reactions involved, and their heat and temperature requirements, are assumed to take place in this bed and not in the gas space above the melt.

Knowing the specific heats and temperatures of the feed streams and the various heats of reaction involved, as given in Section III, and the mass balance from Figure 2 in Section IV, one can perform a heat balance around the reducer if the heat loss can be either estimated or assumed.

An estimate of heat loss depends not only upon estimates of heat transfer coefficients and thermal conductances for the evaluation of the heat flux, but also upon the heat transfer area across which this heat flows. This area can only be determined once the physical dimensions of the reducer melt bed are known, and these are derived from the results of the heat balance.

The heat balance was therefore performed as a function of an independent heat loss parameter, Q_L, the heat loss from the reducer melt bed normalized to a sulfur oxide flow of 1 lb mole per hour in the feed gas to the scrubber. All calculations were performed as a function of this parameter. The heat flux across the reducer vessel walls was then obtained from the assumed heat loss and the physical dimensions thus calculated, and matched with anticipated heat transfer rates.

The heat balance around the reducer melt bed is presented in Figure 3. The results are summarized in the reacted carbon and total coke requirements given by equations (1) through (4) of this figure. The numerical values, of course, are based on the parameters and data given in Section III, and specifically feed stream temperatures of 850, 60 and 600 °F, respectively, for the melt, the coke, and the air.

The reducer coke and air requirements are plotted in Figures 4 and 5, respectively, as functions of the normalized heat loss parameter, Q_L, of the sulfur compound concentration in the melt, $[S]$, and of the sulfate fraction, $\frac{[SO_4]}{[S]}$, of the sulfur compounds in the melt leaving the scrubber. These figures also provide typical coke cost and air compression horsepower data for a power plant burning 3 wt % sulfur, 12,800 Btu/lb coal with a heat rate of 9,000 Btu/Kwh. A discussion of these results is provided in Section IX. 3. a.

Definition of Constants

A = Net heat available in coke, taking into account the heat required for preheating of both the coke and the air for its combustion, Btu/lb-mole of carbon

$$= -\left(\Delta H_{CO_2} + m\Delta H_{SO_2} + \frac{n}{2}\,\Delta H_{H_2O}\right) - \frac{c_{p_C}}{1-\lambda} - \left(1 + m + \frac{n}{4}\right) c_{p_A}$$

For $\lambda = 0.05$ $\quad A = 128,760 + 99,500\,m + 44,980\,n$

For $m = 0.025$, $n = 0$ $\quad A = 131,200$

B = Heat required for reduction of sulfur in coke to sulfide, plus heat made unavailable by consumption of carbon for this reduction, Btu/lb-mole of sulfur

$$= -\left(\frac{1}{2}\,\Delta H_{CO_2} + \Delta H_{SO_2} - \Delta H_{S \rightarrow S^{=}}\right) \quad \frac{3}{2}\, c_{p_A} = 220,700$$

E = Heat required for reduction of sulfate in melt to sulfide, plus heat made unavailable by consumption of carbon for this reduction, Btu/lb-mole of sulfate

$$= -\left(2\,\Delta H_{CO_2} - \Delta H_{SO_4^{=} \rightarrow S^{=}}\right) - 2\, c_{p_A} = 346,700$$

K = Calculation constant, Btu/lb-mole

$$a^{*}\left\{E\left(1 - \frac{a}{4}\right) + \frac{c_{p_M}}{e\,[S]} + \frac{1-p}{e}\, a\, \Delta H_{Disp}\right\}$$

For $e = 0.95$, $p = 0.10$ $\quad K = a^{*}\left(346,700 + \frac{29,800}{[S]} - 107,000\,a\right)$

Figure 3. Molten Carbonate Reducer Heat Balance

HEAT BALANCE ⟶ CARBON REQUIREMENT, lb-mole C/lb-mole SO_x

Heat Available in Coke + Heat of Disproportionation =

= Heat for Coke Sulfur Reduction + Heat for Sulfate Reduction +

+ Heat for Preheat of Melt + Heat Loss

$$AC_o + \left(-\Delta H_{Disp}\right)\frac{1+u}{e}\,a^*(1-p)\,a =$$

$$= BmC_o e + E\frac{1+u}{e}\,a^*\left(1-\frac{a}{4}\right)e + c_{p_M}\frac{1+u}{e}\,a^*\frac{1}{[S]} + Q_L$$

$$(A - Bme)\,C_o = (1+u)\,K + Q_L = K + Q_L + K_m(1\ \ e)\,C_o$$

$$C_o = \frac{K + Q_L}{A - m\left[Be + K(1\ \ e)\right]} \qquad (1)$$

For $\lambda = 0.05$, $m = 0.025$, $n = 0$, $e = 0.95$, $p = 0.10$

$$C_o = \frac{a^*\left(346,700 + \frac{29,800}{[S]}\ \ 107,000\,a\right) + Q_L}{126,000 - a^*\left(433 + \frac{37.3}{[S]} - 134\,a\right)} \qquad (2)$$

$$\cong a^*\left(2.7635 + \frac{0.2375}{[S]} - 0.8529\,a\right) + 0.7971\left(\frac{Q_L}{10^{-5}}\right) \qquad (3)$$

COKE REQUIREMENT, lb Coke/lb Sulfur

For coke containing 90 wt % carbon, and same parameters as above

$$\text{Coke} \cong a^*\left\{0.838 + \frac{0.1042}{[S]} + 0.374\,[SO_4^{=}]\right\} + 0.350\left(\frac{Q_L}{10^5}\right) \qquad (4)$$

with $a^* = \dfrac{1}{1 + \dfrac{1 - [SO_4^{=}]}{76}} \cong 1$

Figure 3. Molten Carbonate Reducer Heat Balance (Cont)

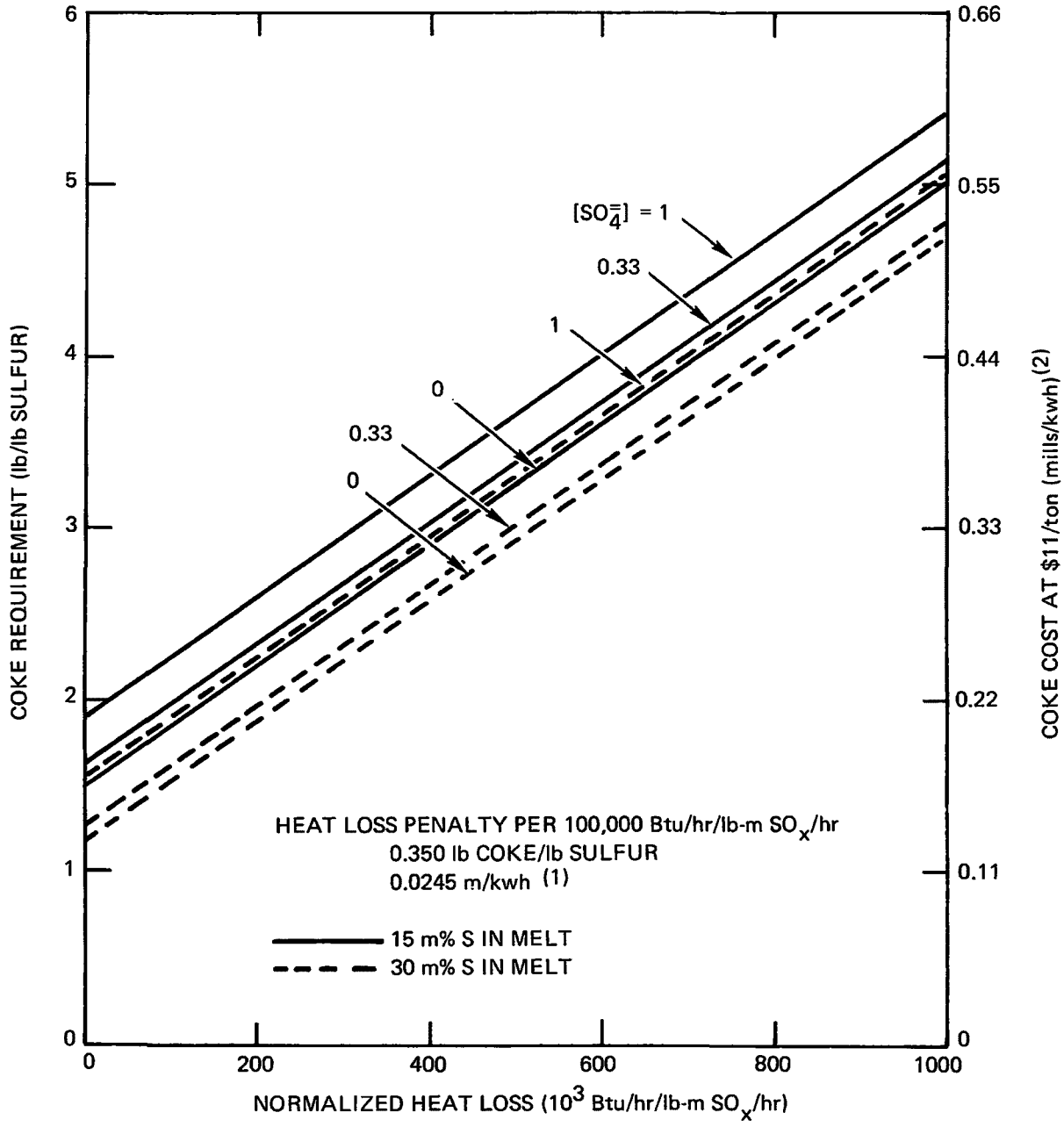

(1) AT 20¢/10^6 Btu THIS HEAT WOULD BE WORTH 0.0125 m/kwh
(2) FOR POWER PLANT BURNING 12,8000 Btu/lb, 3 wt% S COAL WITH A HEAT RATE OF 9000 Btu/kwh

Figure 4. Reducer Coke Requirement

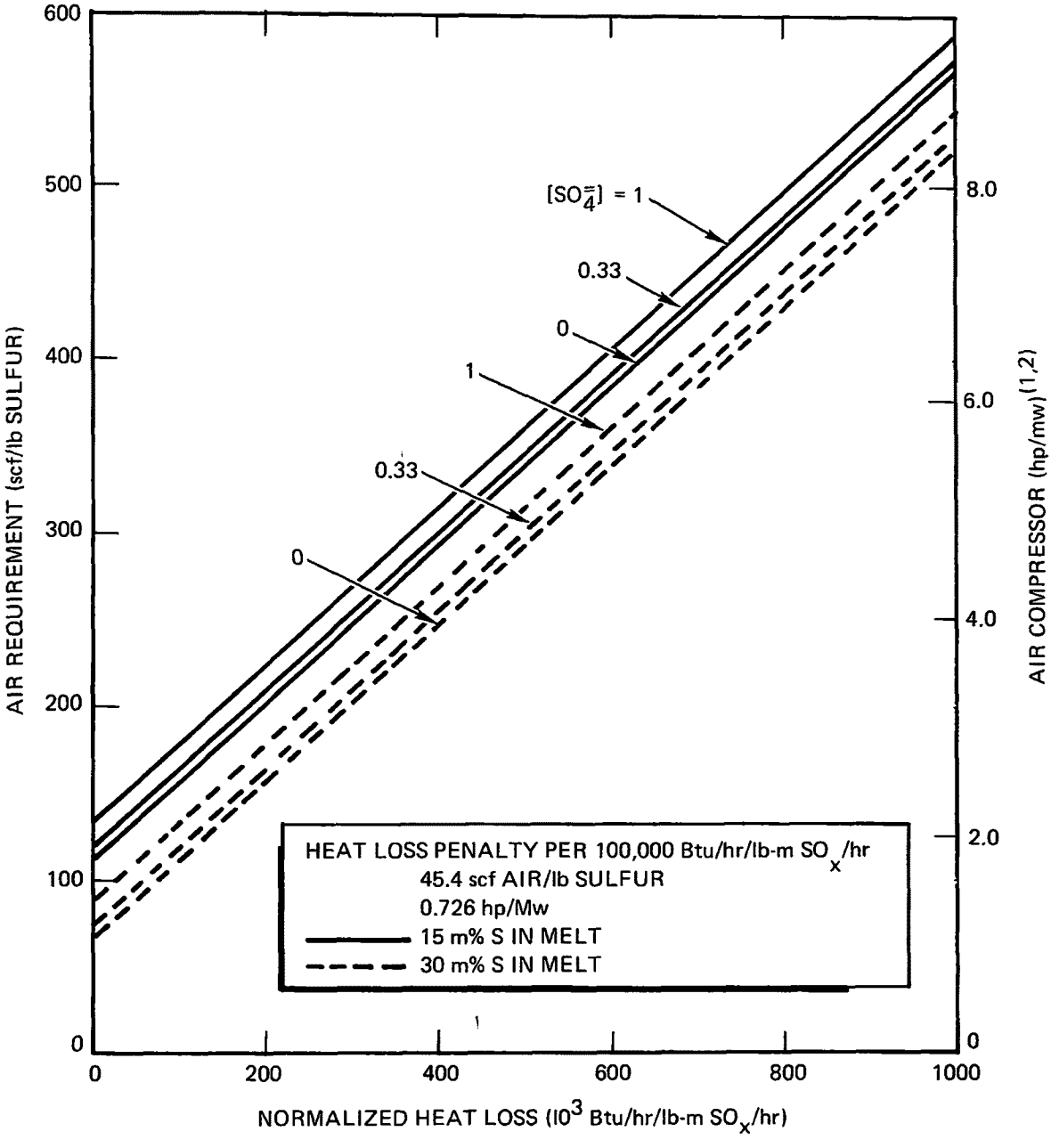

(1) FOR POWER PLANT BURNING 12,800 Btu/lb, 3 wt % S COOL WITH A HEAT RATE OF 9000 Btu/kwh

(2) ASSUMING A PRESSURE REQUIREMENT OF 10 psig AND A COMPRESSOR EFFICIENCY OF 75%

Figure 5. Reducer Air Requirement

VI. PHYSICAL DIMENSIONS OF REDUCER MELT BED

The physical size of the reducer melt bed was determined by calculating the cross-sectional areas of the oxidation and reduction regions as a function of bed depth at various values of the normalized heat loss parameter, Q_L, assuming maximum allowable superficial gas velocity and minimum reduction region residence time to be the controlling parameters (the melt recirculation rate between the oxidation and reduction regions does not appear to be controlling, as will be shown in Section VIII). The depth of the reducer melt bed was then optimized to achieve a minimum heat transfer area of reducer wall surfaces in contact with the melt. This optimization was only approximately correct as it was performed at constant value of the normalized heat loss parameter, Q_L, rather than at constant value of the heat flux across the wall surface, Q/A, which is the truly independent variable in the design of the reducer, as shown in Section VII. It is to be noted that such an optimization based exclusively on heat transfer considerations may be of only limited value in a low heat loss reducer in which heat loss considerations may prove to be secondary to structural considerations.

The general relationships developed in this section express the various parameters as functions of both the normalized heat loss parameter, Q_L, and the normalized amount, O_2, of oxygen consumed in the reducer. O_2 is actually a function of the amount of carbon consumed, C_o, per the mass balance of Figure 2, and C_o in turn is a function of the sulfur compound concentration in the melt, $[S]$, and of the normalized heat loss parameter, Q_L, per the heat balance of Figure 3. In the general case the equations are simpler when written with O_2 left in as an explicit parameter rather than expressed as a function of $[S]$ and Q_L which it actually is. In the specific case of the present study, however, the sulfate mole fraction in the sulfur compounds in the melt leaving the scrubber was not varied and was assumed to be equal to 0.33. Under these conditions, the approximate equation (3) of Figure 3 can be used to express the value of C_o and therefore that of O_2 as a linear function of $[S]$ and Q_L and thus to provide an explicit relationship between the various parameters and $[S]$ and Q_L.

For $1-a = [M_2SO_4] \Big/ \left([M_2SO_3] + [M_2SO_4] \right) = 0.33$, equation (3) of Figure 3 becomes:

$$C_o = 2.1758 + \frac{0.2354}{[S]} + 0.7971 \left(\frac{Q_L}{10^5} \right), \text{ lb moles/lb mole } SO_x \quad (5)$$

From Figure 2, using the value of C_o given by equation (5):

$$O_2 = 0.4960\ F_1, \text{ lb moles/lb mole } SO_x \quad (6)$$

with $F_1 = 1 + \frac{0.4685}{[S]} + 1.5867 \left(\frac{Q_L}{10^5} \right)$

Equation (6) provides the relationship used to express all the other parameters as explicit functions of $[S]$ and Q_L for the specific sulfate-sulfite concentration ratio assumed in this study.

1. Cross Sectional Area of Oxidation Region

The oxidation of sulfide to sulfate with air at around 1500 °F is rapid. The residence time of the melt in the oxidation region is therefore not considered to be a controlling factor in determining the volume of the melt bed in this region. The upper limit on the maximum allowable superficial gas velocity thus becomes the controlling parameter determining the cross-sectional area of the oxidation region.

The mass balance of Figure 2 shows the amount of air required as equal to $4.87\ O_2$ lb moles/hr per lb mole/hr of SO_x in the feed gases to the scrubber. The present calculations were based on the superficial velocity of the air at 1500 °F. This is conservative since the oxygen from the air is removed by reaction with the sulfide as it progresses through the oxidation region.

$$\therefore \text{ Air flow at } 1500\,^\circ F = 1.935\ O_2, \text{ acfs per lb mole/hr } SO_x$$

If the maximum allowable superficial gas velocity is v ft/sec, the minimum area, A_o, of the oxidation region is given by the equation:

$$A_o = 1.935 \frac{O_2}{v}, \text{ ft}^2 \text{ per lb mole/hr } SO_x \quad (7)$$

Hence, per equation (6):

$$A_o = 0.9597 \frac{F_1}{v}, \text{ ft}^2 \text{ per lb mole/hr } SO_x \quad (8)$$

2. Internal Melt Recirculation Requirement

The amount of melt recirculation required between the oxidation and reduction regions of the reducer is determined by the amount of heat which must be transported from the oxidation to the reduction region, and the allowed temperature rise of the melt. The temperature rise was selected as equal to 300 °F for purposes of the present study (Section III). The heat conduction through the separation baffle was assumed to be negligible.

The amount of heat to be transported can be calculated most easily by determining what happens in the oxidation region. In this region heat is generated by only one chemical reaction, the oxidation of sulfide to sulfate, which consumes all the oxygen fed to the reducer. Part of this heat release is utilized in the oxidation region as preheat of the air feed and as heat loss, Q_{L_o}. The remainder is transported to the reduction region in the form of increased sensible heat of the recirculated melt.

$$\therefore \text{Heat Release} = -(\Delta H_{S^= \longrightarrow SO_4^=}) \frac{O_2}{2} = 207{,}600\ O_2, \text{ Btu/hr per lb mole/hr } SO_x$$

$$\text{Air Preheat} = c_{p_A}\ O_2 = 33{,}900\ O_2, \text{ Btu/hr per lb mole/hr } SO_x$$

$$\text{Heat Loss} = Q_{L_o}, \text{ Btu/hr per lb mole/hr } SO_x$$

$$\text{Heat Transport} = Q_T = -(1/2\Delta H_{S^= \longrightarrow SO_4^=} + c_{p_A})\ O_2 - Q_{L_o}$$

$$= 173{,}700\ O_2 - Q_{L_o}, \text{ Btu/hr per lb mole/hr } SO_x$$

A simplifying approximation was made at this point by assuming the heat loss from the reducer to be equally distributed between the oxidation and the reduction regions: $Q_{L_o} = \frac{1}{2} Q_L$. Then:

$$Q_T = 173{,}700\ O_2 - Q_L/2, \text{ Btu/hr per lb mole/hr } SO_x \quad (9)$$

Using equation (6):

$$Q_T = 86{,}160\ F_2, \text{ Btu/hr per lb mole/hr } SO_x \quad (10)$$

with

$$F_2 = 1 + \frac{0.4685}{[S]} + 1.0064 \left(\frac{Q_L}{10^5}\right).$$

For a melt temperature rise of 300 °F with a specific heat at these temperatures of about 45 Btu/lb mole °F, this heat transport requires:

$$\text{Melt Recirculation} = 12.87\ O_2 - 3.704\left(\frac{Q_L}{10^5}\right),\ \text{lb moles/hr per lb mole/hr } SO_x \tag{11}$$

Using equation (6):

$$\text{Melt Recirculation} = 6.3819\ F_2,\ \text{lb moles/hr per lb mole/hr } SO_x \tag{12}$$

Should it prove desirable or necessary to use a melt temperature rise, ΔT, different from the 300 °F assumed in this analysis, equation (12) can be rewritten as follows:

$$\text{Melt Recirculation} = \frac{1915}{\Delta T}\ F_2,\ \text{lb moles/hr per lb mole/hr } SO_x \tag{12a}$$

3. Cross-Sectional Area of Reduction Region

The volume and cross-sectional area of the reduction region can be determined from the melt flow through this region and the residence time required to allow the reduction reaction to proceed to the desired degree of completion. The melt flow is calculated as follows:

Reduction Region Melt Flow = Melt Recirculation + Melt Feed

$$= 12.87\ O_2 - 3.704\left(\frac{Q_L}{10^5}\right) + \frac{1+u}{e}\ a^*\ \frac{1}{[S]}$$

$$\simeq 12.87\ O_2 - 3.704\left(\frac{Q_L}{10^5}\right) + \frac{1.05}{[S]},\ \text{lb moles/hr per lb mole/hr } SO_x \tag{13}$$

Using equation (6):

$$\text{Reduction Region Melt Flow} = 6.3819\ F_3,\ \text{lb moles/hr per lb mole/hr } SO_x \tag{14}$$

with $F_3 = 1 + \frac{0.6330}{[S]} + 1.0064\left(\frac{Q_L}{10^5}\right)$

If one assumes a specific volume of 1.6 ft^3/lb mole for the expanded melt bed (equivalent to a 75% bed expansion due to gas flow and suspension of coke), a minimum reduction region residence time of θ minutes requires a minimum expanded bed volume, V_r, in this region such that:

$$V_r = 1.6 \frac{\theta}{60} \text{ (Reduction Region Melt Flow)}$$

$$= \left\{0.3431\ O_2 - 0.09877 \left(\frac{Q_L}{10^5}\right) + \frac{0.028}{[S]}\right\}\theta, \text{ ft}^3 \text{ per lb mole/hr } SO_x \quad (15)$$

$$= 0.1702\ F_3\ \theta, \text{ ft}^3 \text{ per lb mole/hr } SO_x \quad (16)$$

For a vertical cylinder reducer geometry, the cross-sectional area of the reduction region, A_r, can be determined as a function of expanded melt bed depth, d:

$$A_r = \left\{0.3431\ O_2 - 0.09877 \left(\frac{Q_L}{10^5}\right) + \frac{0.028}{[S]}\right\} \frac{\theta}{d}, \text{ ft}^2 \text{ per lb mole/hr } SO_x \quad (17)$$

$$= 0.1702\ F_3 \frac{\theta}{d}, \text{ ft}^2 \text{ per lb mole/hr } SO_x \quad (18)$$

Should it prove desirable or necessary to use a melt temperature rise, ΔT, different from the 300 °F assumed in this analysis, equations (14), (16), and (18) can be rewritten as follows:

$$\text{Reduction Region Melt Flow} = \frac{1915}{\Delta T} F_3, \text{ lb moles/hr per lb mole/hr } SO_x \quad (1$$

$$\text{with } F_3 = 1 + \frac{0.4685 + 0.5484 \times 10^{-3} \Delta T}{[S]} + 1.0064 \left(\frac{Q_L}{10^5}\right)$$

$$V_r = \frac{51.06}{\Delta T} F_3\ \theta, \text{ ft}^3 \text{ per lb mole/hr } SO_x \quad (16a)$$

$$A_r = \frac{51.06}{\Delta T} F_3 \frac{\theta}{d}, \text{ ft}^2 \text{ per lb mole/hr } SO_x \quad (18a)$$

In general it is found that the cross-sectional area of the reduction region thus determined on the basis of minimum melt residence time is greater than that obtained on the basis of maximum superficial gas velocity:

$$A_{r_{\text{Gas Velocity}}} = 0.3973 \left(1 + m + \frac{n}{2}\right) \frac{C_o}{v}, \text{ ft}^2 \text{ per lb mole/hr } SO_x \quad (19)$$

Using equation (5):

$$A_{r_{\text{Gas Velocity}}} = \frac{1}{v} \left\{0.9898 + \frac{0.1071}{[S]} + 0.3626 \left(\frac{Q_L}{10^5}\right)\right\},$$

$$\text{ft}^2 \text{ per lb mole/hr } SO_x \quad (20)$$

Under the conditions of this study the reduction region residence time is therefore the controlling parameter in determining the cross-sectional area of this region.

4. Melt Bed Diameter and Heat Transfer Area - Vertical Cylinder Reducer Geometry

The total cross-sectional area of the reducer, A_t, is the sum of the cross-sectional areas of the oxidation and reduction regions:

$$A_t = A_o + A_r \tag{21}$$

The actual cross-sectional area, A_{cs}, of a reducer with a capacity to handle N lb moles/hr of SO_x in the feed gas to the scrubber is:

$$A_{cs} = NA_t \tag{22}$$

For a vertical cylinder reducer geometry the diameter of the reducer, D, is:

$$D = 2\sqrt{\frac{A_{cs}}{\pi}} \tag{23}$$

The heat loss from the melt bed takes place across the area of the walls in contact with the melt (side walls and bottom, assumed to be flat, of the reducer vessel), and, by thermal radiation, across the free surface of the melt. If one assumes that the radiation heat flux at the free surface of the melt amounts to a fraction, ϵ, of the convection heat flux at the walls,* the effective heat transfer area, A_{ht}, in a vertical cylinder reducer geometry, can be expressed as follows:

$$A_{ht} = A_{cs}(1+\epsilon) + \pi Dd = A_{cs}(1+\epsilon) + 2d\sqrt{\pi A_{cs}} \tag{24}$$

$$= \left(NA_o + \frac{NV_r}{d}\right)(1+\epsilon) + 2\sqrt{\pi Nd(A_o d + V_r)} \tag{25}$$

* The value of ϵ is difficult to determine as it depends upon the emissivity of the surface and the amount of radiation shielding which may take place. In all the numerical calculations in this report it was assumed to be negligible ($\epsilon \cong 0$)

5. Melt Bed Diameter and Depth Optimization - Vertical Cylinder Reducer Geometry

The optimization of the diameter and depth of the reducer melt bed was directed toward achieving a minimum heat loss from the bed, neglecting any structural considerations which may actually prove to be the controlling factors. At a given rate of heat transfer across the walls of the reducer in contact with the melt, such an optimization is equivalent to minimizing the area, A_{ht}, available for this heat transfer. To be completely rigorous the optimization must be done at constant heat flux. This, however, would have become excessively complex for the present scope of the analysis. A simplifying approximation was used by performing the necessary differentiation of Equation (25) at constant normalized heat loss, Q_L, instead of constant heat flux, $\left(\frac{Q}{A}\right)$, such that:

$$\left(\frac{Q}{A}\right) = \frac{NQ_L}{A_{ht}} \tag{26}$$

The optimization was therefore performed by minimizing the value of the effective heat transfer area, A_{ht}, in equation (25), with respect to bed depth, d, at constant normalized heat loss, Q_L. The heat transfer area, A_{ht}, is minimum when the following relationships prevail:

$$N = \frac{\pi d^3}{V_r} \quad \frac{(1+2b)^2}{1+b} \quad \frac{1}{(1+\epsilon)^2} \tag{27}$$

$$D = 2d\,(1+2b) \quad \frac{1}{1+\epsilon} \tag{28}$$

$$\left(\frac{Q}{A}\right) = \frac{Q_L}{A_o} \quad \frac{b(1+2b)}{(1+b)\,(3+2b)} \quad \frac{1}{1+\epsilon} \tag{29}$$

$$\delta = \frac{\pi}{8} \frac{1-b}{1+b} \quad \frac{2}{\frac{\gamma}{\sin\gamma} + \cos\gamma} \tag{30}$$

$$\cong \frac{\pi}{8} \frac{1-b}{1+b} \quad \frac{1}{1 - \frac{2\delta^2}{3} - \frac{2\delta^4}{5} \quad \frac{4\delta^6}{7}} \,.$$

with $b = \frac{A_o d}{V_r}$ = ratio of volume of oxidation region to volume of reduction region

$= 5.639 \frac{F_1}{F_3} \frac{d}{v\theta}$ for the case of the present analysis with a 0.33 mole fraction sulfate in the sulfur compounds in the melt leaving the scrubber*.

$\delta = \frac{j}{D}$,

j = distance from axis of reducer vessel to separation baffle, ft, positive or negative depending upon whether the volume of the oxidation region is smaller or larger than that of the reduction region, respectively.

$\gamma = \text{arc sin } \frac{j}{D/2} = \text{arc sin } 2\delta.$

It is to be noted that the value of the ratio b increases with increasing reducer processing capacity, becoming equal to unity when

$$N = \frac{9\pi}{2} \frac{V_r^2}{A_o^3} \frac{1}{(1+\epsilon)^2}$$

6. Horizontal Cylinder Reducer Geometry with Separation Baffle Perpendicular to Cylinder Axis

For the horizontal cylinder reducer geometry with the separation baffle perpendicular to the axis of the cylinder, the lengths, L_o and L_r, of the oxidation and reduction regions are given by the following equations:

$$L_o = \frac{NA_o}{D \sin \alpha} \tag{31}$$

$$L_r = \frac{4NV_r}{D^2 \alpha \left(1 - \frac{\sin 2\alpha}{2\alpha}\right)} \tag{32}$$

with $\alpha = \text{arc cos } (1 - \frac{2d}{D})$ and therefore $d = \frac{D}{2}(1 \quad \cos \alpha)$.

---

* It is to be noted that there is an inconsistency in the time units used in the numerical equations as N is expressed in lb moles/hr, v in ft/sec, and θ in minutes.

The total length, L, of the reducer is therefore:

$$L = \frac{NA_o}{D \sin\alpha} \left\{1 + \frac{1}{b\left(\frac{\alpha}{\sin\alpha} - \cos\alpha\right)}\right\} \tag{33}$$

with $b = \frac{A_o D}{4V_r}$ (note the difference between this definition and that used in Section VI-5).

The effective heat transfer area, A_{ht}, across which the heat loss from the melt bed takes place is the area of the walls in contact with the melt (lower part of the cylindrical section plus end plates which for purposes of this calculation are assumed to be flat) and the partially effective free surface of the melt:

$$A_{ht} = LD\alpha\left(1 + \epsilon\frac{\sin\alpha}{\alpha}\right) + \frac{D^2}{2}\alpha\left(1 - \frac{\sin 2\alpha}{2\alpha}\right) \tag{34}$$

An optimization of reducer dimensions similar to the one performed for the vertical cylinder reducer geometry yields a minimum value of the effective heat transfer area, A_{ht}, at constant values of the normalized heat loss parameter, Q_L, when the following relationships prevail:

$$D^3 = \frac{4NV_r}{\alpha\left(1 - \frac{\sin 2\alpha}{2\alpha}\right)^2}\left(1 + \epsilon\frac{\sin\alpha}{\alpha}\right) \tag{35}$$

$$d = \frac{D}{2}(1 - \cos\alpha) \tag{36}$$

$$L = D\left(1 - \frac{\sin 2\alpha}{2\alpha}\right)\left\{1 + b\left(\frac{\alpha}{\sin\alpha} - \cos\alpha\right)\right\}\frac{1}{1+\epsilon\frac{\sin\alpha}{\alpha}} \tag{37}$$

$$\left(\frac{Q}{A}\right) = \frac{Q_L}{A_o}\,\frac{2b\left(1 - \frac{\sin 2\alpha}{2\alpha}\right)}{3 + 2b\left(\frac{\alpha}{\sin\alpha} - \cos\alpha\right)}\,\frac{1}{1+\epsilon\frac{\sin\alpha}{\alpha}} \tag{38}$$

$$\delta = \frac{1}{2}\,\frac{1 - b\left(\frac{\alpha}{\sin\alpha} - \cos\alpha\right)}{1 + b\left(\frac{\alpha}{\sin\alpha} - \cos\alpha\right)} \tag{39}$$

with $b = \frac{A_o D}{4V_r}$

$$\alpha = \arccos\left(1 - \frac{2d}{D}\right)$$

$$\delta = \frac{j}{L}$$

j = distance from vertical midplane of reducer vessel to separation baffle, ft, positive or negative depending upon whether the volume of the oxidation region is smaller or larger than that of the reduction region, respectively.

As in the case of the vertical cylinder reducer geometry, the ratio of the volume of the oxidation region to that of the reduction region increases with increasing reducer processing capacity, becoming equal to unity when

$$b = \frac{1}{\frac{\alpha}{\sin\alpha} - \cos\alpha}$$

and hence

$$N = \frac{16\ V_r^2}{A_o^3} \quad \frac{\sin\alpha}{\frac{\alpha}{\sin\alpha}\left(\frac{\alpha}{\sin\alpha} - \cos\alpha\right)} \quad \frac{1}{1 + \epsilon\ \frac{\sin\alpha}{\alpha}}$$

The free surface of the melt should preferably be somewhat below the horizontal midplane of the reducer vessel, with, for instance, a value of expanded melt bed depth to diameter ratio d/D = 0.40. Assuming $\epsilon = 0$, equations (35) through (39) can then be written:

$$D^3 = 3.9779\ N\ V_r \tag{40}$$

$$d = 0.4\ D \tag{41}$$

$$L = 0.8569\ D\ (1 + 1.1977\ b) \tag{42}$$

$$\left(\frac{Q}{A}\right) = \frac{Q_L}{A_o} \quad \frac{1.7138\ b}{3 + 2.3954\ b} \tag{43}$$

$$\delta = \frac{1}{2} \quad \frac{1 - 1.1977\ b}{1 + 1.1977\ b} \tag{44}$$

with $b = \frac{A_o D}{4V_r} = 1.410\ \frac{F_1}{F_3}\ \frac{D}{v\theta}$ for the case of the present analysis with a 0.33 mole fraction sulfate in the sulfur compounds in the melt leaving the scrubber.*

* See footnote on page 31

7. Horizontal Cylinder Reducer Geometry with Separation Baffle Parallel to Cylinder Axis

For the horizontal cylinder reducer geometry with the separation baffle parallel to the axis of the cylinder, the basic equations can be written:

$$NA_o = \frac{LD}{2}(\sin\alpha \quad \sin\gamma) \tag{45}$$

$$NV_r = \frac{LD^2}{8}\left\{\alpha\left(1 - \frac{\sin 2\alpha}{2\alpha}\right) + \gamma\left(1 - \frac{\sin 2\gamma}{2\gamma}\right) + 2\sin\gamma(\cos\gamma - \cos\alpha)\right\} \tag{46}$$

$$A_{ht} = LD\alpha\left(1 + \epsilon\frac{\sin\alpha}{\alpha}\right) + \frac{D^2}{2}\alpha\left(1 - \frac{\sin 2\alpha}{2\alpha}\right) \tag{47}$$

with: $\alpha = \arccos\left(1 - \frac{2d}{D}\right)$

$\gamma = \arcsin 2\delta$

$\delta = \frac{j}{D}$

j = distance from axis of reducer vessel to separation baffle, ft, positive or negative depending upon whether the volume of the oxidation region is smaller or larger than that of the reduction region, respectively.

An optimization of reducer dimensions similar to the one performed for both the vertical cylinder reducer geometry and the horizontal cylinder reducer geometry with the separation baffle perpendicular to the axis of the cylinder yields a minimum value of the effective heat transfer area, A_{ht}, at constant values of the normalized heat loss parameter, Q_L, when the following relationships prevail:

$$D^3 = \frac{8\,NV_r\left(1 + \epsilon\frac{\sin\alpha}{\alpha}\right)}{\left(1 - \frac{\sin 2\alpha}{2\alpha}\right)\left\{\alpha\left(1 - \frac{\sin 2\alpha}{2\alpha}\right) + \gamma\left(1 - \frac{\sin 2\gamma}{2\gamma}\right) + 2\sin\alpha(\cos\gamma - \cos\alpha)\right\}} \tag{48}$$

$$d = \frac{D}{2}(1 \quad \cos\alpha) \tag{49}$$

$$L = D\left(1 - \frac{\sin 2\alpha}{2\alpha}\right)\left\{1 + 2b(\cos\gamma - \cos\alpha)\right\}\frac{1}{1 + \epsilon\frac{\sin\alpha}{\alpha}} \tag{50}$$

$$\left(\frac{Q}{A}\right) = \frac{Q_L}{A_o}\,\frac{b\left\{\alpha\left(1 - \frac{\sin 2\alpha}{2\alpha}\right) + \gamma\left(1 - \frac{\sin 2\gamma}{2\gamma}\right) + 2\sin\alpha(\cos\gamma - \cos\alpha)\right\}}{\alpha\left\{3 + 4b(\cos\gamma - \cos\alpha)\right\}\left(1 + \epsilon\frac{\sin\alpha}{\alpha}\right)} \tag{51}$$

$$\delta = \frac{\sin\alpha}{2} \quad \frac{1 - b\left(\frac{\sin\alpha}{\alpha} - \cos\alpha\right)}{1 + b\left(\frac{\gamma}{\sin\gamma} + \cos\gamma - 2\cos\alpha\right)} \tag{52}$$

with $b = \frac{A_o D}{4V_r}$.

As in the previous cases, the ratio of the volume of the oxidation region to that of the reduction region increases with increasing reducer processing capacity, becoming equal to unity when

$$b = \frac{1}{\frac{\alpha}{\sin\alpha} - \cos\alpha}$$

and hence

$$N = \frac{8\,V_r^{\,2}}{A_o^{\,3}} \frac{\sin\alpha\left\{1 + \frac{\sin\alpha}{\alpha}(2 - 3\cos\alpha)\right\}}{\left(\frac{\alpha}{\sin\alpha} - \cos\alpha\right)^2} \quad \frac{1}{1 + \epsilon\frac{\sin\alpha}{\alpha}}$$

If one assumes, as before, a typical case with a value of expanded melt bed depth to diameter ratio $d/D = 0.40$, and a value of $\epsilon = 0$, equations (48) through (52) become:

$$D^3 = \frac{3.4058\,NV_r}{1 + 0.3648\gamma\,(1 \quad \frac{\sin 2\gamma}{2\gamma}) \quad 0.7149\,(1 \quad \cos\gamma)} \tag{53}$$

$$d = 0.4\,D \tag{54}$$

$$L = 0.8569\,D\left\{1 + 2\,b\,(\cos\gamma - 0.2)\right\} \tag{55}$$

$$\left(\frac{Q}{A}\right) = \frac{Q_L}{A_o} \quad \frac{2.0017\left\{1 + 0.3648\gamma\,(1 \quad \frac{\sin 2\gamma}{2\gamma}) - 0.7149\,(1 \quad \cos\gamma)\right\}}{3 + 4\,b\,(\cos\gamma - 0.2)} \tag{56}$$

$$\delta = 0.4899 \quad \frac{1 \quad 1.1977\,b}{1 + b\left(\frac{\gamma}{\sin\gamma} + \cos\gamma - 0.4\right)} \tag{57}$$

$$\cong 0.4899 \quad \frac{1 \quad 1.1977\,b}{1 + 1.6\,b\left(1 - \frac{5\delta^2}{6} - \frac{\delta^4}{2} - \frac{5\delta^6}{7} \ldots\right)} \tag{58}$$

with $b = \frac{A_o D}{4V_r} = 1.410 \frac{F_1}{F_3} \frac{D}{v\theta}$ for the case of the present analysis

with a 0.33 mole fraction sulfate in the sulfur compounds in the melt leaving the scrubber.*

8. Results

The results of the dimensional optimization of the reducer melt bed for a vertical cylinder reducer geometry are plotted as a function of reducer processing capacity in Figures 6 through 9.

Equations (27) through (29) were used to calculate the melt bed diameter, expanded bed depth, and heat flux for various values of the normalized heat loss parameter (Figures 6, 7, and 8). Since the heat flux is the real independent variable rather than the heat loss parameter, this parameter was plotted in Figure 9 (a cross-plot of Figure 8) as a function of reducer processing capacity at various values of the heat flux.

Special emphasis was given to reducer processing capacities corresponding to 3.125 and 166.7 lb moles/hr of SO_x in the feed gas entering the scrubber, meeting respective requirements of electric power generating capacities of 5 and 267 Mw (pilot plant size, and full scale size of one of three reducers of an 800 Mw plant, respectively).

Equations (23), (24), and (26) were used to calculate the melt bed diameter and heat loss as a function of heat flux for the 5 Mw reducer with expanded melt bed depths of 2 to 4 ft, and the 267 Mw reducer with expanded melt bed depths of 6 to 10 ft. The results are presented in Figures 10 through 15 for the reference case of a maximum superficial gas velocity of 3 ft/sec and a minimum reduction region residence time of 15 minutes, and the two additional cases of a superficial gas velocity of 5 ft/sec with a residence time of 15 minutes, and a superficial gas velocity of 3 ft/sec with a residence time of 30 minutes.

The scope of the present analysis did not allow calculation of optimized reducer dimensions as a function of reducer capacity for the horizontal cylinder reducer geometries. On the basis of Equations (26), (33), and (34), Figures 16 and 17 were plotted to show the reducer length and heat loss as a function of heat flux for the special cases of the 5 and 267 Mw reducers with diameters ranging

---

* See footnote on page 31

from 5 to 10 ft, and from 20 to 30 ft, respectively, with separation baffle perpendicular to the axis of the cylinder.

A discussion of these results is provided in Sections IX. 3. b and IX. 3. c.

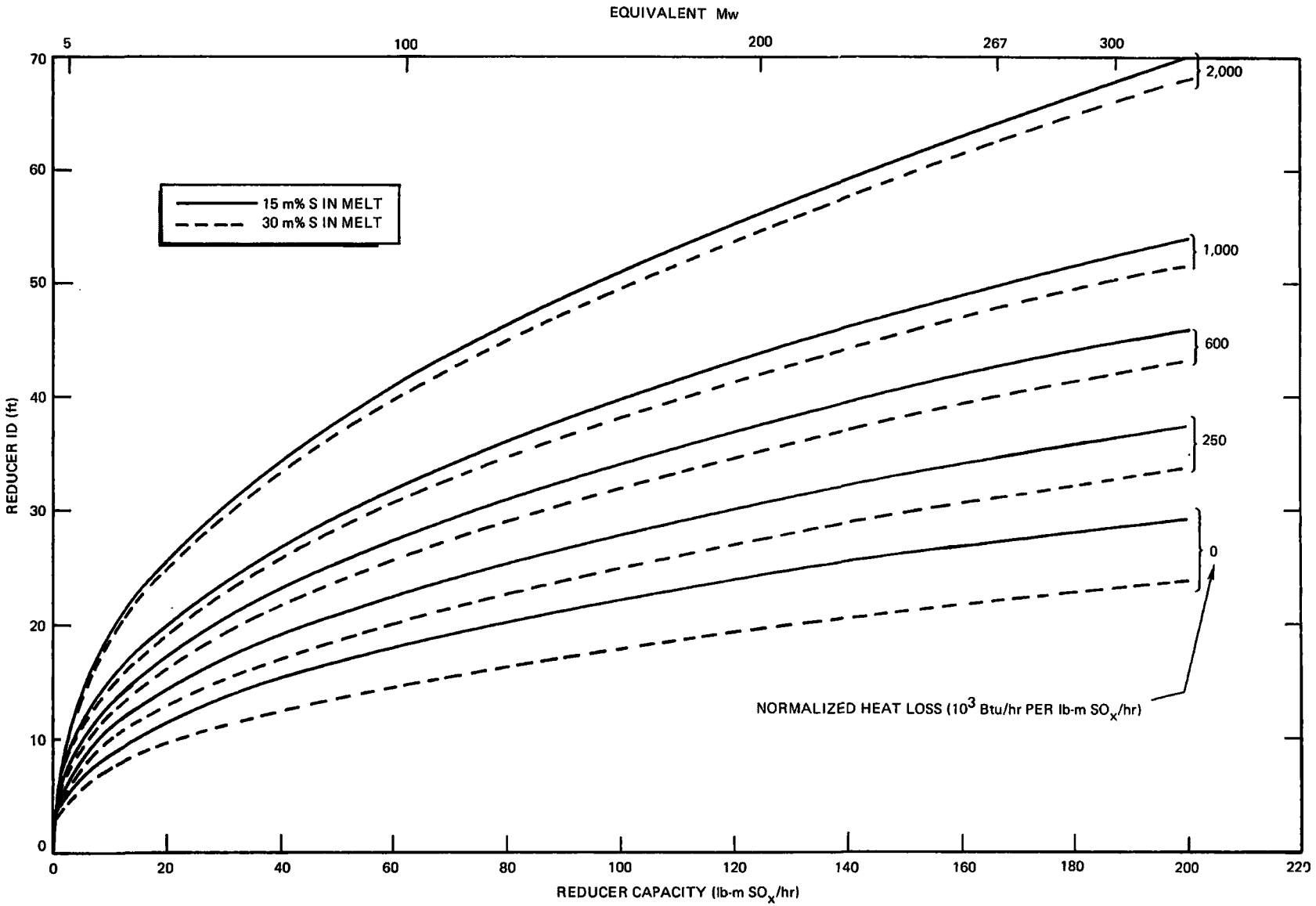

Figure 6. Reducer Diameter as a Function of Processing Capacity

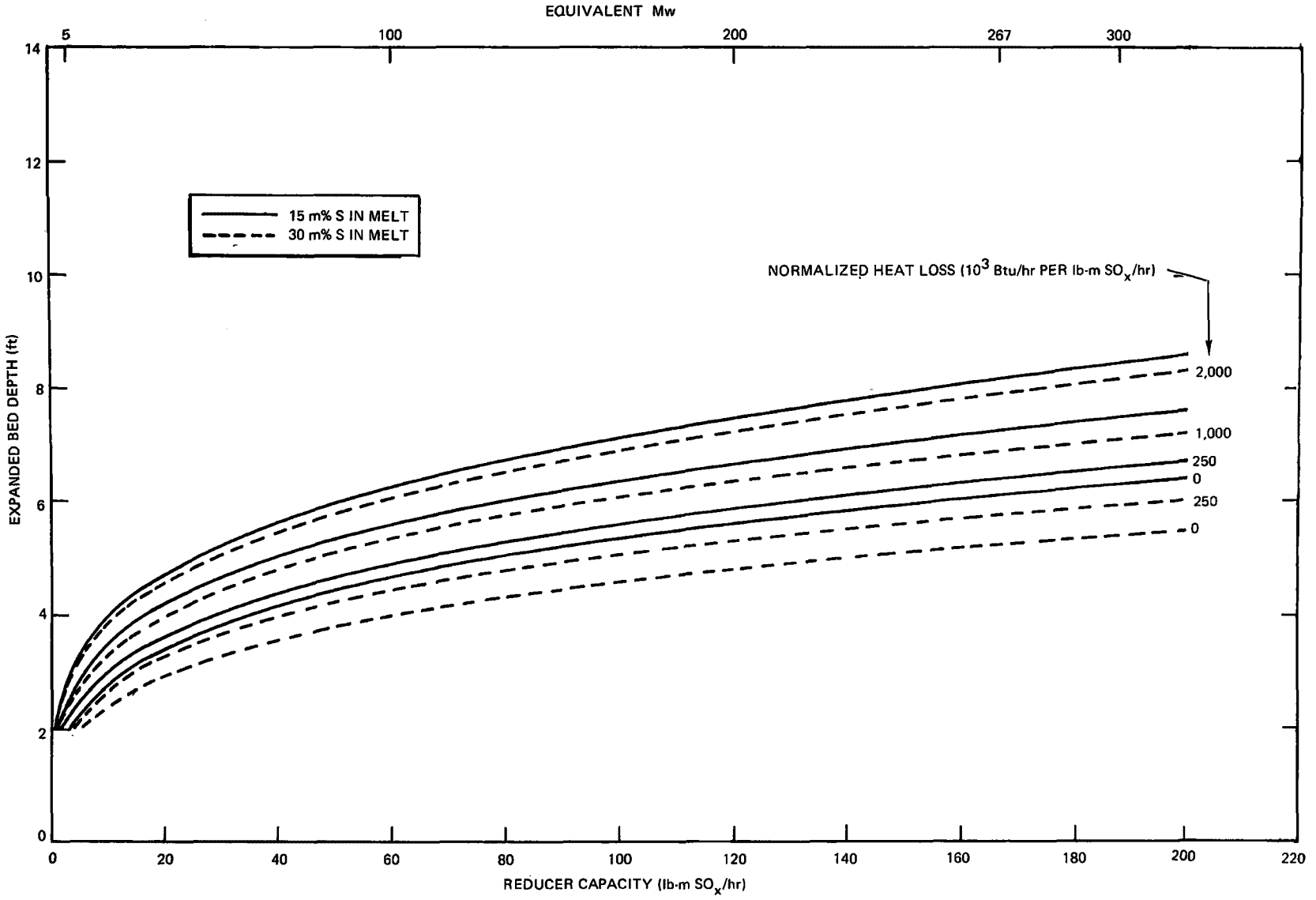

Figure 7. Reducer Bed Depth as a Function of Processing Capacity

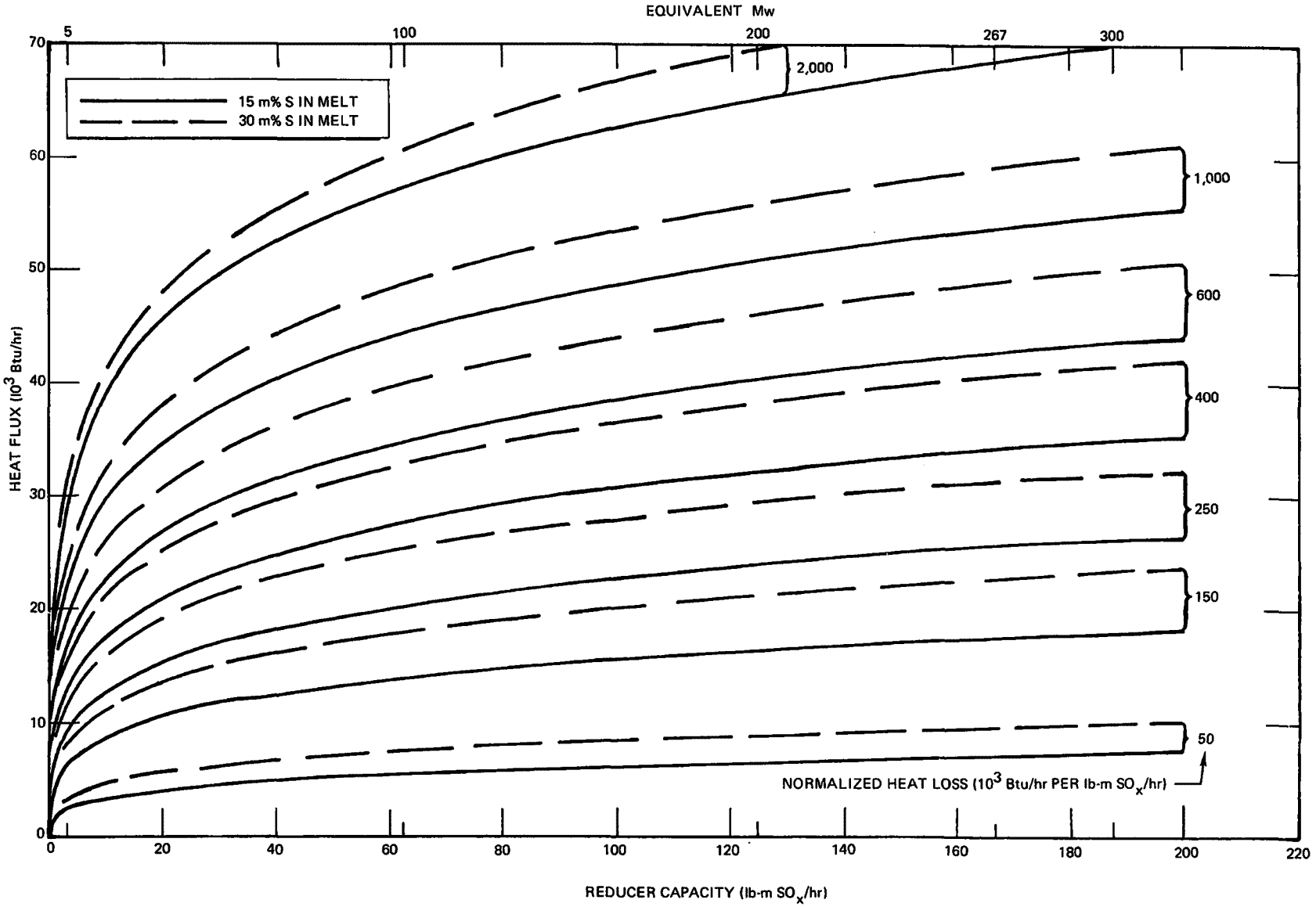

Figure 8. Reducer Wall Heat Flux as a Function of Processing Capacity

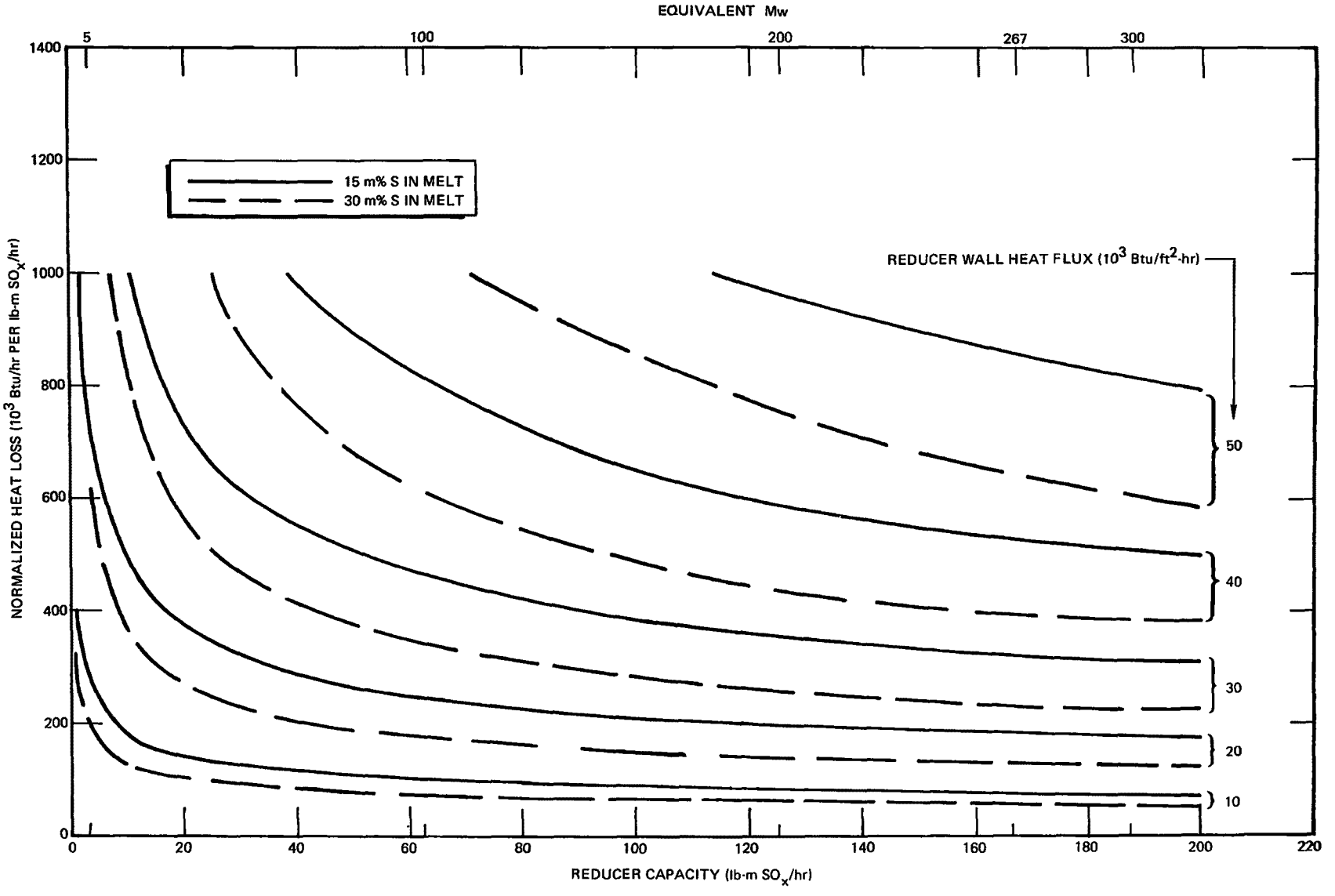

Figure 9. Normalized Heat Loss as a Function of Processing Capacity (Cross-Plot of Figure 8)

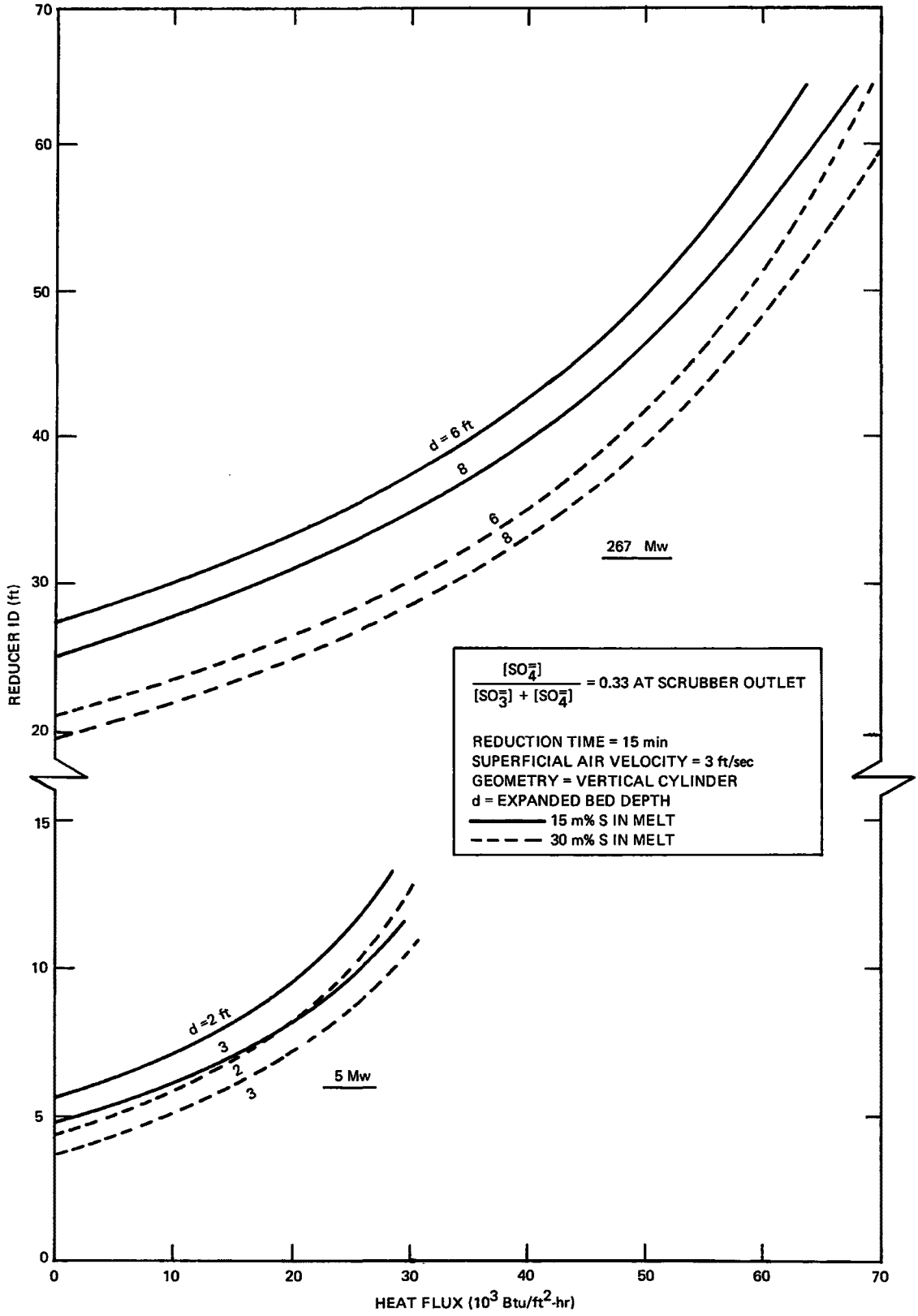

Figure 10. Effect of Heat Flux on Reducer Diameter

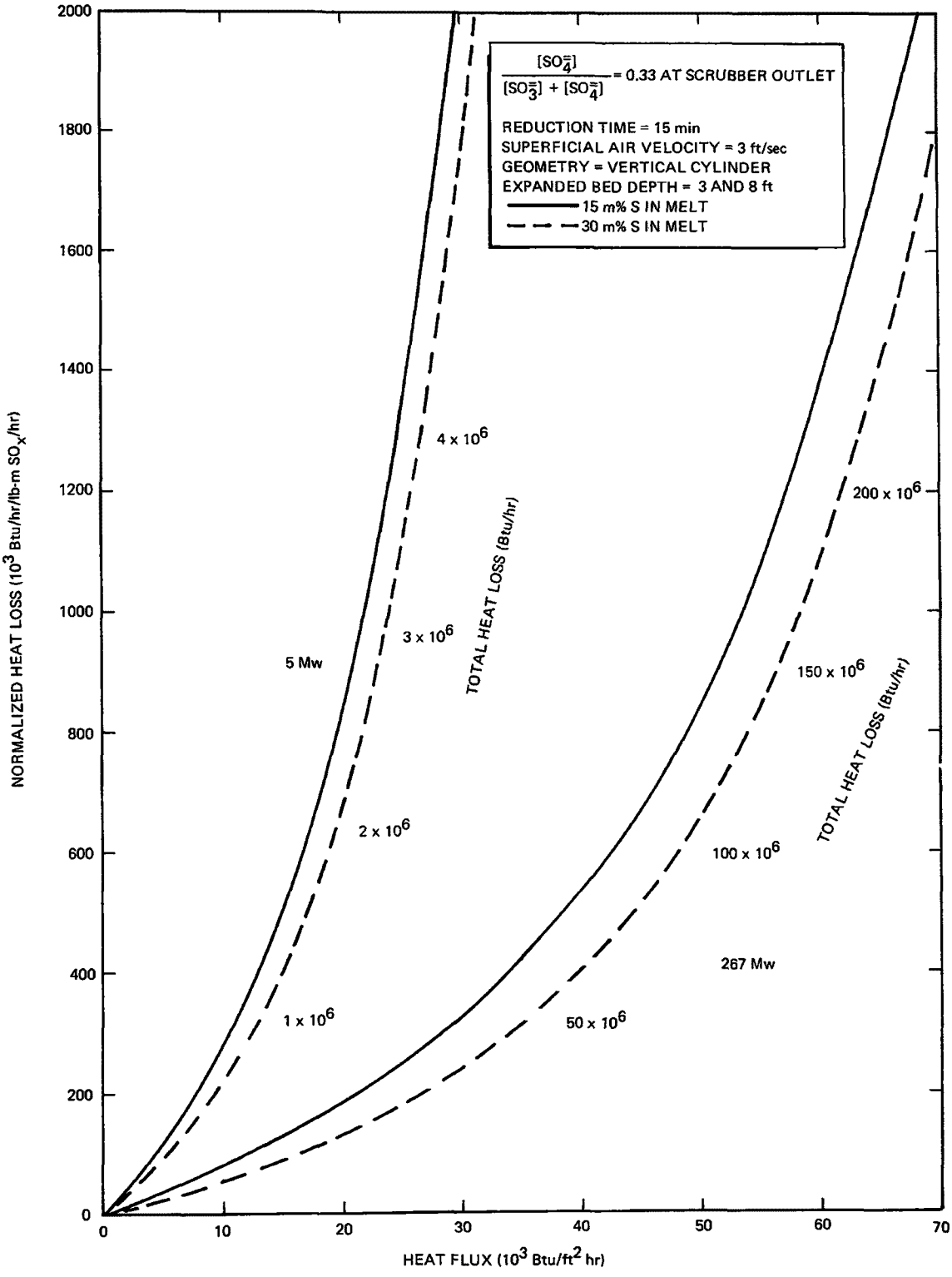

Figure 11. Reducer Bed Heat Loss

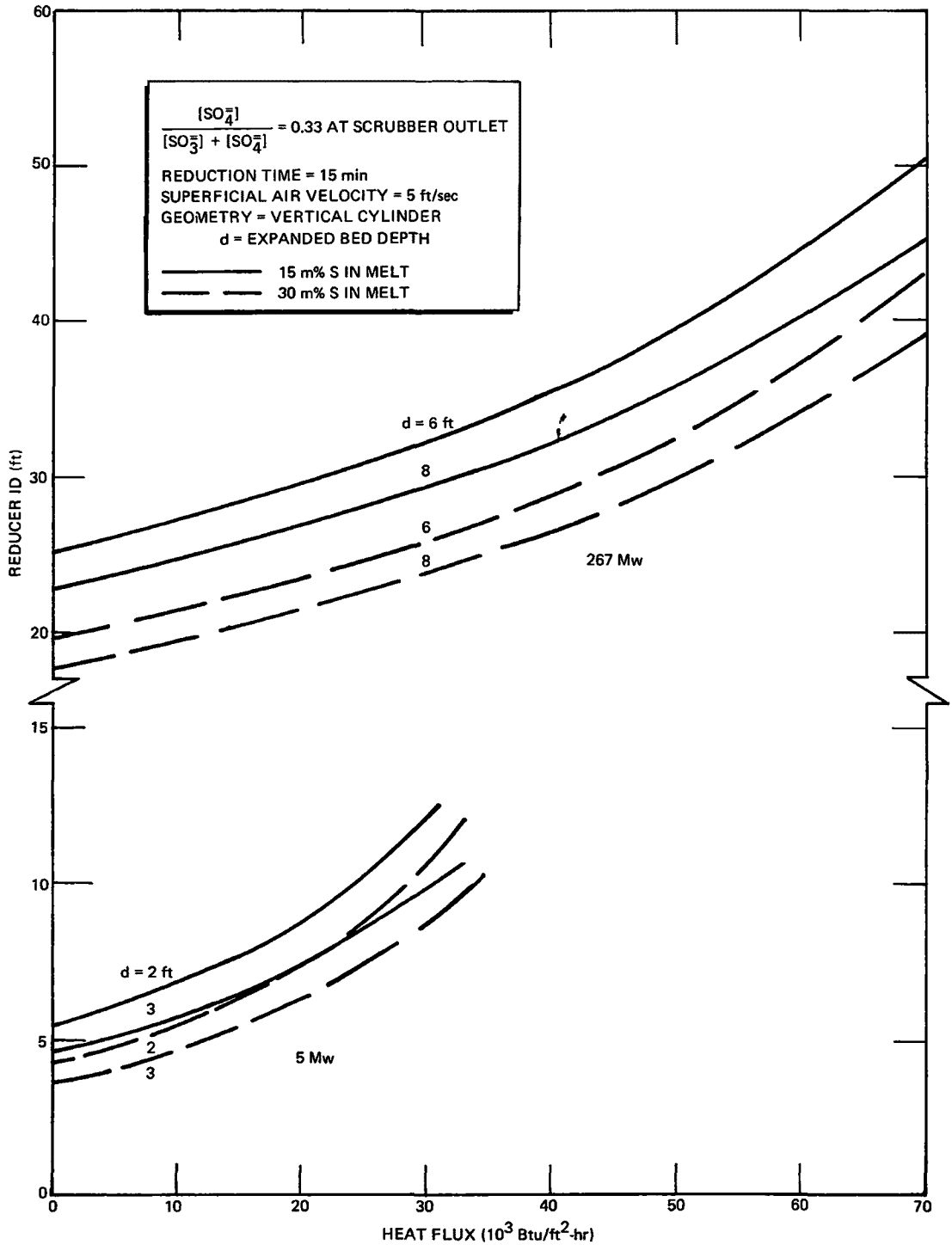

Figure 12. Effect of Heat Flux on Reducer Diameter

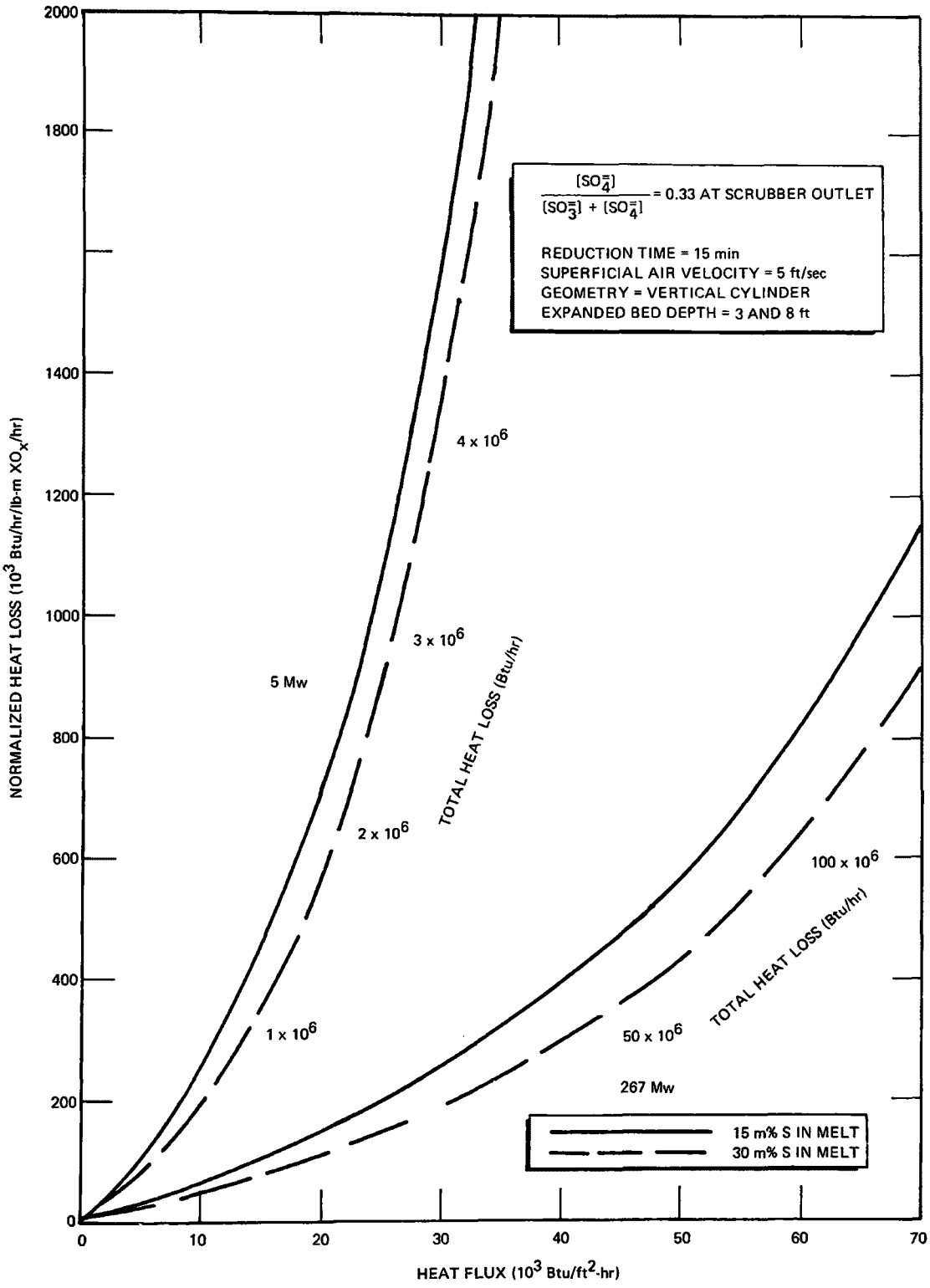

Figure 13. Reducer Bed Heat Loss

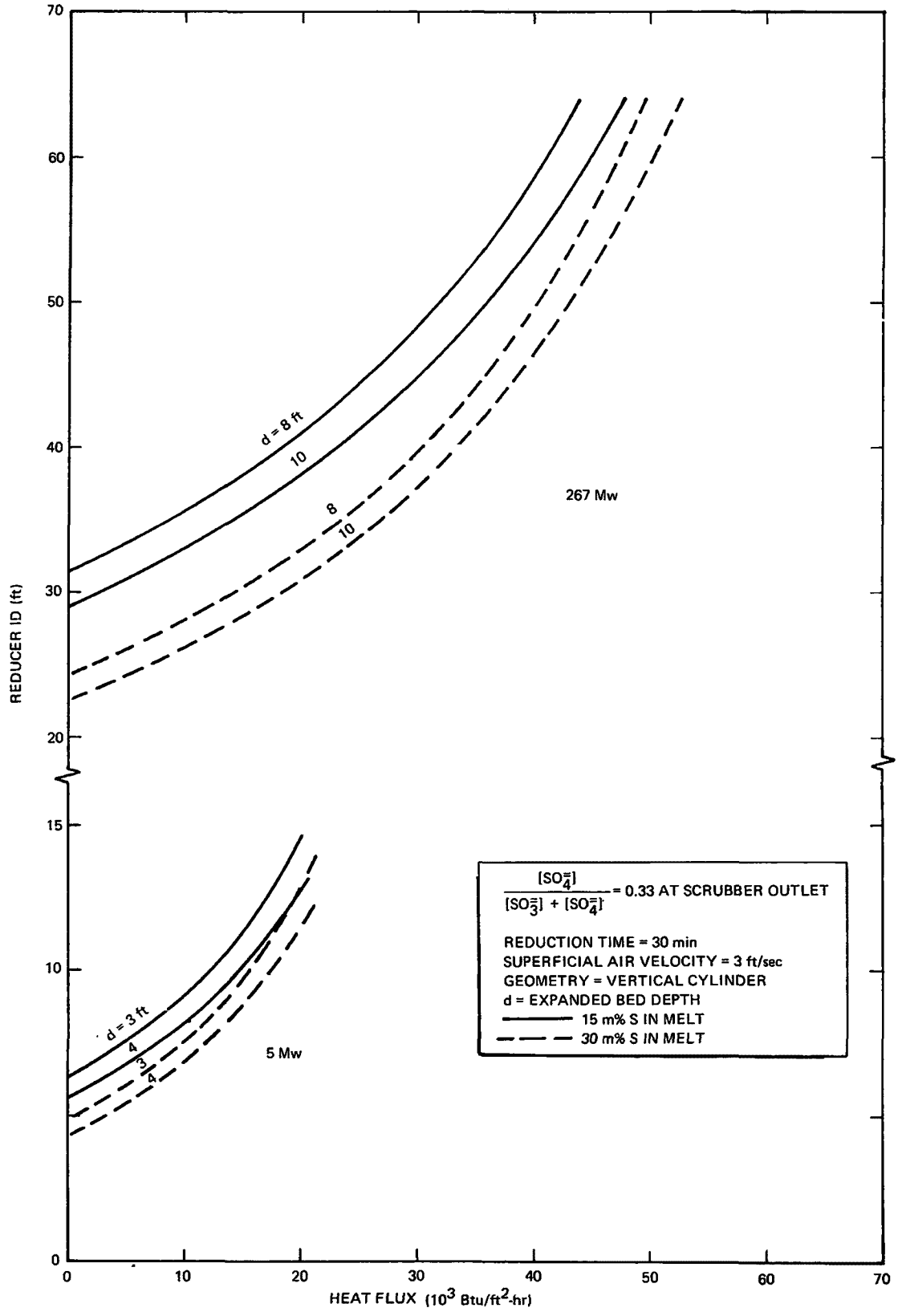

Figure 14. Effect of Heat Flux on Reducer Diameter

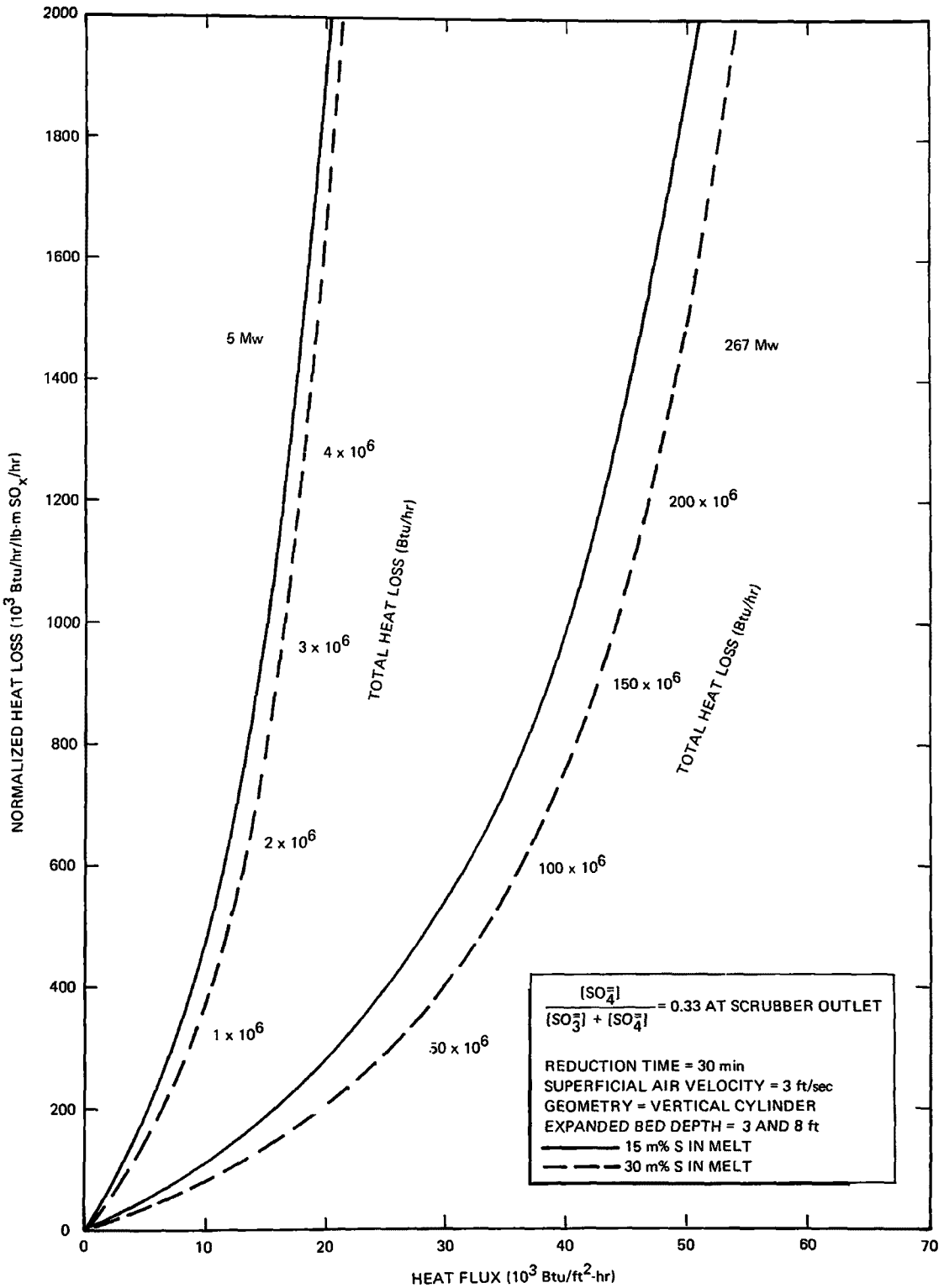

Figure 15. Reducer Bed Heat Loss

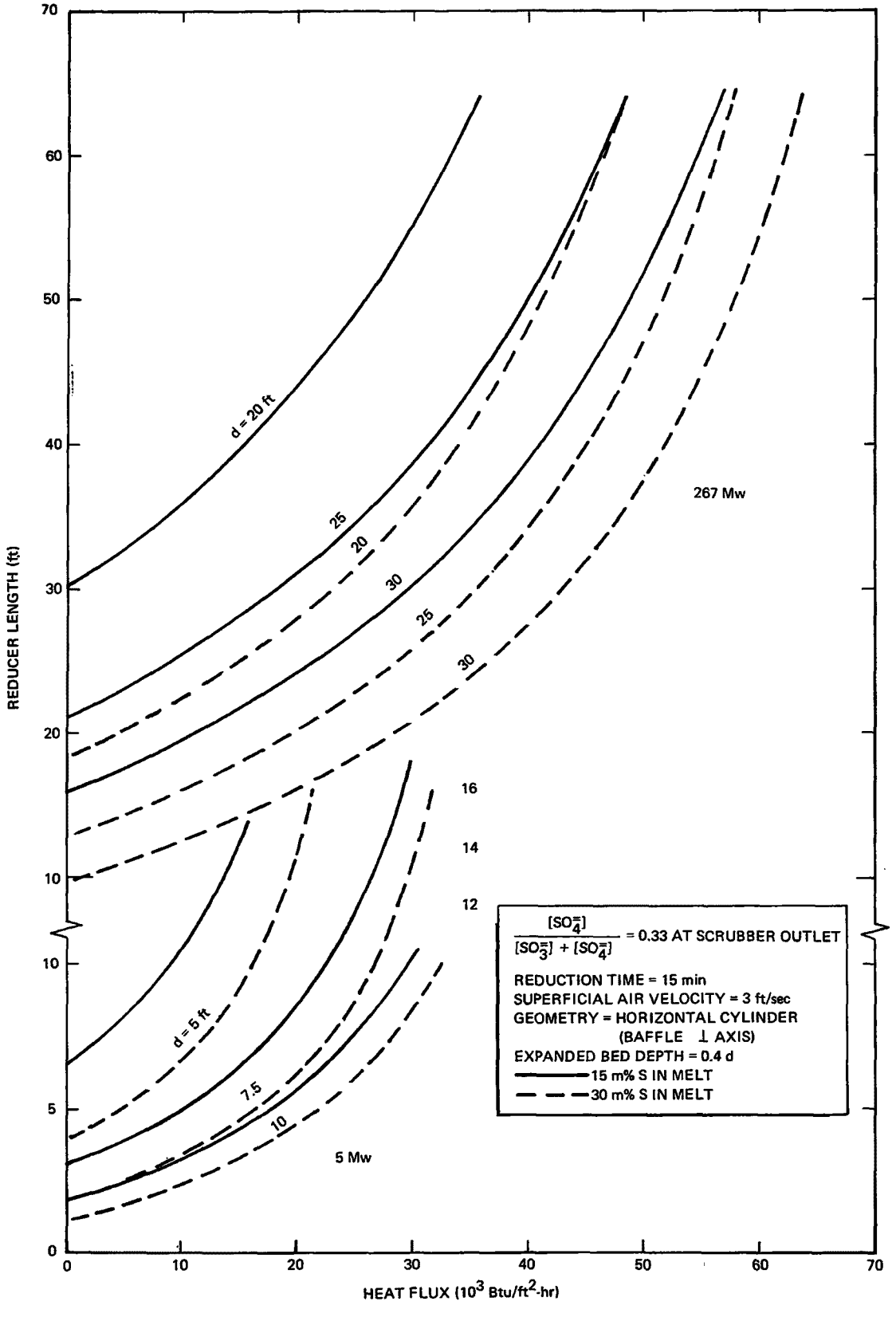

Figure 16. Effect of Heat Flux on Reducer Length

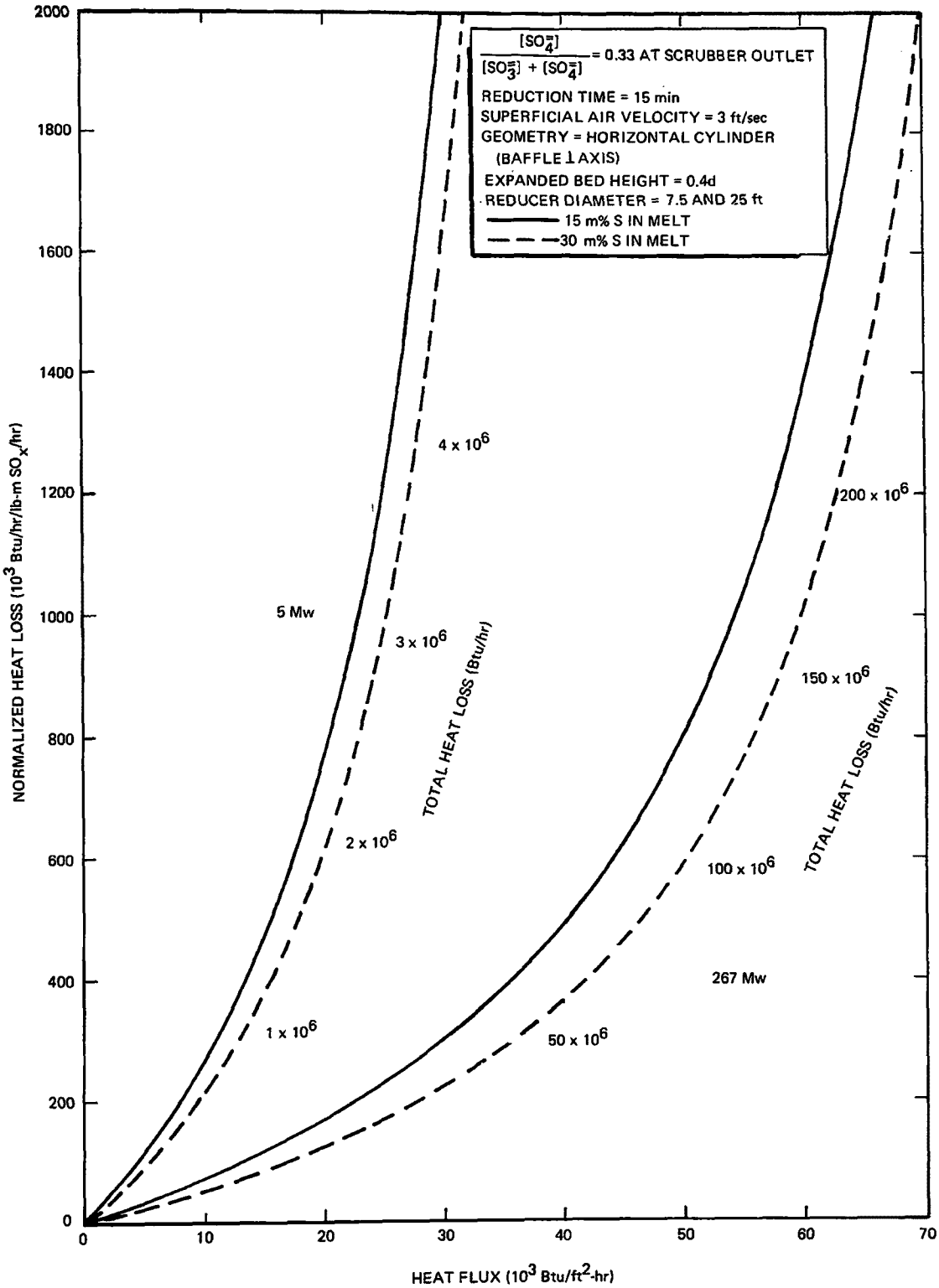

Figure 17. Reducer Bed Heat Loss

VII. REDUCER HEAT LOSS

The previous sections of this report have shown that the coke and air consumption of the reducer and its physical dimensions must be determined on the basis of a heat balance around the reducer melt bed. This heat balance was performed and the key parameters were defined as a function of the independent variable parameter, Q_L, the normalized heat loss from the melt bed, or of the heat flux, (Q/A), at the walls of the reducer vessel in contact with the melt, which is the truly independent variable determining the magnitude of Q_L. The question which must therefore be answered is "What is the magnitude of the heat flux, (Q/A), and how can it be minimized? "

The heat flux at the walls of the reducer vessel is determined by the temperature driving force between the melt and whatever heat sink is provided, and by the thermal resistance between the melt and this heat sink. Both of these can be controlled by the selection of the design concept. As stated in Section IV, the two concepts evaluated in this study are the "frozen melt skull (cold wall)" and the "alumina-liner (hot wall)" concepts. This section of the report provides an estimate of the heat fluxes which one may expect to encounter at the reducer vessel walls in contact with the melt in these two concepts.

1. Estimate of Melt Heat Transfer Coefficient

The heat transfer coefficient across the melt film in contact with the surface of the walls of the reducer vessel controls the heat transfer rate from the melt to the outside of the vessel in the frozen skull design concept. In this concept the temperature of the skull in contact with the melt is fixed (at the freezing point temperature of the melt or approximately 750 °F) and therefore the temperature driving force is fixed. The heat flux at the reducer wall in the frozen skull concept is:

$$(Q/A) = h\,(T_{melt} \quad T_{MP}) \cong h\,(1550\text{-}750) = 800\,h \qquad (59)$$

An accurate knowledge of the expected magnitude of the melt film heat transfer coefficient is therefore essential to the evaluation of the frozen skull reducer design concept.

In the alumina-liner reducer design concept on the other hand, the resistance of the film of melt represents only a small part of the overall resistance to the heat transfer across the walls of the reducer vessel. There is therefore little need for an accurate knowledge of the film heat transfer coefficient in the evaluation of this concept.

The liquid film at the walls of the reducer vessel consists of the carbonate-sulfate-sulfide process melt, containing suspended particles of partially reacted coke. This melt is kept in a highly turbulent state by the flow of air in the oxidation region and by the flow of gases generated in the reduction region. The melt thus represents a multiphase environment with complex circulation patterns for which reliable heat transfer coefficient values can only be obtained experimentally.

Using many simplifying assumptions an attempt was made to obtain an estimate of the magnitude of the melt heat transfer coefficient which one might expect to prevail at the walls of the reducer vessel. For this purpose the film was assumed to consist of a single liquid phase with the physical properties of the carbonate melt at the prevailing temperatures. Preliminary calculations showed that at the low net flow velocities and the relatively high temperature differences encountered in the reducer, natural convection would provide the main contribution to the heat transfer at the walls. The estimate of the heat transfer coefficient was therefore based on McAdams' recommended correlation for natural convection heat transfer for vertical planes and vertical cylinders in the turbulent range:[8]

$$h = 0.13\, k \left(g \frac{\rho^2 c_p}{\mu k} \beta \Delta t\right)^{1/3} = 0.13\, k \left[\frac{g\left(-\frac{\Delta t}{\rho}\frac{d\rho}{dt}\right)}{\left(\frac{\mu}{\rho}\right)\left(\frac{k}{\rho c_p}\right)}\right]^{1/3} \qquad (60)$$

The physical properties used were those of the carbonate melt at the average temperature of the film (approximately 1150 °F in the case of the frozen skull reducer design and 1400 °F in the case of the alumina-liner reducer design).

With these assumptions, the correlation yielded heat transfer coefficient values of 317 and 303 Btu/ft^2 hr °F for the frozen skull and the alumina-liner design concepts, respectively.

Obviously many factors which may have significant effects upon the magnitude of these heat transfer coefficients were neglected in such a calculation. These include the increased turbulence attributable to the flow of gases and to the suspended particulates, the increased effective viscosity due to the presence of the particulates, and the possible effect of gas phase heat transfer. In addition, there are uncertainties in our knowledge of the properties of the melt at the prevailing temperatures and in the correctness of the use of these properties in the correlation at an arithmetic average temperature between that of the bulk melt and that of the walls. It must be noted, however, that even a 10-fold increase in the viscosity values used in the calculations would still yield the relatively high heat transfer coefficient values of 117 and 112 Btu/ft^2 hr °F, respectively.

From the practical point of view, a melt heat transfer coefficient in excess of 50 Btu/ft^2 hr °F yields a reducer wall heat flux in excess of 40,000 Btu/ft^2 hr in the frozen skull design concept (per Equation (59)). Figures 4 through 17 clearly show that a heat flux of this magnitude results in an unacceptably high heat loss from the reducer, with consequent excessive coke and air consumption and large vessel dimensions. The present analysis of the frozen skull design concept was therefore based on a range of melt heat transfer coefficients from 10 to 70 Btu/ft^2 hr °F, which is realistic only if actual melt heat transfer coefficients are found to be lower than predicted on the basis of the simplifying assumptions made above.

In the case of the alumina-liner design concept, a value of 50 Btu/ft^2 hr °F was assumed for the melt heat transfer coefficient. As stated before, this represents only a small fraction of the total heat transfer resistance in this concept and therefore has little effect on its analysis and evaluation.

2. Reducer Wall Heat Transfer in Frozen Melt Skull Concept

The heat transfer rate across the walls of the reducer vessel in the frozen skull design concept can be expressed as follows:

$$(Q/A) = h\,(T_{melt} - T_{MP}) = \frac{T_{MP} - T_{heat\ sink}}{(t/k)_{skull} + (1/U)} \qquad (61)$$

where t_{skull} is the thickness and k_{skull} the thermal conductivity of the skull, and U is the overall thermal conductance from the outer (cold) surface of the skull to the cooling medium of the heat sink.

Equation (61) gives:

$$t_{skull} = k_{skull} \left\{ \frac{T_{MP} \quad T_{heat\ sink}}{h(T_{melt} \quad T_{skull})} - \frac{1}{U} \right\}$$

$$= k_{skull} \left(\frac{r}{h} - \frac{1}{U} \right) \tag{62}$$

with

$$r = \frac{T_{MP} - T_{heat\ sink}}{T_{melt} - T_{MP}} \tag{63}$$

Figure 18 presents a plot of frozen skull thickness as a function of melt film resistance for various values of the temperature parameter, r, and of the thermal conductance to the heat sink, U (the appropriate equivalent skull thickness, k_{skull}/U, must be subtracted from the skull thickness shown on the ordinate for $U \longrightarrow \infty$). The thermal conductivity of the skull was assumed to be 0.5 Btu/ft hr °F.

With a skull freezing temperature of approximately 750 °F and cooling with boiling water at 50 and 600 psia, the parameter r takes values of 0.59 and 0.33, respectively. If one assumes a melt heat transfer coefficient of 50 Btu/ft^2 hr °F and a thermal conductance from the skull to the heat sink of 200 Btu/ft^2 hr °F, the thickness of the skull becomes 40 and 10 mils, respectively. No skull could be maintained if the melt heat transfer coefficient were to be greater than 118 Btu/ft^2 hr °F with 50 psia cooling water and 67 Btu/ft^2 hr °F with 600 psia cooling water.

The temperature parameter, r, is relatively small in the molten carbonate process which uses the low melting eutectic as the molten salt mixture. Other processes may be able to use a higher melting point melt, such as sodium carbonate, with resulting higher values of r. These higher values of r would make it considerably easier to maintain a protective frozen skull of appreciable thickness on the walls of the reducer vessel. A typical value of r in a Kraft furnace,[9] for instance, might be about 1.5, which for the above-considered conditions of h = 50 and U = 200 Btu/ft^2 hr °F would yield a skull thickness of 150 mils with 600 psia cooling water.

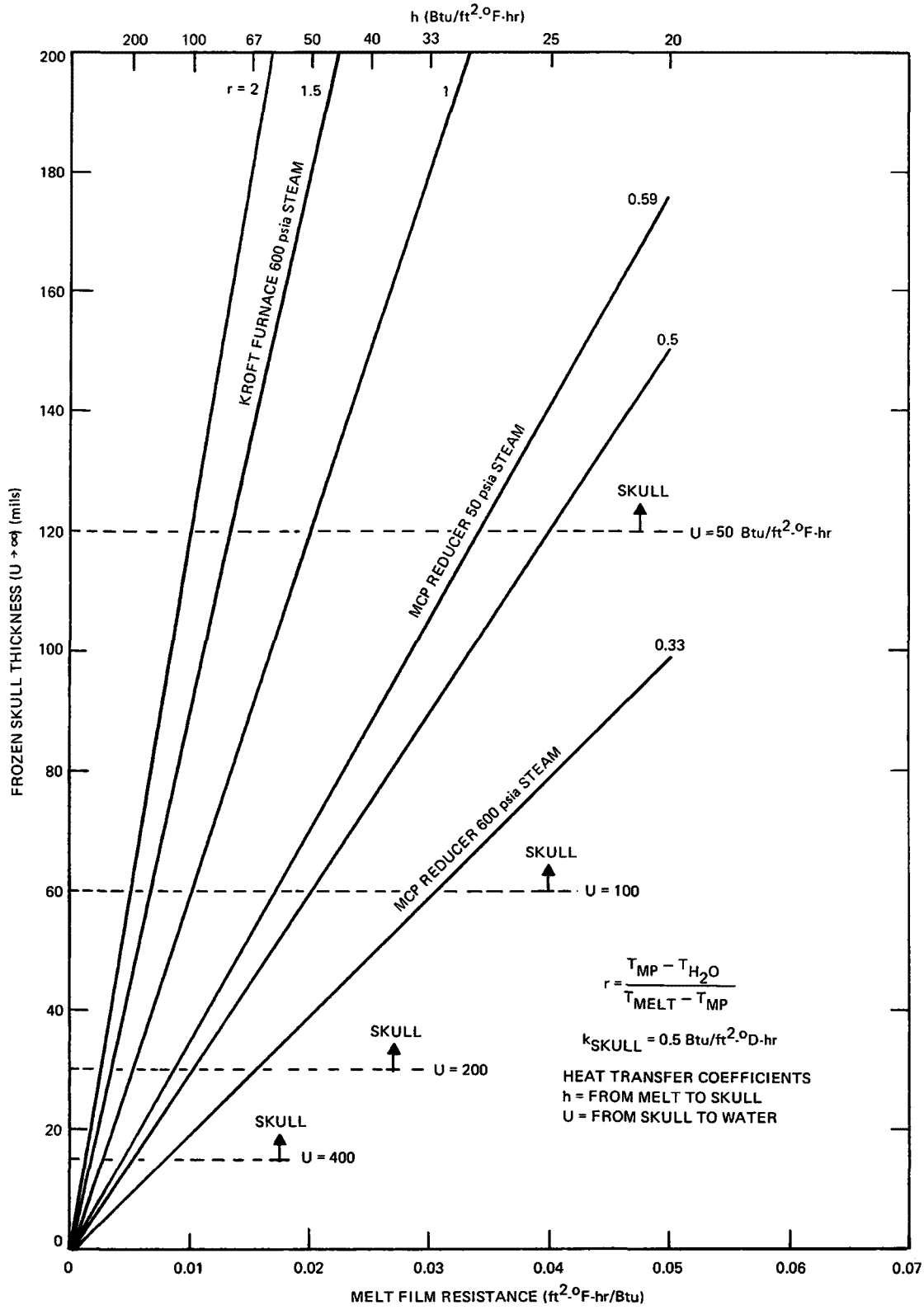

Figure 18. Effect of Parameters h, U, and r on Frozen Skull Thickness

Figure 19 provides a plot of heat flux and frozen skull thickness as a function of melt heat transfer coefficient in the range of 0 to 70 Btu/ft^2 hr °F. It clearly shows how rapidly the heat flux and therefore heat loss increases and the skull thickness decreases with increasing magnitude of the melt heat transfer coefficient.

3. Reducer Wall Heat Transfer in Alumina Liner Concept

In the alumina liner reducer design concept the temperature of the walls in contact with the melt is no longer fixed as it was in the frozen skull concept. The only fixed temperature is that of whatever heat sink is used to absorb the heat loss from the reducer. The heat transfer rate equation across the reducer walls can therefore be written:

$$(Q/A) = \frac{T_{melt} \quad T_{heat\ sink}}{\frac{1}{h} + \left(\frac{t}{k}\right)_{alumina} + \frac{1}{U}} \tag{64}$$

where $t_{alumina}$ is the thickness and $k_{alumina}$ the thermal conductivity of the alumina lining, and U is the overall thermal conductance from the outer (cold) surface of the alumina to the cooling medium of the heat sink.

In this concept it is highly desirable and possibly essential that liquid melt not be allowed to penetrate all the way through the alumina liner to the structural steel of the reducer vessel. The outer (cold) surface of the alumina liner must therefore be kept below the 750 °F freezing point temperature of the melt.

To give visibility to this requirement, the overall thermal resistance across the walls of the reducer was divided into two series components, the thermal resistance from the melt to the outer surface of the alumina, and the thermal resistance from the outer surface of the alumina to the heat sink. For this purpose Equation (64) can be rewritten in the form:

$$(Q/A) = \frac{T_{melt} \quad T_{outer\ alumina}}{\frac{1}{h} + \left(\frac{t}{k}\right)_{alumina}} = U\,(T_{outer\ alumina} \quad T_{heat\ sink}) \tag{65}$$

Figure 20 presents a plot of Equation (65). It shows the heat flux at the walls of the reducer vessel as a function of the outer (cold) side temperature of the alumina lining. The straight lines with the negative slope show the heat flux

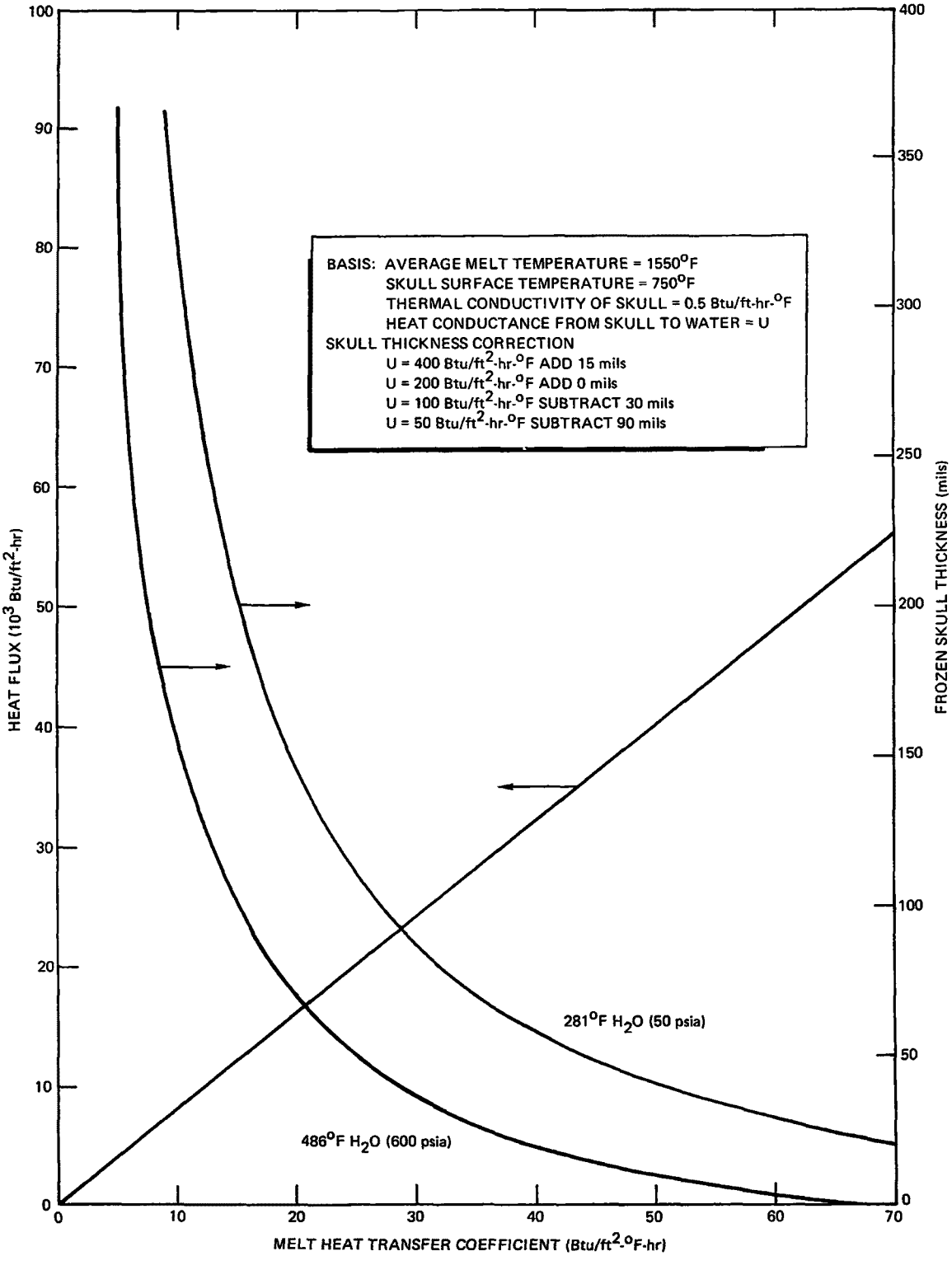

Figure 19. Frozen Skull Reducer Concept — Heat Flux and Skull Thickness

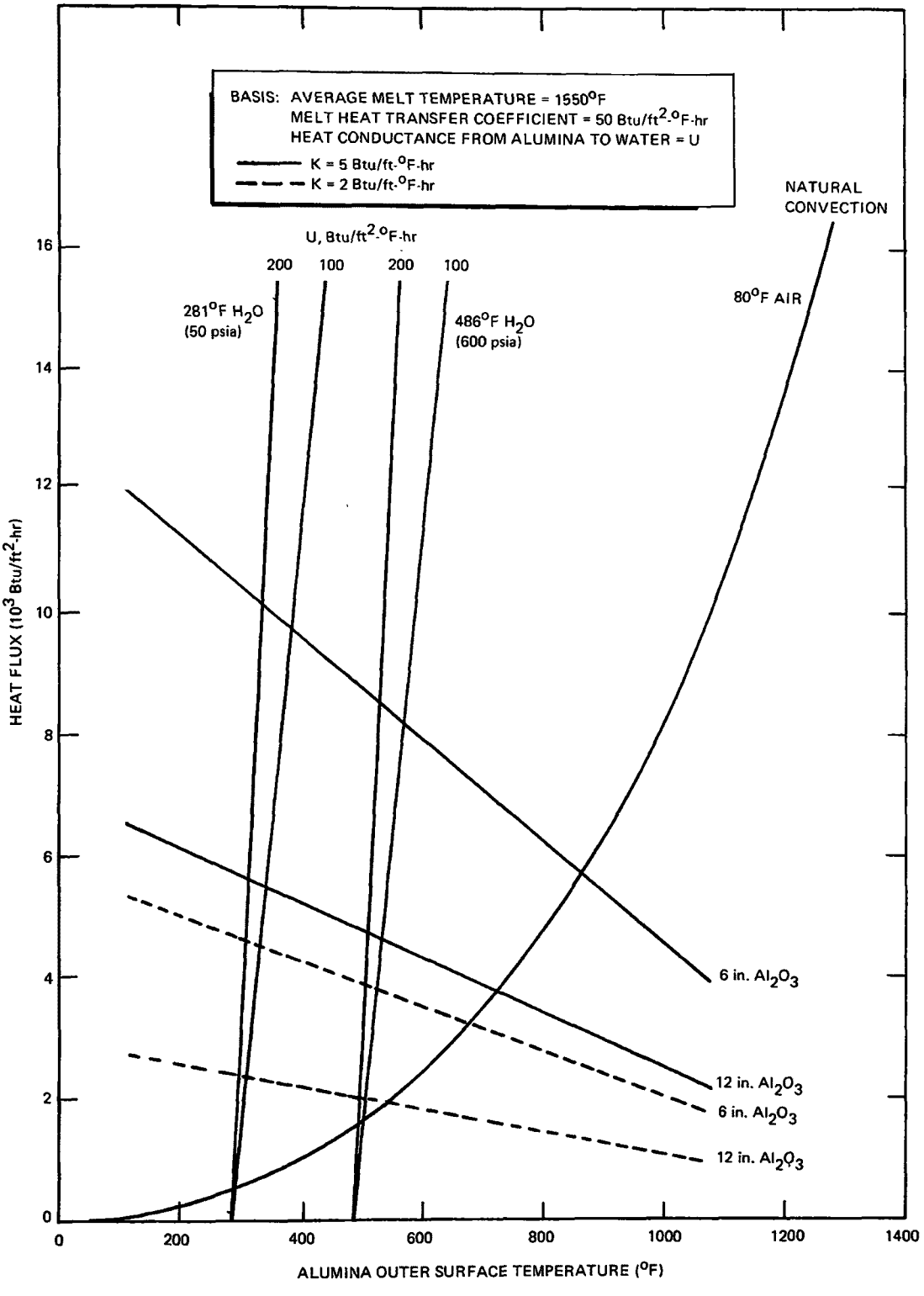

Figure 20. Alumina-Liner Reducer Concept — Heat Transmission and Rejection Capability

transmitted through various alumina linings. The straight lines with the positive slope and the curve show the heat flux which can be rejected from the outside of the lining to various cooling systems. The intersections of the negative slope lines with the positive slope lines and curve provide solutions to the overall heat transfer rate Equation (65) from the melt through the walls of the reducer vessel to an external heat sink.

Figure 20 shows that with natural convection air cooling, approximately 12 inches of high thermal conductivity alumina, such as Monofrax A, are required to keep the temperature of the outer surface of the alumina below 750 °F (a major part of the alumina not in direct contact with the melt could be replaced with a thermally equivalent amount of higher porosity but lower thermal conductivity alumina such as alundum). The corresponding heat flux at the walls of the reducer vessel in contact with the melt is less than 4000 Btu/ft^2 hr. The temperature at the outside surface of the steel reducer vessel is below 750 °F and can be lowered to below 650 °F by a slight increase in thickness of the lining, thus possibly allowing the use of carbon steel for the reducer vessel.

Natural convection air cooling requires a high temperature at the outside surface of the steel reducer vessel and thus does not allow installation of thermal insulation on this surface. If it should prove desirable that the outside temperature of the reducer be below 200 °F, water cooling of the outside surface of the alumina liner, or of the steel surrounding it, is required. Thermal insulation can then be installed around the outside of the cooling pipes to lower the outside temperature of the reducer to whatever temperature is desired. The heat flux at the walls of the reducer in contact with the melt will be around 5000 Btu/ft^2 hr if one uses the equivalent of a 12 inch high thermal conductivity alumina lining. The thickness of lining required can be decreased in this case, but at the penalty of increasing the heat flux and thus the heat loss from the reducer.

In view of the major incentive to minimize heat loss from the melt, the actual design of the reducer will involve the use of a combination of liner materials between the melt and the steel shell of the vessel. Low porosity high thermal conductivity alumina will provide the inner lining in contact with the melt. It will in turn be surrounded by one or several layers of more porous alumina with better thermal insulation properties. Figure 20 shows that a reduction of the heat flux at the walls to below 2000 Btu/ft^2 hr is thus readily achievable with either natural convection air cooling or water cooling of the outside walls of the reducer vessel.

VIII. INTERNAL RECIRCULATION BETWEEN OXIDATION AND REDUCTION REGIONS

The two-region reducer concept is based on the use of melt recirculation between the oxidation and reduction regions to transport the heat generated in the oxidation region into the reduction region. This recirculation must be fast enough on the one hand to transport the required amount of heat without exceeding the specified temperature differential between the top and the bottom of the melt bed. On the other hand it must be slow enough to allow for the required minimum residence time of the melt in the reduction region and thus permit the reduction reaction to proceed to the required degree of completion.

Internal melt recirculation takes place as a result of the difference in effective average densities of the melt in the oxidation and reduction regions. The melt density in the oxidation region is lower than that in the reduction region because:

1) The greater superficial gas velocity in the oxidation region results in a greater bed expansion in that region than in the reduction region.

2) The anticipated non-linearity with distance of heat generation in the oxidation region and heat consumption in the reduction region results in the major part of the melt temperature rise taking place in the lower section of the oxidation region and the major part of the melt temperature drop occurring in the upper section of the reduction region, thus yielding an effective difference in average melt temperature between the two regions and a consequent difference in average melt density.

The density difference of the melt provides the driving force necessary to establish a natural circulation flow pattern between the oxidation and reduction regions of the reducer. Opposing this driving force is the pressure drop resulting from the circulation thus established. The actual internal circulation rate is determined by the equalization of these two forces. Since the main resistance to the flow is provided by the baffle openings connecting the oxidation and reduction regions at the top and bottom of the melt bed, these openings will control the melt recirculation rate and must therefore be sized to provide the rate required to allow transport of the heat and adequate residence time for completion of the reduction reaction.

1. Natural Convection Driving Force

The natural convection driving force is generated by the differences in effective average melt densities between the oxidation and reduction regions of the reducer. Experimental information is presently not available on either the difference in bed expansion which one might expect to prevail, or the non-linearity with distance of the chemical reactions taking place which would establish the average temperature differential between the two regions. The analysis was therefore based on the following somewhat arbitrary assumptions:

1) The net effect of the difference in superficial gas velocity on melt bed expansion and therefore melt density was assumed to be approximately 5 percent. A melt bed expansion by a factor of 1.75 was assumed for the oxidation region and a factor of 1.75/1.05 = 1.67 for the reduction region.

2) The average temperature differential between the oxidation and reduction regions was assumed to be approximately one-third of the temperature rise from the bottom to the top of the melt bed.

The natural convection driving force, ΔP, can be expressed as:

$$\Delta P = d\Delta\rho \tag{66}$$

with:

$$\Delta\rho = \rho_r - \rho_o = 1.05 \frac{\rho_{T_r}}{1.75} - \frac{\rho_{T_o}}{1.75}$$

$$= \frac{0.05}{1.75} \rho_{T_r} + \frac{\rho_{T_r} - \rho_{T_o}}{1.75} \tag{67}$$

where ρ_r and ρ_o are the effective average densities of the melt in the reduction and oxidation regions, respectively, and ρ_{T_r} and ρ_{T_o} are the unexpanded melt densities at the average temperatures prevailing in these regions. It is to be noted that of the two terms on the right hand side of Equation (67) the first represents the effect attributable to different gas flow rates and the second the effect attributable to the prevailing temperature differential.

Using the melt density data of Section III, and assuming an average melt temperature of 1500 °F in the reduction region and an overall temperature rise ΔT from the bottom to the top of the melt bed:

$$\Delta\rho = \frac{0.05}{1.75}\ 110.61 + \frac{18.87 \times 10^{-3}}{1.75}\ \frac{\Delta T}{3}$$

$$= 3.160\ (1 + 1.137 \times 10^{-3}\ \Delta T),\ \text{lb/ft}^3 \tag{68}$$

for $\Delta T = 300\ ^\circ F$:

$$\Delta\rho = 3.160 + 1.078 = 4.238\ \text{lb/ft}^3 \tag{69}$$

Equations (68) and (69) show that, under the conditions of the specific assumptions made above, the effect of differences in gas flow rates is considerably more important than the effect of temperature differences between the oxidation and the reduction regions.

The natural convection driving force is therefore:

$$\Delta P = 3.160\ d\ (1 + 1.137 \times 10^{-3}\ \Delta T),\ \text{lb/ft}^2 \tag{70}$$

2. Pressure Drop

Internal recirculation of the melt between the oxidation and reduction regions of the reducer results in a pressure drop across the openings (orifices) in the baffle between these two regions at the top and bottom of the melt bed, plus an additional pressure drop for the flow through each region. The pressure drop across the orifices can be expected to form the major part of the total pressure drop. For simplifying purposes one can write:

$$\Delta P = q\ \Delta P_{or} \tag{71}$$

where ΔP_{or} is the pressure drop across both orifices and q is a proportionality factor somewhat larger than unity.

The orifice equation can be written:

$$\Delta P_{or} = \left\{\frac{1}{2g}\ \left(\frac{V}{cA_{or}}\right)^2 \rho\right\}_1 + \left\{\frac{1}{2g}\left(\frac{V}{cA_{or}}\right)^2 \rho\right\}_2 \tag{72}$$

where V is the volumetric flow rate, A_{or} the orifice area, c the orifice discharge coefficient, and the subscripts 1 and 2 refer to each of the two orifices.

Assuming both orifices to have the same area and approximately the same volumetric flow, and using an average value of the melt density, Equation (72) becomes:

$$\Delta P_{or} = \frac{\rho}{g} \left(\frac{V}{cA_{or}}\right)^2 \tag{73}$$

Therefore:

$$\Delta P = \frac{q\rho}{g} \left(\frac{V}{cA_{or}}\right)^2 \tag{74}$$

V can be expressed as a function of the heat transported from the oxidation to the reduction region and the temperature difference between the top and bottom of the melt:

$$V = \frac{NQ_T}{\rho c_p \Delta T} \tag{75}$$

where Q_T is the normalized heat transport, as given by Equations (9) or (10).

$$\therefore \Delta P = \frac{q}{g\rho} \left(\frac{NQ_T}{c_p \Delta T} \frac{1}{cA_{or}}\right)^2 \tag{76}$$

Arbitrarily assuming that the unaccounted-for pressure drop may represent about 20% of the pressure drop across the orifices results in an approximate value of $q = 1.20$. Substitution in Equation (76) of the appropriate average values of ρ and c_p and a typical orifice discharge coefficient of 0.61 yields:

$$\Delta P = 6.127 \times 10^{-10} \left(\frac{NQ_T}{A_{or} \Delta T}\right)^2, \text{ lb/ft}^2 \tag{77}$$

This is the pressure drop resulting from the required melt recirculation between the oxidation and reduction regions of the reducer. The value of Q_T can be obtained from equations (9) or (10).

3. Orifice Size

From equations (70) and (77):

$$A_{or} = 2.475 \times 10^{-5} \frac{NQ_T}{\Delta T \sqrt{\Delta P}}$$

$$= 1.392 \times 10^{-5} \frac{NQ_T}{\Delta T \sqrt{d\,(1 + 1.137 \times 10^{-3}\, \Delta T)}}, \text{ ft}^2 \tag{78}$$

Substitution of the value of Q_T from equation (10) yields:

$$A_{or} = \frac{1.2\ F_2}{\Delta T \sqrt{1 + 1.137 \times 10^{-3}\ \Delta T}} \frac{N}{\sqrt{d}},\ ft^2 \tag{79}$$

For $\Delta T = 300\ °F$:

$$A_{or} = 0.003453\ F_2\ \frac{N}{\sqrt{d}},\ ft^2 \tag{80}$$

Typically the openings in the baffle at the top and bottom of the melt between the oxidation and reduction regions may be rectangular, with a length possibly equal to one-quarter of the internal diameter, D, of the reducer. Under these conditions the width, w, of these openings would be:

$$w = 0.1657\ F_2\ \frac{N}{D\sqrt{d}},\ \text{inches} \tag{81}$$

Figure 21 presents a plot of orifice width as a function of reducer capacity, based on the use of Equation (81) with the values of D and d obtained in Section VI (Figures 6 and 7). In view of the several rather arbitrary assumptions made it cannot be considered to represent anything more than trends and a very rough approximation of the actual size of the orifices required. Nevertheless it does show that no difficulty should be expected in obtaining adequate recirculation of the melt and that the orifices must be rather small even in large reducer units to control the recirculation rate to provide the minimum melt residence time in the reduction region required for completion of the reduction reaction.

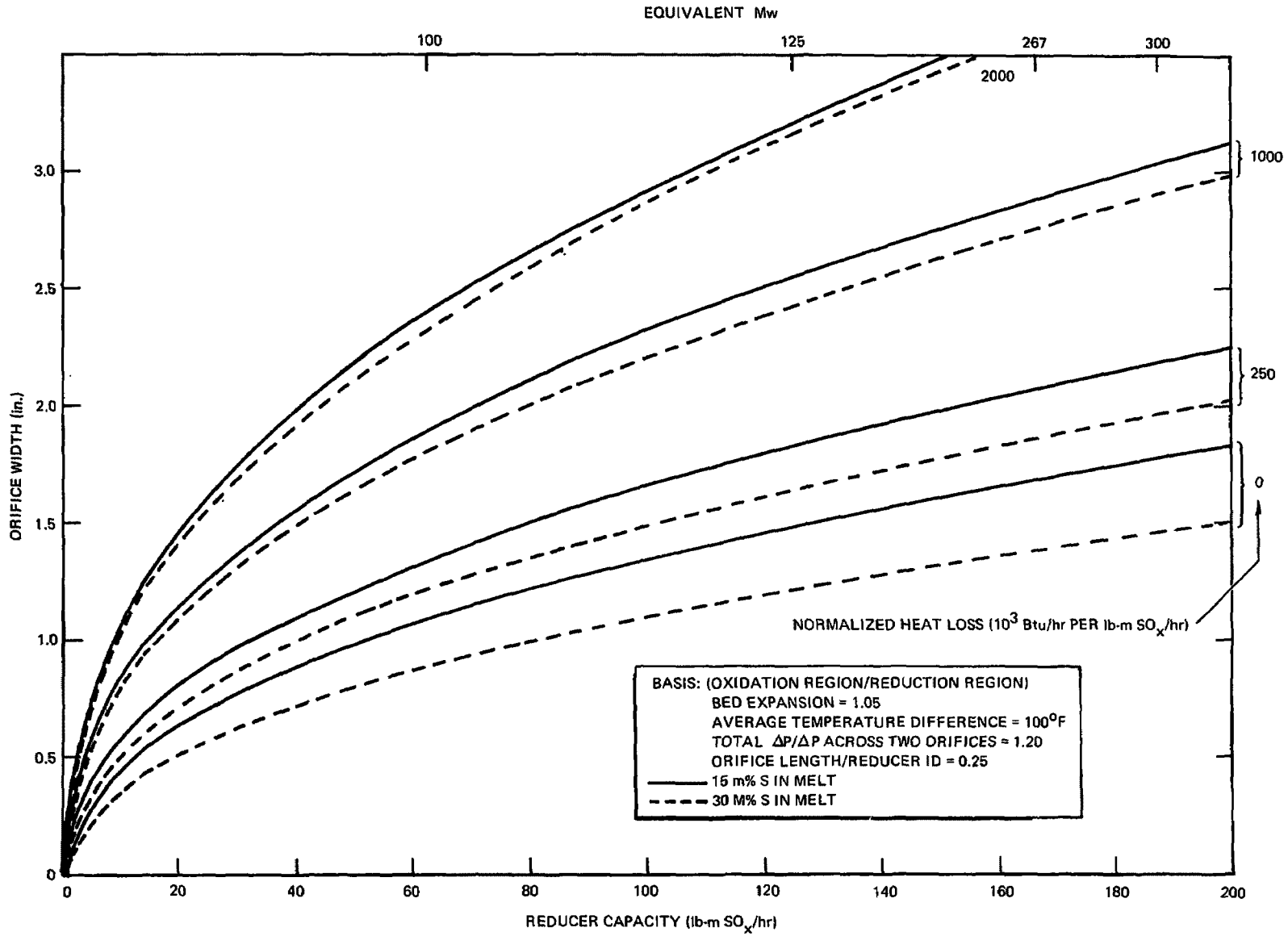

Figure 21. Reducer Baffle Orifice Width as a Function of Processing Capacity

IX. DISCUSSION AND CONCLUSIONS

1. Basis of Analysis

A meaningful discussion of the results obtained in this study of the molten carbonate reducer requires a review of the technical approach and parameters on which it has been based. A diagrammatic flow-sheet of the steps involved in the procedure used to size the reducer and determine its coke and air requirements is shown in Figure 22. This figure also lists the independent variables considered, the system constraints involved, and the results obtained.

a. Technical Approach

Starting from a mass balance around the reducer, a heat balance (1) yields the coke (2) and air (3) requirements. The air requirement combined with a superficial air velocity limitation determines the cross-sectional area of the oxidation region of the reducer (4). The air requirement also determines the amount of heat which must be transported from the oxidation region to the reduction region of the reducer and therefore, in combination with the temperature rise from the bottom to the top of the melt bed, determines the melt recirculation rate required to transport this heat (5). The melt recirculation rate, and the required minimum melt residence time in the reduction region determine the required volume of the melt bed in this region (6). This volume in conjunction with an assumed bed depth yields the cross-sectional area of the reduction region (7). Adding the cross-sectional areas of both regions gives the normalized total cross-sectional area of the reducer per unit SO_x input into the molten carbonate system (8). The cross-sectional area for the actual SO_x input is then calculated, yielding the reducer diameter (9). This in turn determines the area for heat transfer from the melt bed to the walls of the reducer in contact with the melt (10). This area is minimized, thus yielding an optimized relationship between the melt bed diameter and depth. Finally the value of the heat flux at the reducer walls in contact with the melt is obtained and matched with the actual design heat transfer rate for a given reducer design concept (11). The

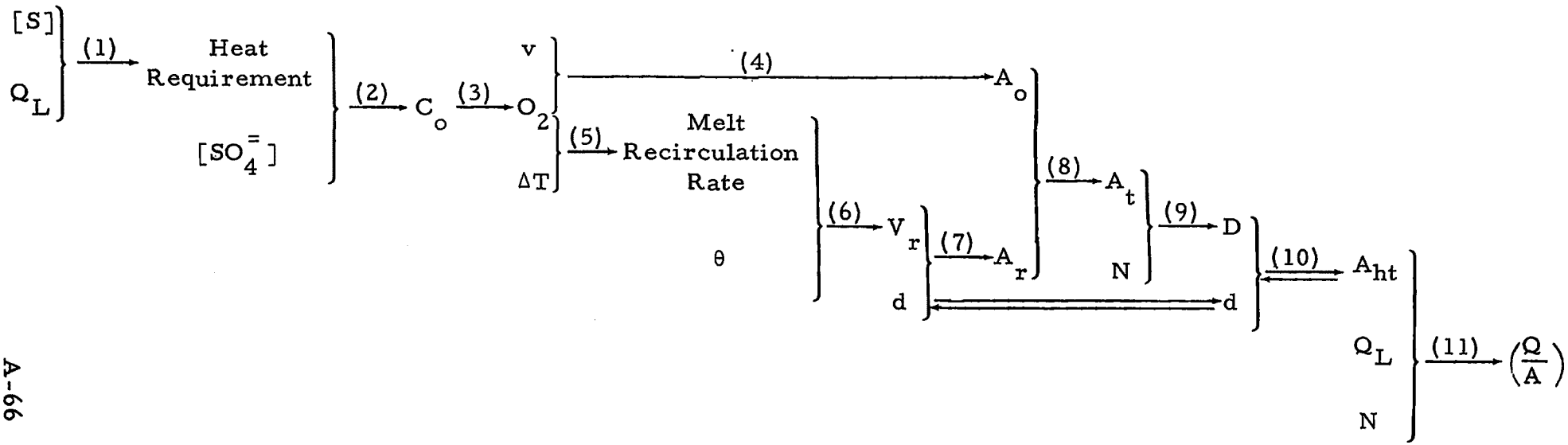

Independent Variables

- N
- Q_L

System Constraints

[S]	=	0.15 + 0.30
$[SO_4^=]$	=	0.33
v	=	3 ft/sec
θ	=	15 min
ΔT	=	300°F

Results

C_o (coke)	Figure 4
O_2 (air)	Figure 5
D	Figure 6
d	Figure 7
$\left(\frac{Q}{A}\right)$	Figure 8 + 9

Figure 22. Reducer Analysis Schematic Diagram

optimization shown by a set of double arrows in Figure 22 is a heat loss minimization and therefore does not take into account any other considerations which may influence the overall optimization of the reducer design.

b. Independent Variables

The key independent variable, aside from the obvious and trivial one of processing throughput, N, is the heat loss from the melt bed to the walls of the reducer vessel in contact with the melt, expressed in this analysis by its normalized value, Q_L. This is as might be expected since the molten carbonate reducer is basically a furnace designed to provide the heat and space requirements for the reduction of the alkali metal sulfates dissolved in the carbonate melt. The net heat generated by the oxidation of the excess coke fed into the reducer provides the heat required for the reduction of the sulfates in the process melt, the heat required for preheating the feed streams to the operating temperature of the reducer, and the heat losses to the walls of the vessel in contact with the melt. Once the processing capacity of the reducer has been specified, the reduction and preheat requirements are established, and the only variable which can be controlled by the design of the unit is the heat loss to the walls. This heat loss is determined by the heat flux at the walls of the vessel in contact with the melt. The heat flux is therefore the real independent variable. It is controlled by the nature of the heat sink and the thermal resistances at and through the walls, and therefore by the design concept and physical dimensions involved. In this analysis the normalized heat loss was varied from 0 to 2×10^6 Btu/hr per lb mole/hr SO_x, with lower values generally achievable in large capacity reducers and higher values prevailing in small capacity units.

c. System Constraints

As shown in Figure 22 the major constraints considered in the present study were the concentration of sulfur compounds in the molten carbonate melt, $[\overline{S}]$, the fraction of these sulfur compounds present in the sulfate state in the melt leaving the scrubber, $[\overline{SO_4^=}] = 1-a$, the superficial air velocity in the oxidation region region, v, the melt residence time in the reduction region, θ, and the temperature differential between the top and the bottom of the melt bed, ΔT. Some of the other constraints listed in Section III include the composition of the coke, and the extent of initial preheat of the air feed into the reducer, the extent of sulfite disproportionation upstream of the reducer, the extent of completion of the chemical reactions involved, and the geometry of the reducer vessel.

The concentration of sulfur compounds in the carbonate melt, $[S]$, should be as high as possible to minimize the melt flow requirement, with consequent minimization of equipment and piping sizes throughout the system. With respect to the reducer, the main effect of melt flow rate is upon the melt preheating requirement and therefore the overall heat requirement. Another effect is on the contribution of the net melt flow through the reducer to the total flow rate of melt through the reduction region and therefore upon the volume of the bed required to meet the reduction reaction residence time requirement.

The maximum allowable concentration of sulfur compounds in the melt is determined by the solubility of the least soluble of these compounds at the operating temperatures of the various steps of the process. The controlling solubility appears to be that of the alkali metal sulfides in the melt to be cooled in the quench tank upon discharge from the reducer (the possibility of the presence of these sulfides in the actual form of thiocarbonates may provide some relief from this constraint). It is expected that a 30 mole per cent concentration will be acceptable, but the possibility exists that the maximum allowable concentration may be as low as 15 mole per cent. The reducer analysis, therefore, was performed for both cases of 30 and 15 mole per cent sulfur compounds in the melt.

The oxidation state of the sulfur compounds in the melt leaving the scrubber is determined by the ratio of SO_3 to SO_2 in the feed gas to the scrubber, the amount of melt recycle directly back to the scrubber, the amount of sulfate returned to the scrubber from the reduction-regeneration system, and the extent of sulfur compound oxidation taking place in the scrubber itself. The greater the extent of oxidation of the sulfur compounds, the greater will be the amount of coke required for their reduction as well as the amount of coke required to supply the heat for this reduction. For purposes of the present study, the effect of the oxidation state of the sulfur compounds in the melt leaving the scrubber upon the coke and air requirements of the reducer has been shown as a function of the variable parameter $[SO_4^{=}]$. In the remainder of the analysis, the scope of the work limited the effort to the case of a single value of the sulfate fraction, 33 mole per cent, as a reasonable approximation to most of the conditions encountered in actual practice.

For a given air feed rate requirement the maximum allowable superficial gas velocity determines the minimum required cross-sectional area of the oxidation region of the reducer. As the gas velocity is increased the expansion of the melt bed increases. On the basis of the experimental data presented in Reference (6) on the expansion of beds with a quiescent height in excess of one foot, a value of 3 ft/sec was selected for the maximum allowable superficial air velocity, v, in the oxidation region. The corresponding total expansion of the melt bed was assumed to be approximately 75 per cent. Most of the analysis was done at this velocity. The possible improvement to be achieved if the superficial air velocity could be increased to 5 ft/sec was evaluated for the special cases of a 5 Mw and a 267 Mw reducer capacity.

For a given melt throughput through the reduction region of the reducer the volume of this region is determined by the minimum residence time required to allow the reduction reaction to proceed to the desired degree of completion. The data of Reference (7) indicate that at temperatures above 1472 °F (800 °C) the reaction time required to achieve 95 per cent reduction is less than half an hour. The present study has been based on a minimum reduction region residence time, θ , of 15 minutes since the reaction temperature ranges from 1700 to 1400 °F. The possible penalty which might result if the residence time had to be increased to 30 minutes was evaluated for the special cases of a 5 Mw and a 267 Mw reducer capacity.

Another parameter which may be considered either as a constraint or an independent variable is the temperature differential, ΔT, between the top and bottom of the reducer melt bed. The larger the temperature differential, the smaller will be the internal melt recirculation requirement, and therefore the volume of the reduction region melt bed required to satisfy the minimum residence time requirement. The temperature at the top of the bed, however, must be kept as low as possible to minimize the potential problems associated with the structural materials of the reducer and the decomposition of the carbonate salts. The temperature at the bottom of the bed must be high enough to allow the reduction reaction to proceed at a reasonable rate. In this analysis the top and bottom temperatures of the melt bed were selected as 1700 and 1400 °F, respectively, with a consequent temperature differential of 300 °F, considered as a fixed constraint throughout the study.

2. Limitations of Present Study

The reducer analysis performed in this study is believed to provide a reasonable approximation to the actual process performance of a two-region molten carbonate reducer, and to the effect of key parameters upon this performance. It also provides a starting baseline for the more detailed process analysis to be performed in conjunction with the actual design of such a reducer and the evaluation of performance data to be developed from future experimental work.

It must be emphasized, however, that this analysis has of necessity had to be based on the limited experimental information available at this time. The following qualifications must be noted:

a) The present study is concerned only with the process engineering aspects of the reducer design. It does not take into account mechanical and structural problems, such as method and location of process stream introduction, distribution, and discharge, minimization of melt carry-over, installation of vessel lining and baffle.

b) The analysis assumes perfect separation of the oxidation and reduction functions. It assumes that all the direct air oxidation takes place through the oxidation of sulfide to sulfate and that the oxidation of the coke occurs only as a result of reduction of sulfate to sulfide. This entails transport of a larger amount of heat between the two regions of the reducer than would otherwise be necessary. The analysis also ignores any potential contribution of oxidation of the hydrogen in the coke to the heat balance around the melt bed, and any lack of contribution or other effects associated with the volatile matter in the coke.

c) The analysis assumes idealized component and flow distributions in the melt bed and thus ignores any potential problems associated with poor flow distribution, differences in the densities of the various components of the melt (feed melt, reduced melt, coke, partially oxidized coke, ash), and differences in particulate sizes.

d) The analysis is based on the limited information presently available on the physical property and thermodynamic data of the process materials involved, and the heat transfer and hydraulic behavior of the three phase system existing in the molten carbonate reducer.

3. Results

a. Coke and Air Requirements

Figures 4 and 5* show the normalized coke and air requirements of the two region molten carbonate reducer as a function of normalized heat loss, at sulfur compound mole fractions in the melt of 0.15 and 0.30, and sulfate mole fractions of the sulfur compounds in the melt leaving the scrubber of 0, 0.33, and 1.

Table I presents typical values of the normalized coke and air requirements at the reference sulfate mole fraction of 0.33:

TABLE I

MOLTEN CARBONATE REDUCER COKE AND AIR REQUIREMENTS

Sulfur Compound Concentration, [S]	Normalized Heat Loss, Q_L, 10^3 Btu/hr per lb mole/ hr SO_x	Normalized Coke Reqmt, lb per lb Sulfur	Normalized Air Reqmt, scf per lb Sulfur	Coke Cost, mills/kwhr	Air Compressor Power Reqmt, HP/Mw
0.15	0	1.64	118	0.180	1.9
"	50	1.82	141	0.200	2.3
"	100	1.99	163	0.218	2.6
"	250	2.52	232	0.276	3.7
"	1,000	5.14	572	0.566	9.2
0.30	0	1.30	73	0.143	1.2
"	50	1.48	96	0.164	1.5
"	100	1.65	119	0.182	1.9
"	250	2.17	187	0.239	3.0
"	1,000	4.79	527	0.526	8.4

It is to be noted that the conversion factors used to obtain the right hand ordinates of Figures 4 and 5 and therefore the last two columns of Table I are based on the use of a 12,800 Btu/lb, 3 wt % sulfur coal in a power plant with a heat rate of 9000 Btu/Kwh.

The coke and air requirements increase linearly with increasing heat loss. An increase in heat loss of 100,000 Btu/hr per lb mole SO_x/hr results in coke and air requirement increases of 0.35 lb and 45 scf per lb of sulfur, respectively.

*Pages 22 and 23

Similarly decreasing the sulfur compound concentration in the melt from a mole fraction of 0.30 to a mole fraction of 0.15 increases the coke and air requirements by 0.34 lb and 45 scf per lb of sulfur, respectively.

The extent of oxidation of the sulfur compounds in the melt leaving the scrubber can be seen from Figures 4 and 5 to result in an increase in coke and air requirements of 0.39 lb and 21 scf per lb of sulfur, respectively, when the sulfate fraction increases from 0 to 1.

If, as is most probable, the oxidation of the coke in the reducer is less than 100 per cent complete, some unreacted coke will be discharged to the quench tank with the reduced melt and ash. Filtration of the melt will then entail the loss of salt associated with a filter cake consisting not only of ash but also of coke, thus requiring increased recovery plus make-up of molten carbonate. For a constant fractional coke usage an increase in coke requirement therefore also results in an increase in carbonate recovery and make-up, with an economic penalty directly proportional to the increase in coke requirement.

If one assumes 95 per cent utilization of the coke, 0.7 per cent ash in the coke, and a 1:1 ratio of melt to coke plus ash in the filter cake, the resulting carbonate recovery and make-up requirement amounts to 113 lb per ton of coke fed into the reducer. At an average carbonate recovery plus make-up cost of 8 cents per lb this would add $9 per ton of coke fed into the reducer to the cost of the coke itself, thereby effectively almost doubling the cost directly associated with the coke requirement (assuming a coke cost of $11 per ton). Major emphasis must therefore be placed on achieving the greatest possible utilization of the coke, possibly through recycle of part of the filter cake back into the reducer (this may be limited by the resulting ash build-up in the melt).

It is therefore essential that:

(1) The heat loss from the reducer melt bed be minimized

(2) The sulfur compound concentration in the melt be as high as possible without exceeding their solubility limits.

(3) The oxidation of the sulfur compounds going through the scrubber be minimized. The two parameters which may be most controllable in this respect are the direct recycle of melt to the scrubber and the return to the scrubber of unreduced sulfate and unregenerated sulfide (which becomes oxidized to sulfate) from the reduction-regeneration system.

(4) The coke utilization in the reducer be maximized. The fraction of unreacted coke can be minimized through good distribution of the coke in the melt and possibly partial recycle of the coke-ash-salt filter cake back to the reducer.

b. Physical Dimensions

Figures 6 through 8* show the melt bed diameter and expanded depth, and the heat flux at the walls of the reducer vessel in contact with the melt, as a function of processing capacity and normalized heat loss. Since the real independent variable is the heat flux rather than the normalized heat loss, Figure 9* presents a cross-plot of Figure 8 showing the normalized heat loss as a function of processing capacity and heat flux. Figures 6, 7 and 9 therefore provide the means for obtaining the physical dimensions of the reducer melt bed as a function of processing capacity and heat flux.

Table II presents typical values of the normalized heat loss, melt bed diameter and expanded depth, at reducer processing capacities of 5, 40, 60, and 200 lb moles/hr SO_x, corresponding to equivalent nominal power plant capacities of 8, 64, 96 and 320 Mw, respectively.

TABLE II

MOLTEN CARBONATE REDUCER HEAT LOSS AND DIMENSIONS

Reducer Capacity, lb m/hr SO_x / Reducer Capacity Equiv. Mw		5 40 / 8 - 64			60 - 200 / 96 - 320		
[S]	Q/A, 10^3 Btu/ft^2 hr	Q_L, 10^3 Btu/hr per lb m/hr SO_x	D, ft	d, ft	Q_L, 10^3 Btu/hr per lb m/hr SO_x	D, ft	d, ft
0.15	0	0	6.5-15	2.2-4.2	0	18-29	4.7-6.5
"	10	240-120	8-17	2.5-4.3	110-70	20-32	4.8-6.6
"	20	640-290	10-19	2.7-4.5	250-170	23-35	4.9-6.7
"	30	>1000-550	>11-23	>2.9-4.7	470-310	26-39	5.2-6.9
"	40	> 1000-980	>11-28	>2.9-5.0	830-500	30-44	5.4-7.1
0.30	0	0	5.5-12	2.0-3.6	0	15-24	4.0-5.5
"	10	170-90	7-14	2.1-3.7	80-50	17-26	4.1-5.6
"	20	540-210	9-16	2.4-3.9	180-120	19-29	4.3-5.8
"	30	>1000-410	>11-19	>2.8-4.2	350-220	22-33	4.6-6.0
"	40	>1000-770	>11-23	>2.8-4.5	620-380	26-37	4.9-6.3

*Pages 38 through 41

It is to be noted that the plots of Figures 6 through 9 and the data of Table II are based on a melt bed diameter to depth relationship optimized for minimum heat loss since this is considered the most important independent process variable. It does not take into account any other factor, such as structural requirements which may affect the detailed design of the reducer. These, however, are not expected to introduce any major changes in either the trends or the actual values presented in the figures and table.

Both Figure 9 and Table II show that at a given reducer processing capacity the normalized heat loss increases exponentially with increasing heat flux. This is as would be expected since an increase in heat flux increases not only the heat loss per unit wall area but also the size of the reducer vessel required to accomodate the resulting higher heat requirements.

At a given heat flux, the normalized heat loss increases with decreasing reducer processing capacity. For pilot plant size reducer units, the normalized heat loss becomes large even at relatively low heat fluxes. At high heat fluxes it becomes so great that a small pilot plant unit cannot provide an adequate technical representation of a high heat flux reducer design (a design which would be of interest only if there were a demand for the production of large amounts of steam).

Table II shows that the actual magnitude of the heat loss from the reducer melt bed will be quite large unless the heat flux at the walls is kept low. At 10,000 Btu/ft^2 hr the heat loss from 60 and 200 lb mole/hr SO_x capacity reducers would amount to 4.8 to 6.6 x 10^6 and 10.0 to 14.0 x 10^6 Btu/hr, respectively, at sulfur compound concentrations in the melt of 0.30 to 0.15.

The following conclusions can be drawn from these results:

(1) The heat flux at the walls of the reducer vessel in contact with the melt must be minimized not only to minimize the heat loss but also to minimize the physical size of the reducer vessel. As discussed in Section IX-3.d, this entails the use of the alumina-liner reducer design concept.

(2) The sulfur compound concentration in the melt must be as high as possible without exceeding their solubility limits.

(3) The data developed in this work do not allow any conclusion to be drawn with respect to the effect of the state of oxidation of the sulfur compounds in the melt leaving the scrubber upon the physical dimensions and heat loss of the reducer. It is evident, however, that here again the sulfate content of these compounds should be minimized as much as possible.

(4) If for some reason there were an interest in developing a frozen skull or other high heat flux reducer design concept, such a reducer could not be mocked up adequately in a small scale pilot plant unit as the excessively high normalized heat loss in such a unit would entail the consumption of disproportionately high amounts of coke and air.

c. Five and 267 Mw Reducer Units

Figures 10 through 17* show the physical dimensions and heat loss for the special cases of 3.125 and 167 lb mole/hr SO_x capacity reducer units, equivalent to reducer units for nominal power plant capacities of 5 and 267 Mw , respectively (pilot plant size, and one of three units of a fullscale 800 Mw plant). The reduction region residence time was varied from 15 to 30 minutes and the superficial air velocity from 3 to 5 ft/sec.

For comparison purposes the results are summarized in Figures 23 through 28 which show the effects of varying reduction region residence time and superficial air velocity upon the reducer dimensions, normalized heat loss, and normalized coke and air requirements. It is to be noted that the abscissa scale on these figures is purely arbitrary and that the shape of the curves drawn represents assumed trend curves since actual data were available only at 15 minutes and 5 ft/sec, 15 minutes and 3 ft/sec, and 30 minutes and 3 ft/sec.

Figures 23 through 28 (and 10 through 17) show that:

(1) There is a greater incentive to decrease the minimum required reduction region residence time from 30 to 15 minutes than to increase the maximum allowable superficial air velocity from 3 to 5 ft/sec. The reduction region residence time could be decreased by increasing the operating temperature of the reducer, at a penalty, however, of increased preheat requirements and potentially greater materials and carbonate salt decomposition problems.

(2) The incentive to achieve these improvements increases with increasing heat flux from the melt bed to the walls of the reducer vessel.

---

*Pages 47 through 49

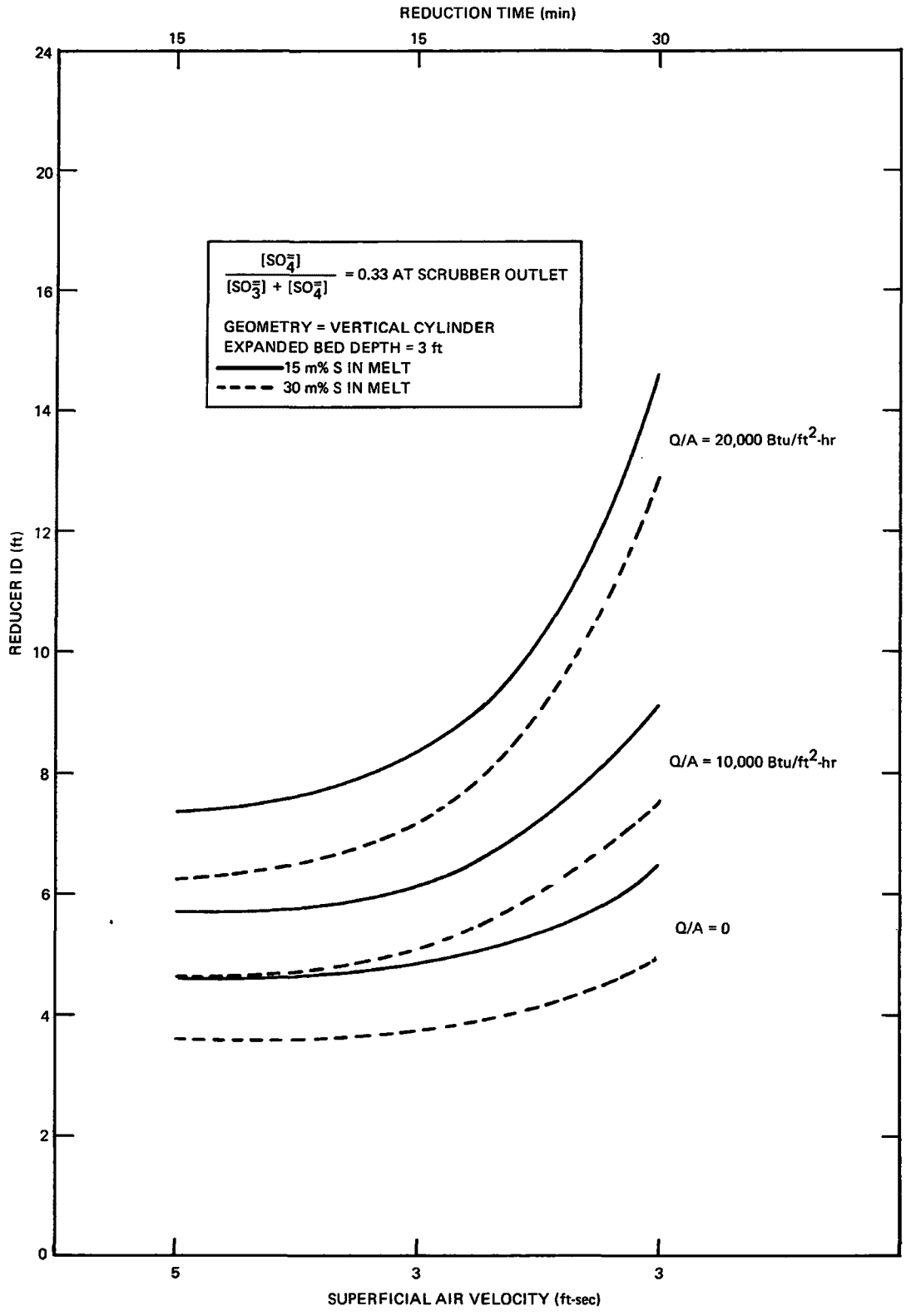

Figure 23. Effect of Reduction Time and Air Velocity on Reducer Diameter

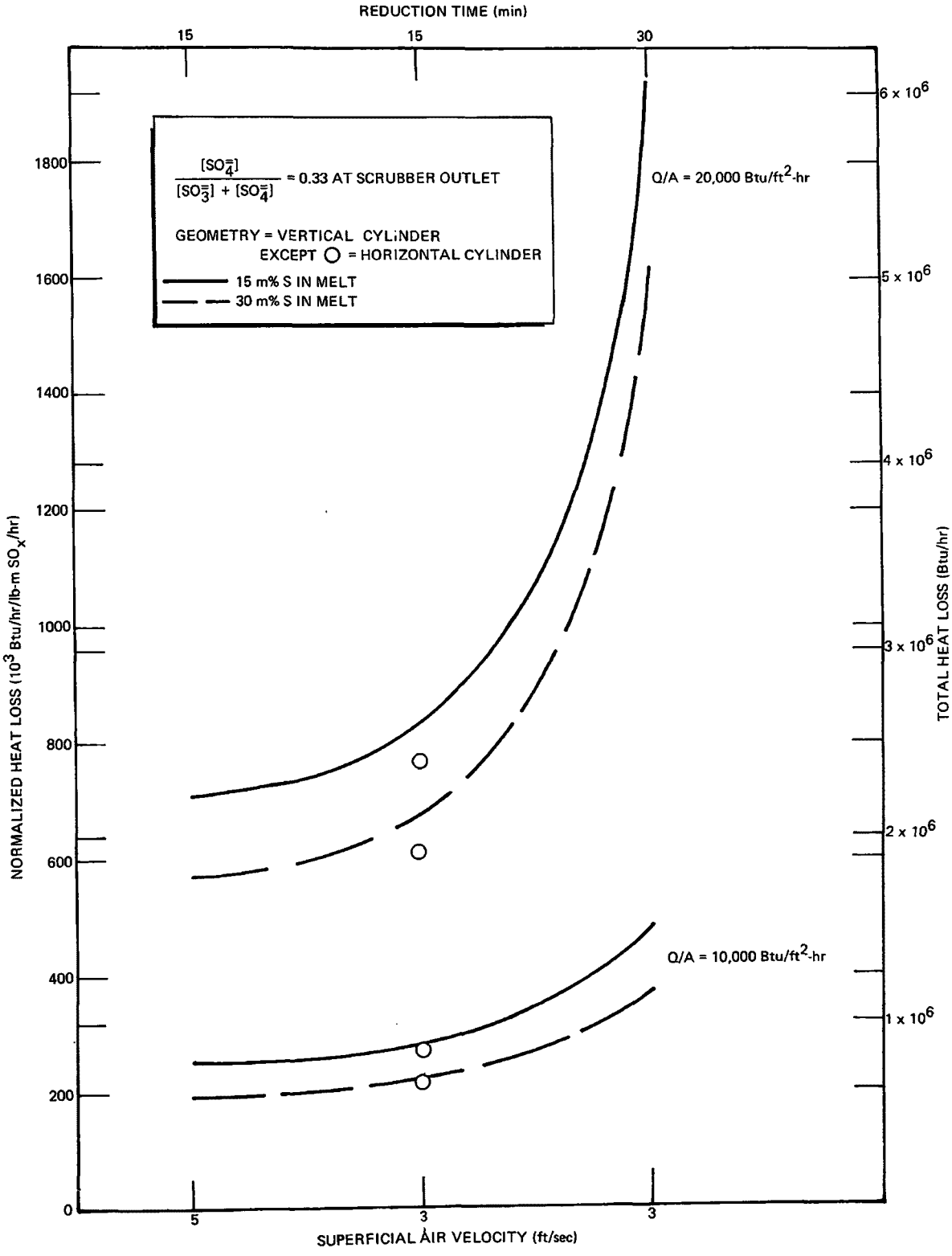

Figure 24. Effect of Reduction Time and Air Velocity on Reducer Bed Heat Loss

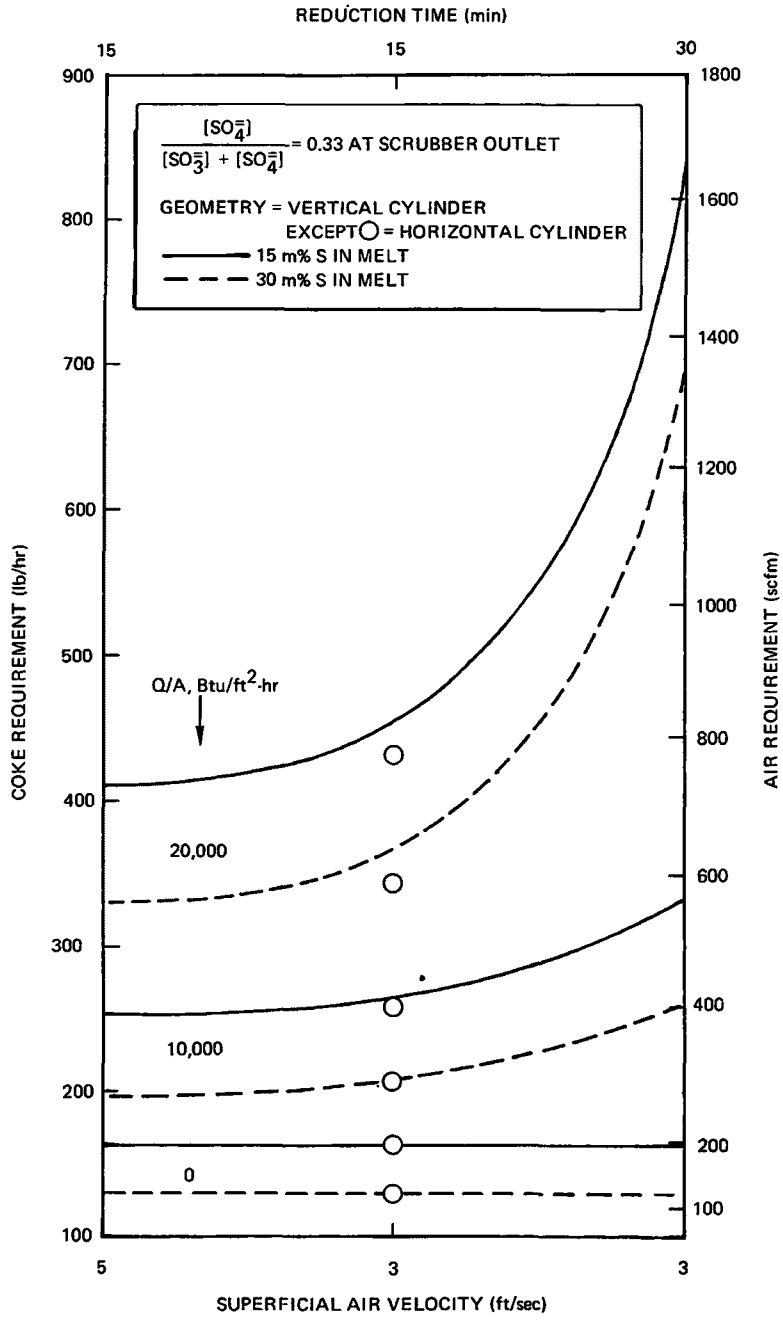

Figure 25. Effect of Reduction Time and Air Velocity on Reducer Coke and Air Requirements, 5-Mw Reducer

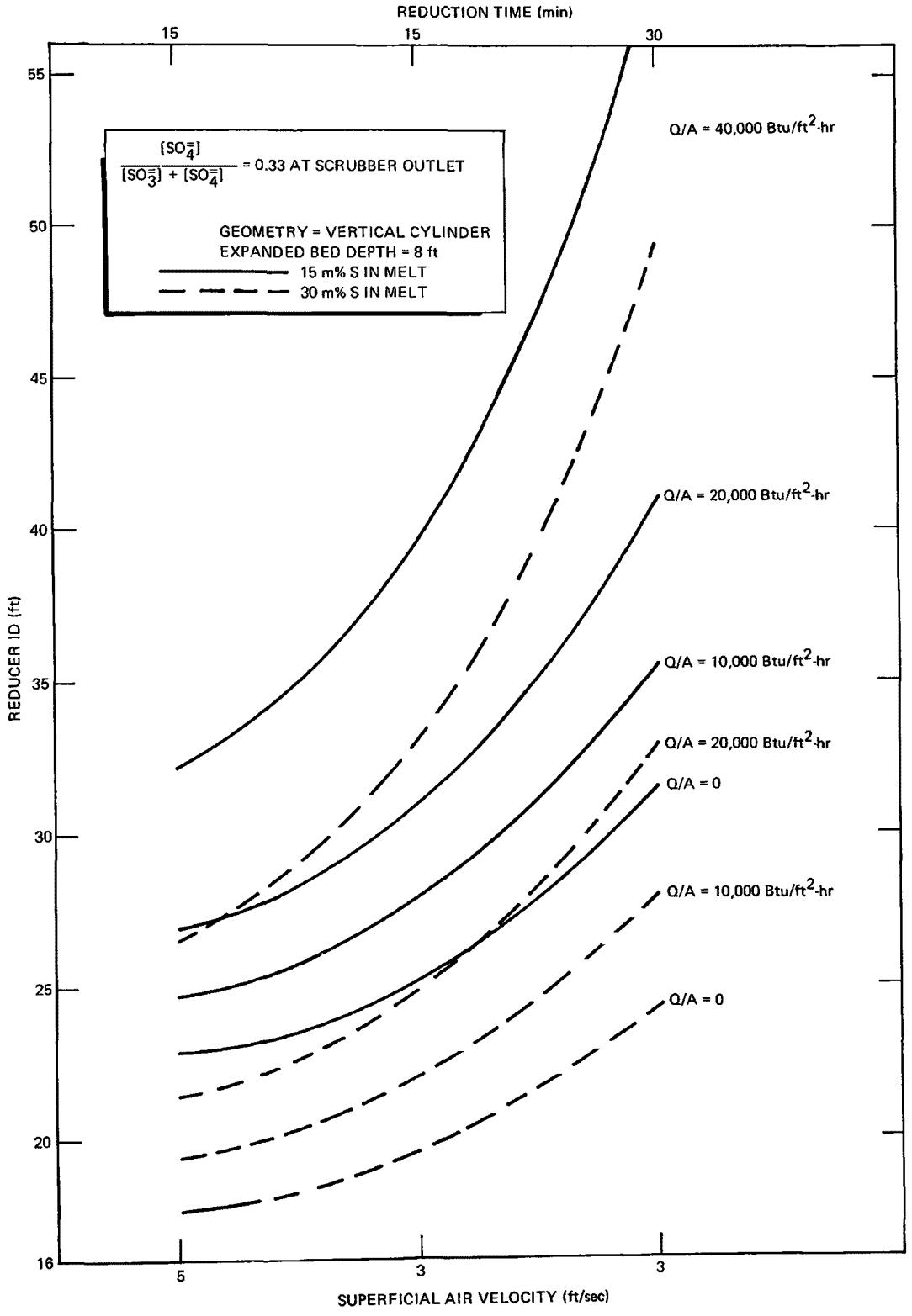

Figure 26. Effect of Reduction Time and Air Velocity on Reducer Diameter, 267-Mw Reducer

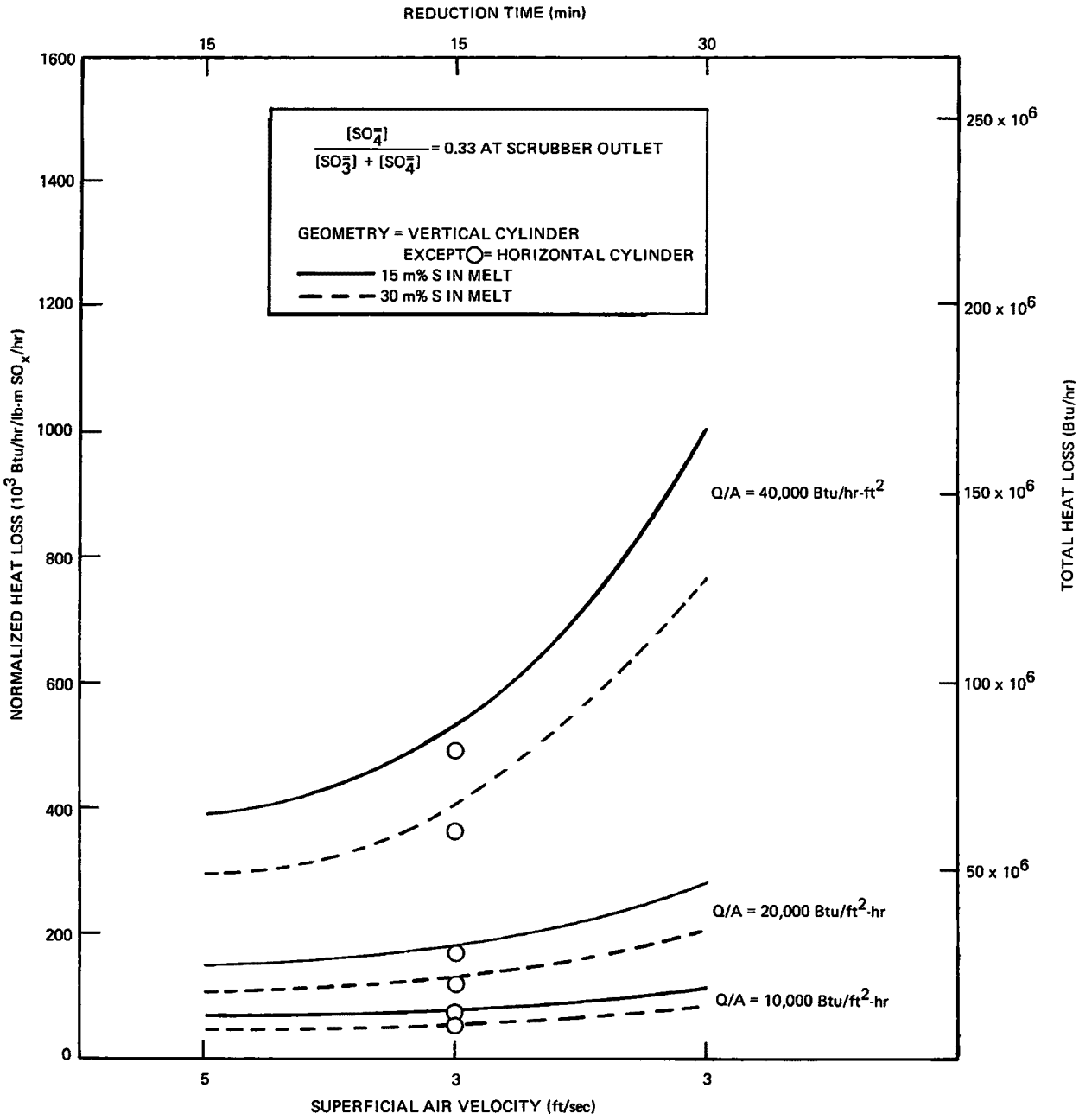

Figure 27. Effect of Reduction Time and Air Velocity on Reducer Bed Heat Loss, 267-Mw Reducer

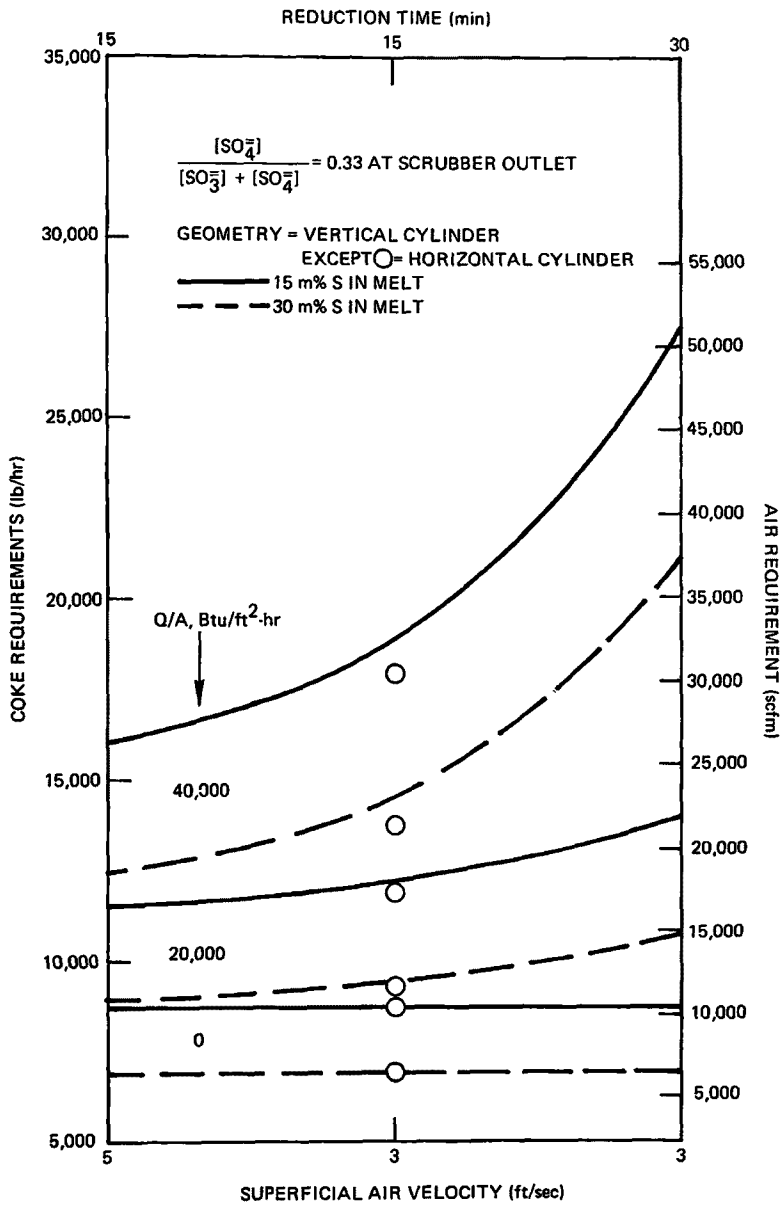

Figure 28. Effect of Reduction Time and Air Velocity on Reducer Coke and Air Requirements, 267-Mw Reducer

(3) On the basis of the very superficial look at a single case of a horizontal cylinder reducer geometry with separation baffle perpendicular to the axis of the cylinder, and within the limitations of the assumptions used in the analysis, there appears to be no significant difference from the process engineering point of view between this geometry and that of a vertical cylinder.

(4) As stated in Section IX-3.b. a small pilot plant unit cannot be used to provide adequately representative technical information on a high heat flux reducer design concept (a concept which would be of interest only if there were a demand for the production of large amounts of steam).

d. Melt Bed Heat Loss

The conclusions reached thus far have all emphasized the essential need for minimizing the heat loss from a molten carbonate reducer and therefore minimizing the heat flux at the walls of the reducer vessel in contact with the melt.

The results of Section VII have shown that the frozen skull (cold wall) reducer design concept does not lend itself to the use of a relatively low melting point melt such as proposed in this process. The high temperature driving force (~800 °F) between the melt and the walls of the vessel combined with a relatively high heat transfer coefficient (> 50 Btu/ft^2 hr) from the melt to the walls yields a heat flux of over 40,000 Btu/ft^2 hr considerably in excess of what would be acceptable in a molten carbonate reducer (Figure 19).* Such a high heat flux also imposes very stringent cooling requirements to allow the maintenance of the frozen melt skull (Figures 18 and 19).* The frozen skull reducer design concept is therefore not suitable for the molten carbonate process. This conclusion, however, must be limited exclusively to the process based on the use of the lithium, sodium and potassium carbonate eutectic as the carrier melt. It does not necessarily apply to a process using a higher melting point salt mixture, such as one based on sodium carbonate as the carrier melt.

The alumina liner (hot wall) reducer design concept on the other hand involves the use of internal insulation which, in the form of a combination of low porosity, high thermal conductivity and high porosity, low thermal conductivity liner materials, allows reduction of the heat flux at the walls of the reducer vessel in contact with the melt to less than 2,000 Btu/ft^2 hr and thus minimizes the heat loss from the reducer vessel (Figure 20).* Though this concept may

*Pages 54, 56 and 57

present some materials problems it appears to be well suited for application to the reduction step. It is to be noted that the minimum heat loss will be achieved with natural convection air cooling of the outside surface of the reducer vessel. Such cooling precludes the installation of thermal insulation at this surface and therefore requires the outside wall of the vessel to run hot (~500 °F). If a cold outside wall temperature should be required, the vessel walls would have to be water-cooled, with thermal insulation installed around the outside of the water-cooled region. The reducer heat loss would then be slightly higher, but could still be kept to a heat flux value of less than 2,000 Btu/ft^2 hr.

It can therefore be concluded that:

(1) The alumina-liner (hot wall) reducer design concept appears to be well suited for the molten carbonate reducer, with achievable heat flux levels of less than 2,000 Btu/ft^2 hr at the surface of the walls in contact with the melt bed.

(2) The reducer heat loss can be minimized with natural convection air cooling of the outside walls of the reducer vessel, which will then operate at relatively high temperatures (> 500 °F).

(3) Water cooling of the walls of the reducer vessel can be used to lower the outside temperature of the vessel, at a penalty, however, of a small increase in heat loss.

(4) The frozen melt skull (cold wall) reducer design concept is not applicable to a molten carbonate reducer using a relatively low melting point salt mixture such as a lithium-sodium-potassium carbonate-based melt. It may, however, be well suited for application to a molten carbonate reducer using a high melting point salt mixture such as a sodium carbonate-based melt.

e. Internal Melt Recirculation

The analysis of Section VIII, though based on very rough assumptions, indicates that there should be no problem in achieving adequate recirculation of the melt between the oxidation and reduction regions of the reducer. The difference in effective densities between the two regions, resulting from a slight difference in superficial gas velocities and, to a lesser extent, a difference in average temperatures, is sufficient to provide the required recirculation. The most important consideration in this respect may involve control of the recirculation rate by correct sizing of the orifices at the top and bottom of the baffle separating the oxidation region from the reduction region.

These orifices must be small enough to regulate the melt flow rate to maintain the minimum residence time of the melt in the reduction region required for carrying out the reduction reaction to the desired degree of completion. Typical orifice dimensions are shown in Figure 21.*

4. Conclusions

A preliminary process analysis of a two-region molten carbonate reducer design concept shows that:

1) The heat loss from the melt bed must be minimized in order to minimize the coke and air requirements of the reducer and its physical dimensions.

2) The sulfur compound concentration in the carbonate melt must be as high as feasible subject to solubility limitations, thus minimizing melt flow rate and melt preheat requirements.

3) The sulfate fraction of the sulfur compounds in the melt leaving the scrubber must be minimized in order to minimize the reduction duty of the reducer.

4) The coke utilization in the reducer must be maximized in order to minimize the melt recovery and make-up requirement resulting from the melt loss associated with the filtration of the unreacted coke.

The controlling constraints in the design of the reducer are the maximum allowable superficial air velocity in the oxidation region and the minimum required residence time of the melt in the reduction region. A decrease in reduction region residence time from 30 to 15 minutes results in a more significant reducer design improvement than an increase in superficial air velocity of 3 to 5 ft/sec.

Typical reducer dimensions have been determined as a function of processing capacity and heat loss. Coke and air requirements have been estimated as a function of heat loss. For a sulfur compound mole fraction in the melt of 0.30, one-third of which is sulfate, the coke and air requirements of a reducer with a negligible heat loss amount to approximately 1.30 lb and 73 scf, respectively, per lb of sulfur fed into the scrubber.

---

*Page 64

The heat loss from the melt bed in the reducer can be minimized through use of an alumina-lined internally insulated (hot wall) reducer design. If it is air-cooled the outside wall of the reducer vessel in this design cannot be insulated and operates at a temperature of around 500 °F. Water cooling surrounded by insulation would allow operation of the outside of the reducer at a lower temperature.

Because of its inherently high heat loss a frozen melt skull (cold wall) reducer design does not appear feasible when a low melting point carbonate mixture such as the lithium-sodium-potassium carbonate eutectic is used as the carrier melt.

Internal melt recirculation between the oxidation and reduction regions of the reducer can be controlled through sizing of the orifices in the baffle between the two regions. These orifices must be small enough to assure satisfaction of the minimum residence time requirement in the reduction region and large enough to allow sufficient flow to transport the required heat without exceeding melt bed temperature rise limitations.

The results obtained are based on the technical information presently available and on various assumptions and approximations which had to be made in lieu of required experimental data. They are therefore preliminary and must be confirmed through a development program. They are, however, believed to provide a sound basis for the conceptual design of a molten carbonate reducer and the planning of the required experimental program.

REFERENCES

1. G. J. Janz, "Molten Carbonate Electrolytes as Acid-Base Solvent Systems," AD 651604, Rensselaer Polytechnic Institute, Troy, New York, February 1967.

2. H. C. Weber, "Thermodynamics for Chemical Engineers," John Wiley & Sons, Inc., New York, 1939, p. 52.

3. Ibid., p. 54

4. PB-168370, "JANAF Thermochemical Tables," Dow Chemical Company, Midland, Michigan, August 1967.

5. J. H. Perry, "Chemical Engineers' Handbook," McGraw Hill Book Co., Inc., Third Edition, 1950, pp 239-243.

6. G. T. Skaperdas, "Commercial Potential for the Kellogg Coal Gasification Process," PB 180358, M. W. Kellogg Company, Piscataway, N.J., September 1967, pp 87-92.

7. "Development of a Molten Carbonate Process for Removal of Sulfur Dioxide from Power Plant Stack Gases, Progress Report No. 2, Part I. Process Chemistry - Radiation. April 1, 1968 to October 27, 1968." AI-70-5, pp. 48-50.

8. W. H. McAdams, "Heat Transmission," McGraw Hill Book Co., Inc., Third Edition, 1954, p. 172.

9. "Chemical Recovery in Alkaline Pulping Processes," Roy P. Whitney, Editor, TAPPI Monograph Series No. 32, 1968, pp. 59-99

APPENDIX B

PRELIMINARY PROCESS ANALYSIS OF A MOLTEN CARBONATE REGENERATOR

I. INTRODUCTION

In the molten carbonate regeneration step, the alkali metal carbonate-sulfide melt from the reduction step is contacted with a carbon dioxide-steam mixture. The reaction converts the sulfide into carbonate and releases hydrogen sulfide. This Appendix describes in detail the results of an analytical study of the regeneration step. The study was conducted to determine the hydrogen sulfide concentrations achievable in the regenerator off-gas and to establish the operating conditions required to attain these concentrations. Specific emphasis was given to the constraints imposed by the thermodynamic equilibrium and heat generation of the regeneration reaction, by the alkali metal sulfide solubility in the melt, and by the composition of the available regeneration feed gas.

II. CONCLUSIONS

1. The operating parameters of the regenerator must be optimized to satisfy the following constraints:

   a. A thermodynamic equilibrium strongly favored by low temperatures
   b. A highly exothermic heat of reaction
   c. A solubility of sulfide in the carbonate melt which increases significantly with increasing temperature

2. The regeneration equilibrium is strongly favored by a high steam concentration in the feed gas, and to a lesser extent by increased total pressure or CO_2 concentration (especially at low temperatures or high CO_2 concentrations). At a given steam concentration the effect of CO_2 concentration is more important than that of total pressure.

3. The maximum hydrogen sulfide concentration achievable in the regenerator off-gas is for all practical purposes independent of the M_2S concentration in the carbonate feed melt.

4. A stoichiometry limitation combined with equilibrium considerations makes it essential that the regeneration gas have as high a concentration as possible of CO_2 and H_2O. This requirement can be adequately satisfied through use of the reducer off-gas from a fluid coke reduction system (about 40 mole % CO_2).

5. As a result of potential solubility limitations, the operating temperature of the regenerator may be determined by the M_2S concentration in the carbonate feed melt. For operation in the temperature range below 1000°F, the M_2S concentration in the carbonate feed melt may have to be kept under about 17 mole %.

6. At atmospheric pressure a typical fluid coke reducer off-gas containing about 25 mole % CO_2 and 25 mole % H_2O (through addition of steam)* allows the production of an off-gas containing a maximum of about 10 mole % H_2S. Adding more steam, available as a by-product of the process, to increase the H_2O content of the gas to 40 mole %, concurrently reducing its CO_2 content to 20 mole %, increases the achievable H_2S concentration in the product gas to about 15 mole %.

7. Approximately nine theoretical plates are required to regenerate 95% of the M_2S in the temperature range of 950 to 1000°F with a feed gas containing 20 mole % CO_2 and 40 mole % H_2O and a feed melt containing 15 mole % M_2S. The corresponding H_2S concentration of the product gas is about 13.7 mole %. Increasing the total pressure to two atmospheres would allow production of a 16 mole % H_2S product gas or a decrease in the number of theoretical plates from 9 to 6.

8. The number of theoretical plates required, and the maximum achievable H_2S concentration in the product gas, are controlled by a pinch point between the operating line and the equilibrium line at the maximum allowable operating temperature of the regenerator. This pinch point is approached as the heat of regeneration raises the temperature of the melt, requiring intercooling to allow regeneration to proceed. Several stages of external cooling, or cooling on every plate, would practically eliminate the pinch point limitation and thus appreciably decrease the number of plates required and increase the H_2S concentration achievable in the product gas. However, a single stage cooling the melt taken off a plate slightly above the middle

*The reducer analysis conducted after completion of the regenerator study has shown that a regeneration gas containing about 40 mole % CO_2 and 40 mole % H_2O will be available from a two-region molten carbonate reducer.

of the regenerator from about 1000°F down to about 900°F appears to be adequate. Approximately 60% of the heat of reaction can thus be removed. The remainder goes into the product gas and the regenerated carbonate melt.

III. BASIS

A. THERMODYNAMIC EQUILIBRIUM

The effective regeneration reaction was assumed to be

$$M_2S(\ell) + CO_2(g) + H_2O(g) \rightleftarrows M_2CO_3(\ell) + H_2S(g) \qquad (1)$$

(where M = mixture of Li, Na, and K cations)
and consideration was not given to any actual reaction mechanism and formation of intermediate compounds such as the thiocarbonate M_2CO_2S.

The equilibrium data used were those obtained experimentally and reported in reference (1). They can be formulated as follows:

$$\frac{[H_2S]}{[CO_2][H_2O]} \frac{[M_2CO_3]}{[M_2S]} = \frac{K_1\pi}{1 + K_2\pi [CO_2]} \qquad (2)$$

with: $K_1 = 1.90 \times 10^{-6}\ e^{50,400/RT}$

$K_2 = 1.24 \times 10^{-3}\ 3^{27,720/RT}$

π = Total pressure, atmospheres

R = Gas constant, Btu/°R lb mole

T = Absolute temperature, °R

Figure 1 presents an arithmetic scale plot of K_1 and K_2 as a function of temperature over the temperature range considered to be of interest, 800 to 1050°F.

B. HEAT OF REACTION

A value of -25.8 kcal/g mole = 46,400 Btu/lb mole, based on estimates from reference (1), was used. While this value had been estimated for a temperature of 850°F, no attempt was made in the present calculations to include the effect

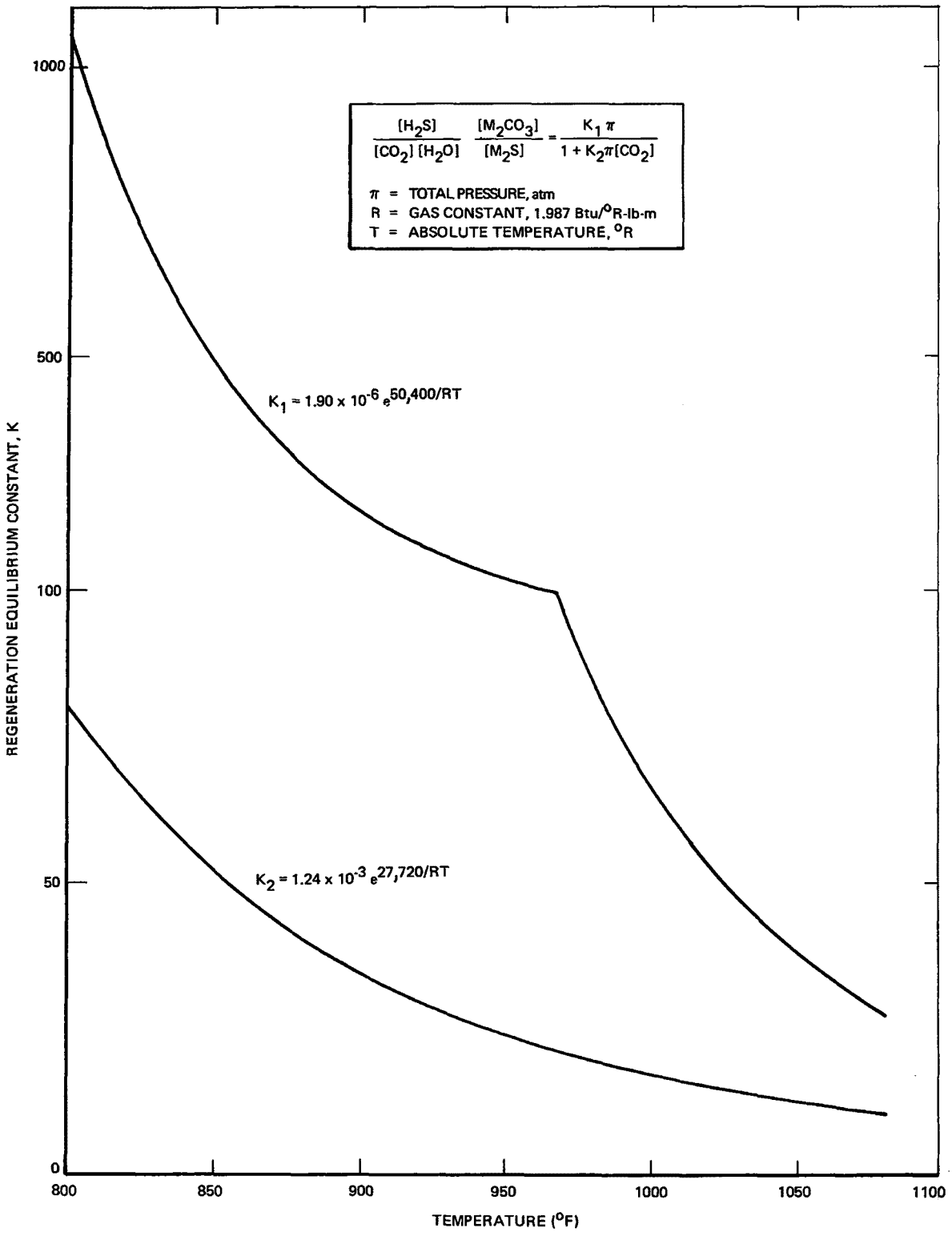

Figure 1. Regeneration Equilibrium Constants

of temperature upon the heat of reaction since this value was used only in the approximate heat balances carried out to establish the number of theoretical plates required for efficient regeneration.

C. SULFIDE SOLUBILITY IN CARBONATE MELTS

The solubility of sulfide (M_2S) in the alkali metal carbonate (M_2CO_3) melts was determined by measuring the initial freezing temperature of fused salt mixtures. The first measurements were done with mixtures made up by combining purified sodium sulfide with lithium, sodium, and potassium carbonate in the proper proportions. The freezing points of these mixtures are shown plotted in Figure 2; the data indicate that about 18 mole % is soluble at 950°F, and that a 32 mole % sulfide mixture started to freeze at 1060°F. The 32 mole % mixture was then treated by bubbling CO_2 through it to simulate melt from the reduction step of the process. This treatment lowered the freezing point to 770°F, probably by converting part of the sulfide to thiocarbonate (M_2CO_2S). The regeneration tests used to determine the equilibrium and heat of reaction data were all done with reduced melts, not synthetic mixtures. Therefore, it is believed that the regeneration tests actually involved carbonate-sulfide-thiocarbonate mixtures; This was discussed in reference (1). Because of this, the initial freezing point of the melts to be regenerated will probably not exceed 770 to 800°F. However, the freezing points and solubilities of the synthetic mixture were used as design constraints in this study, to be conservative.

IV. METHOD OF CALCULATION

The basic thermodynamic equilibrium equation, equation (2), was written in the form:

$$\gamma = K_1 \frac{\alpha \beta / [H_2S]}{\frac{1}{\pi} + K_2 \alpha} \qquad (3)$$

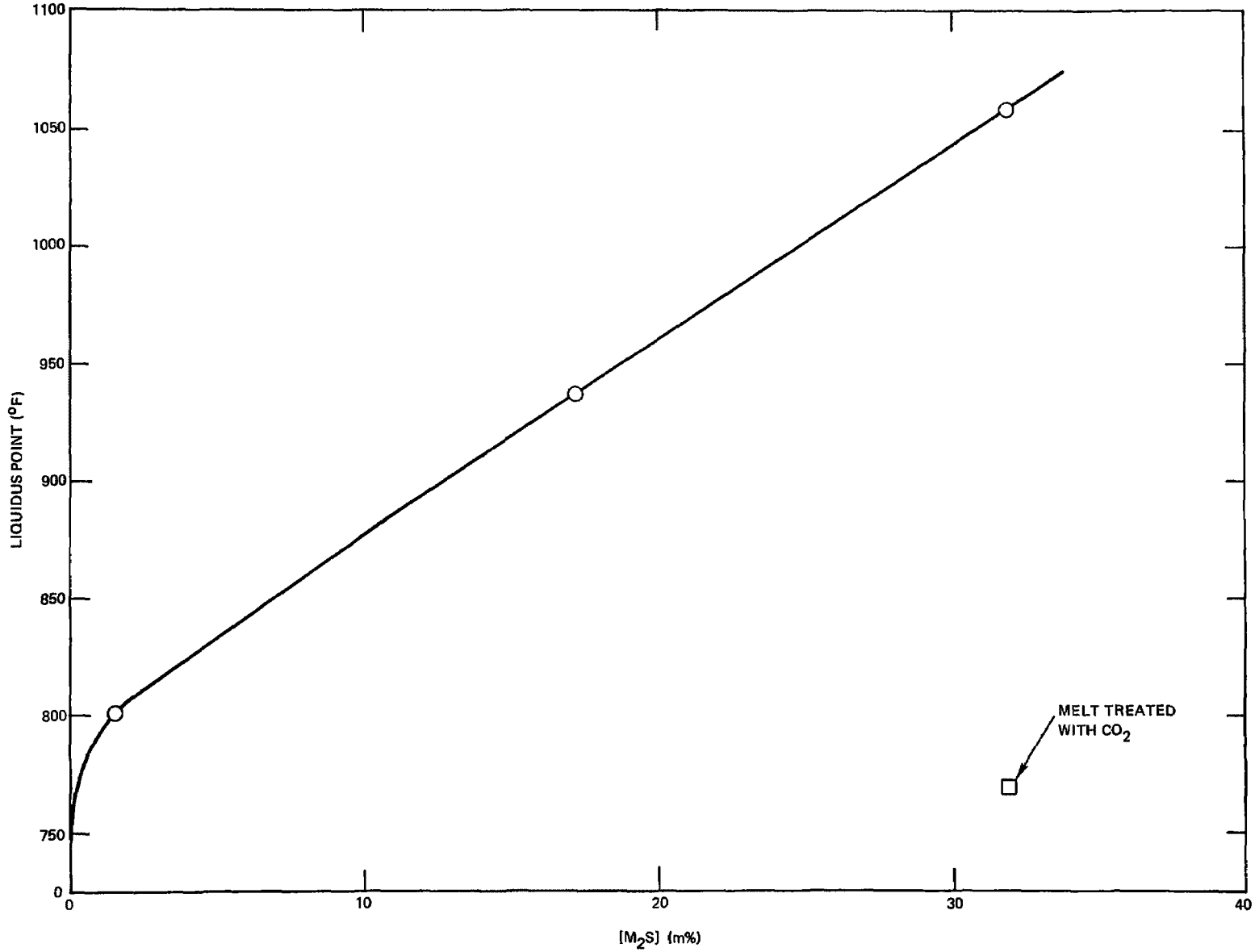

Figure 2. M_2S Solubility in Molten Carbonate Melts

with: $\gamma = \dfrac{[M_2CO_3]}{[M_2S]}$, ratio of mole fractions in the melt on a regenerator plate in equilibrium with the gas leaving the plate,

$\left.\begin{array}{l} \alpha = [CO_2] \\ \beta = [H_2O] \\ \qquad [H_2S] \end{array}\right\}$ mole fractions in the gas leaving a plate in equilibrium with the melt on the plate,

K_1 and K_2 = regeneration reaction equilibrium constants, from Fig. 1,

π = total pressure, atmospheres.

If it is assumed that the regeneration feed gas introduced at the bottom of the regenerator contains only CO_2, H_2O, and N_2, without any H_2S, the stoichiometry of the regeneration reaction, Eq (1), is such that:

$$\alpha = \frac{\left\{[CO_2]_F / \left(1-[CO_2]_F\right)\right\} - [H_2S]}{1 + \left\{[CO_2]_F / \left(1-[CO_2]_F\right)\right\}} \qquad (4)$$

$$\beta = \frac{\left\{[H_2O]_F / \left(1-[H_2O]_F\right)\right\} - [H_2S]}{1 + \left\{[H_2O]_F / \left(1-[H_2O]_F\right)\right\}} \qquad (5)$$

with the subscript F being applied to mole fractions in the feed gas.

It is important to note that stoichiometry thus limits the maximum achievable concentration of H_2S in the product gas to the lesser of $[CO_2]_F / \left(1-[CO_2]_F\right)$ or $[H_2O]_F / \left(1-[H_2O]_F\right)$.

Given the composition of the regenerator feed gas, and the H_2S concentration in the gas in equilibrium with the melt on a plate, one calculates α and β by means of equations (4) and (5), and then γ by means of equation (3).

Knowing γ, one obtains the M_2S concentration in the melt in equilibrium with the H_2S concentration in the gas:

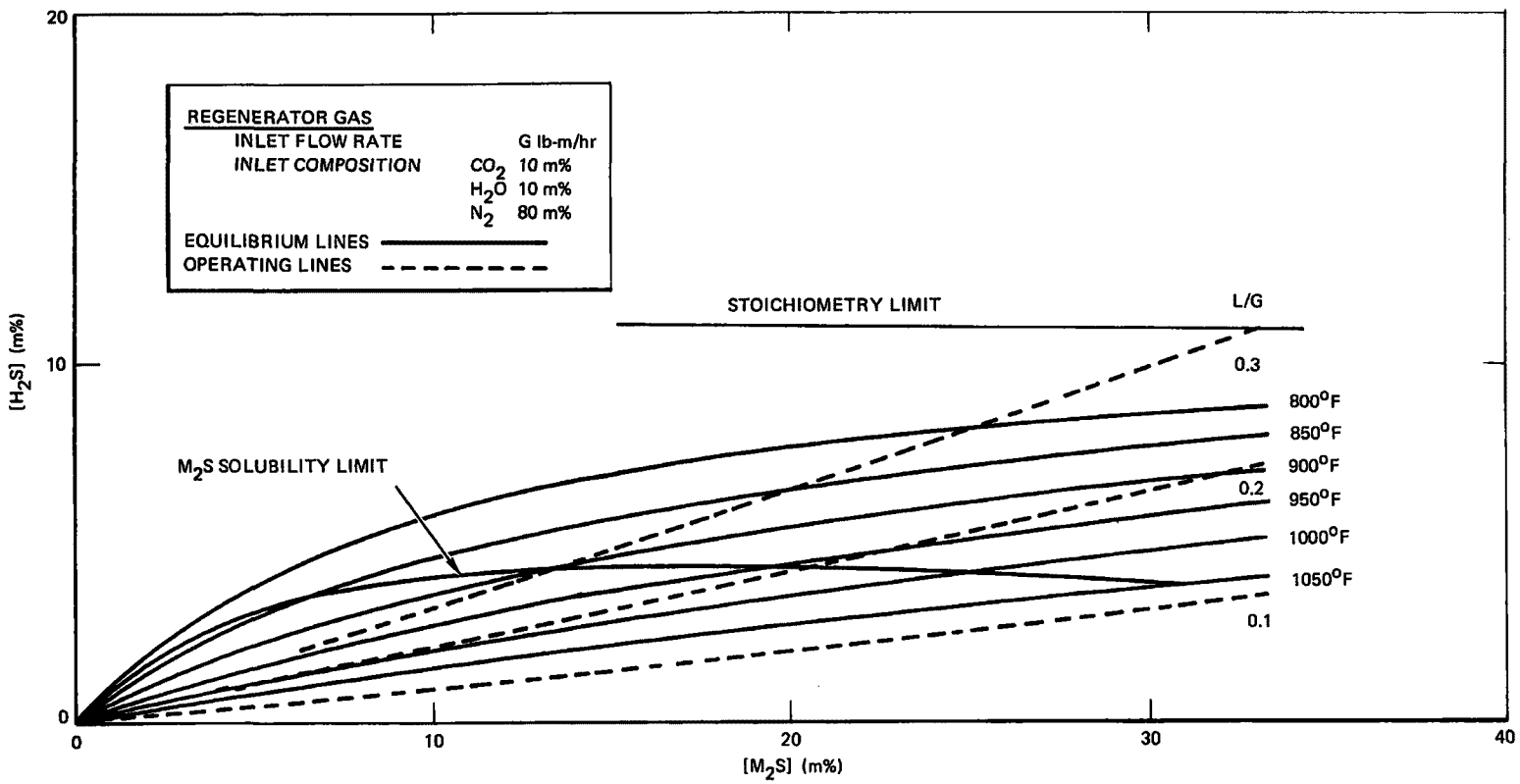

Figure 3. Molten Carbonate Regenerator Equilibria (A)

$$[M_2S] = \frac{1-[I]}{1+\gamma}$$

with [I] = concentration of inerts, such as M_2SO_4, in the melt. In general [I] will be small. It has been neglected in all further calculations, but could be corrected for very simply by multiplying the $[M_2S]$ scale (abscissa) values on all the graphs by the constant factor 1- [I].

Values of $[M_2S]$ in the melt in equilibrium with $[H_2S]$ in the gas were thus obtained at temperatures ranging from 800 to 1050°F, and plotted as a function of each other for various regeneration feed gas compositions. The compositions selected were:

Case A	10% CO_2, 10% H_2O, 80% N_2,	Figure 3
Case B	10% CO_2, 25% H_2O, 65% N_2,	Figure 4
Case C	15% CO_2, 15% H_2O, 70% N_2,	Figure 5
Case D	20% CO_2, 20% H_2O, 60% N_2,	Figure 6
Case E	20% CO_2, 40% H_2O, 40% N_2,	Figures 7 and 8
Case F	25% CO_2, 25% H_2O, 50% N_2,	Figure 9
Case G	30% CO_2, 30% H_2O, 40% N_2,	Figure 10
Case H	40% CO_2, 40% H_2O, 20% N_2,	Figure 11
Case I	50% CO_2, 50% H_2O, 0% N_2,	Figure 12

With the exception of compositions B and E, all these compositions had equal mole fractions of CO_2 and H_2O, ranging from the concentrations achievable from the combustion of natural gas to those achievable through the combustion of pure carbon or calcination of limestone.

Figures 4, 7 and 8 show the effect of addition of extra quantities of steam to the regenerator feed gas (compositions B and E).

Figure 8 shows the effect of operation at a total pressure of two atmospheres as compared with the atmospheric pressure on which all the other calculations were based. Gas composition E was used.

M_2S solubility *vs* temperature values from Figure 2 were then superimposed on the equilibrium curves of Figures 3 through 12, yielding the curves of "M_2S solubility limit" for each of these figures.

Operating lines were also included in these figures to show the H_2S-M_2S mass balance relationship from plate to plate in the regenerator. The lines shown are ideal lines assuming complete (100%) stripping of the hydrogen sulfide from the melt and represented by the following equation which takes into account the stoichiometrically decreasing mole flow rate of gas as it passes through the regenerator:

$$[H_2S] = \frac{L/G\,[M_2S]}{1-L/G\,[M_2S]} \qquad (7)$$

with: L = liquid flow rate, lb moles/hr

G = gas flow rate at regenerator inlet, lb moles/hr

Actual operating lines follow the relationship:

$$[H_2S] = \frac{\frac{L}{G}\left\{[M_2S] - (1-\eta)[M_2S]_F\right\}}{1-\frac{L}{G}\left\{[M_2S] - (1-\eta)\,[M_2S]_F\right\}} \qquad (8)$$

with: η = hydrogen sulfide stripping efficiency

and $[M_2S]_F$ = metal sulfide concentration in the feed melt to the regenerator.

The three cases of Figures 7, 8 and 9 (gas compositions E and F) were selected for layouts of theoretical plate diagrams of the regenerator, since all three apply directly to gas compositions achievable through use of the fluid coke reducer off-gas, with various steam additions, as the regenerator feed gas.* The regenerator feed melt was assumed to have an M_2S concentration of 15 mole % and be at a temperature of 950°F.

The plates were laid out in Figures 13, 14, and 15 in a standard McCabe-Thiele diagram fashion, including a very rough heat balance around each plate. This heat balance determined the temperature on the plate and therefore the

---

*As mentioned in an earlier footnote, gas composition H (Fig. 11) may actually be available from a two region reducer.

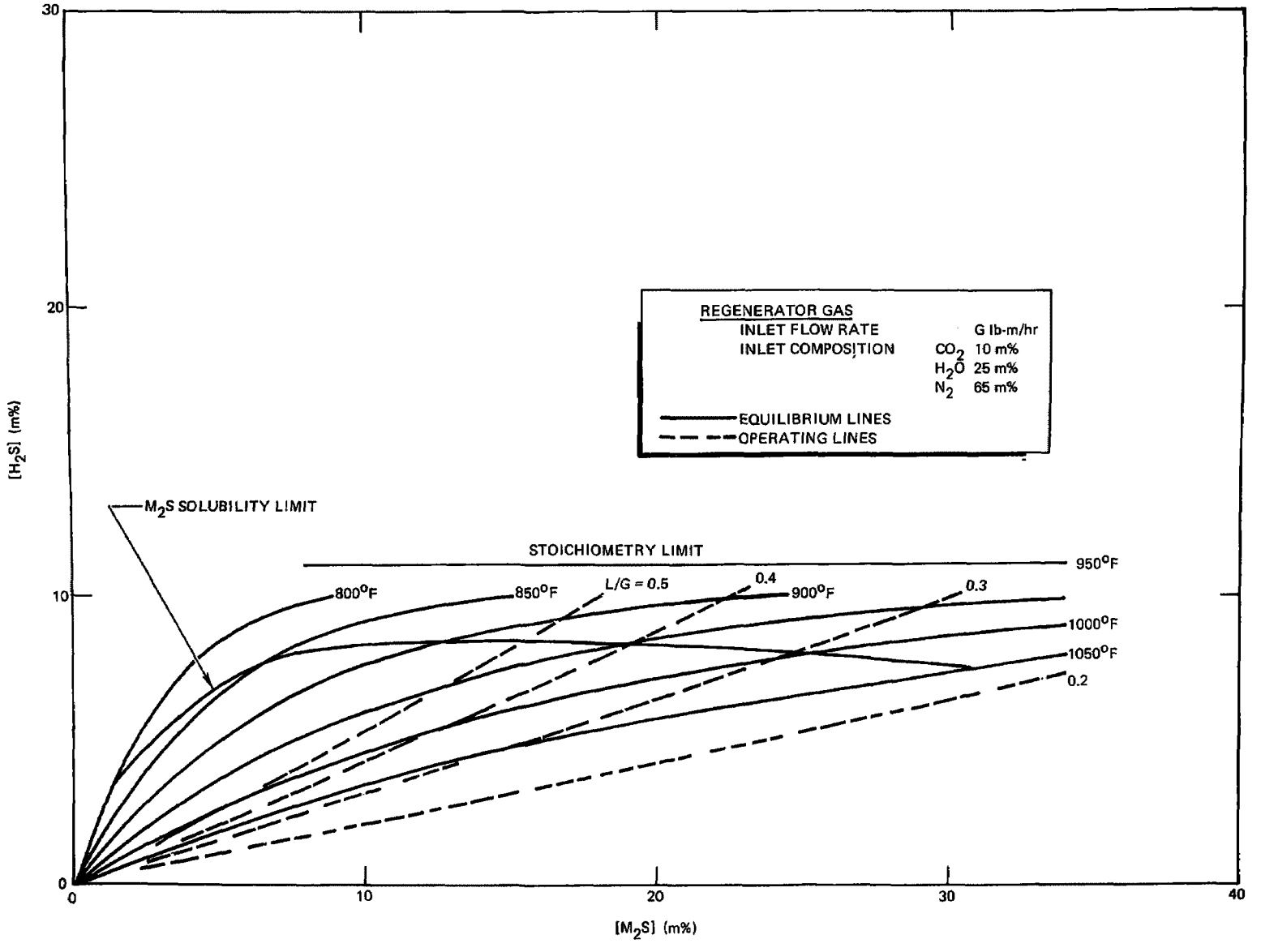

Figure 4. Molten Carbonate Regenerator Equilibria (B)

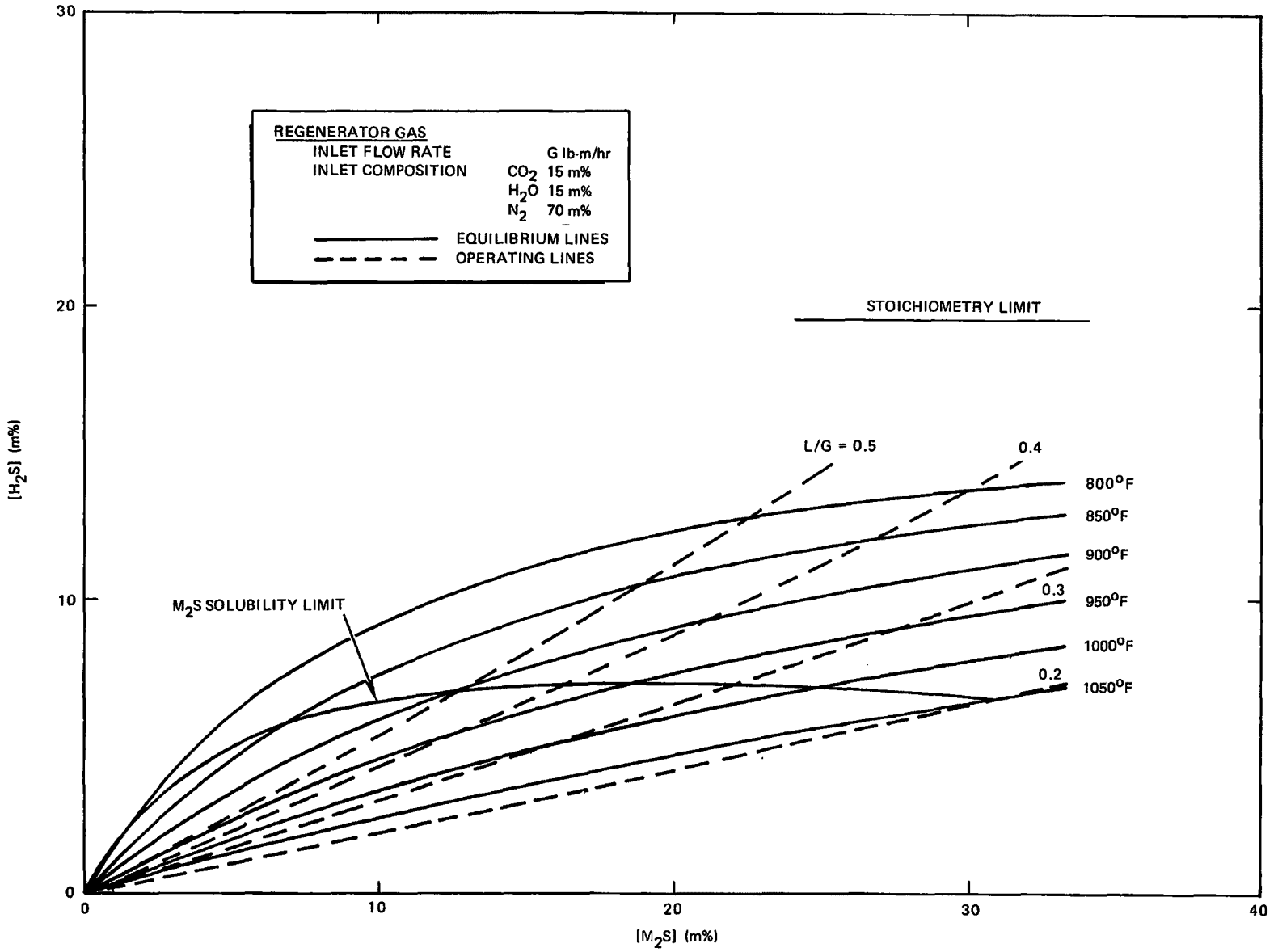

Figure 5. Molten Carbonate Regenerator Equilibria (C)

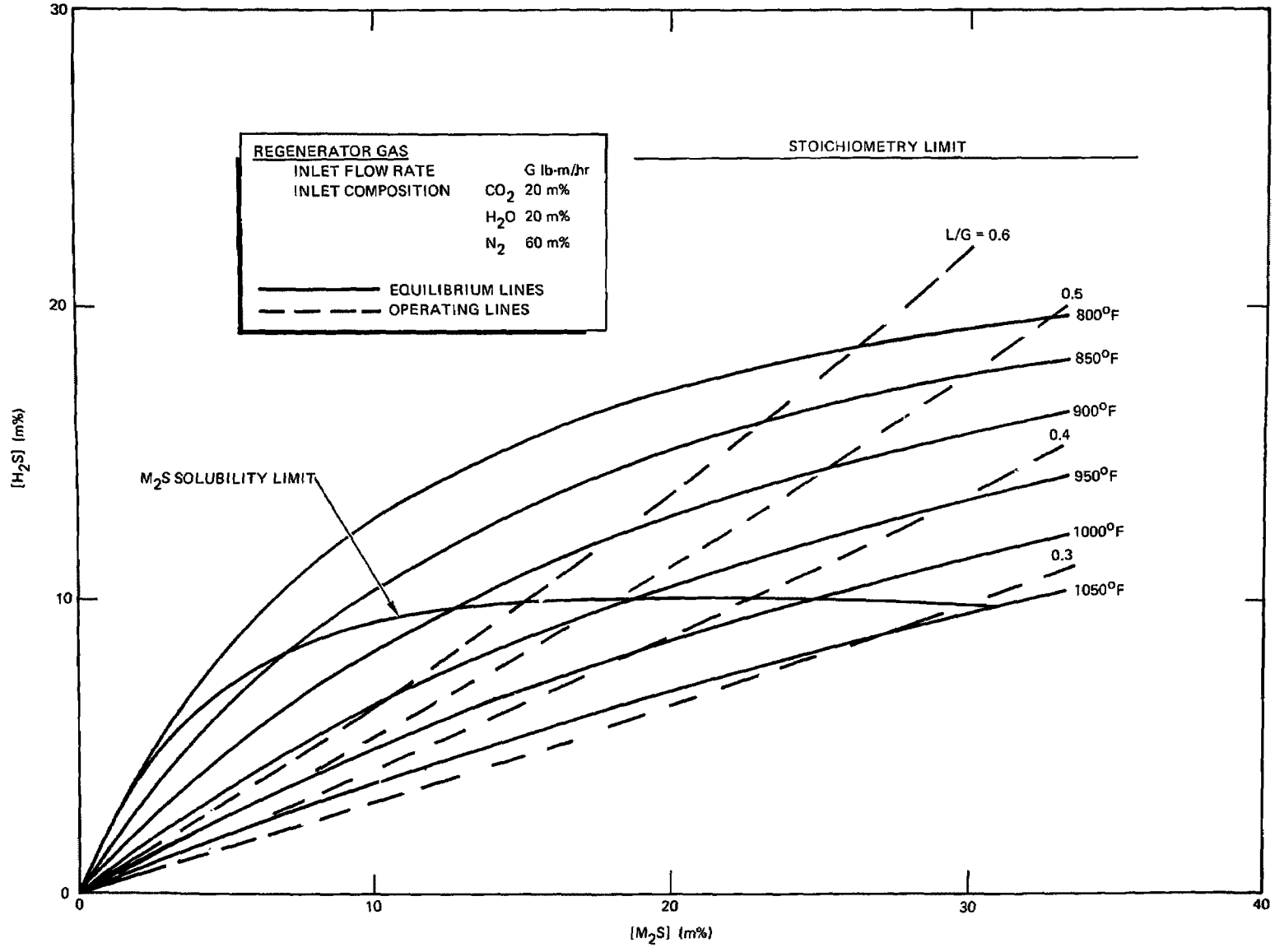

Figure 6. Molten Carbonate Regenerator Equilibria (D)

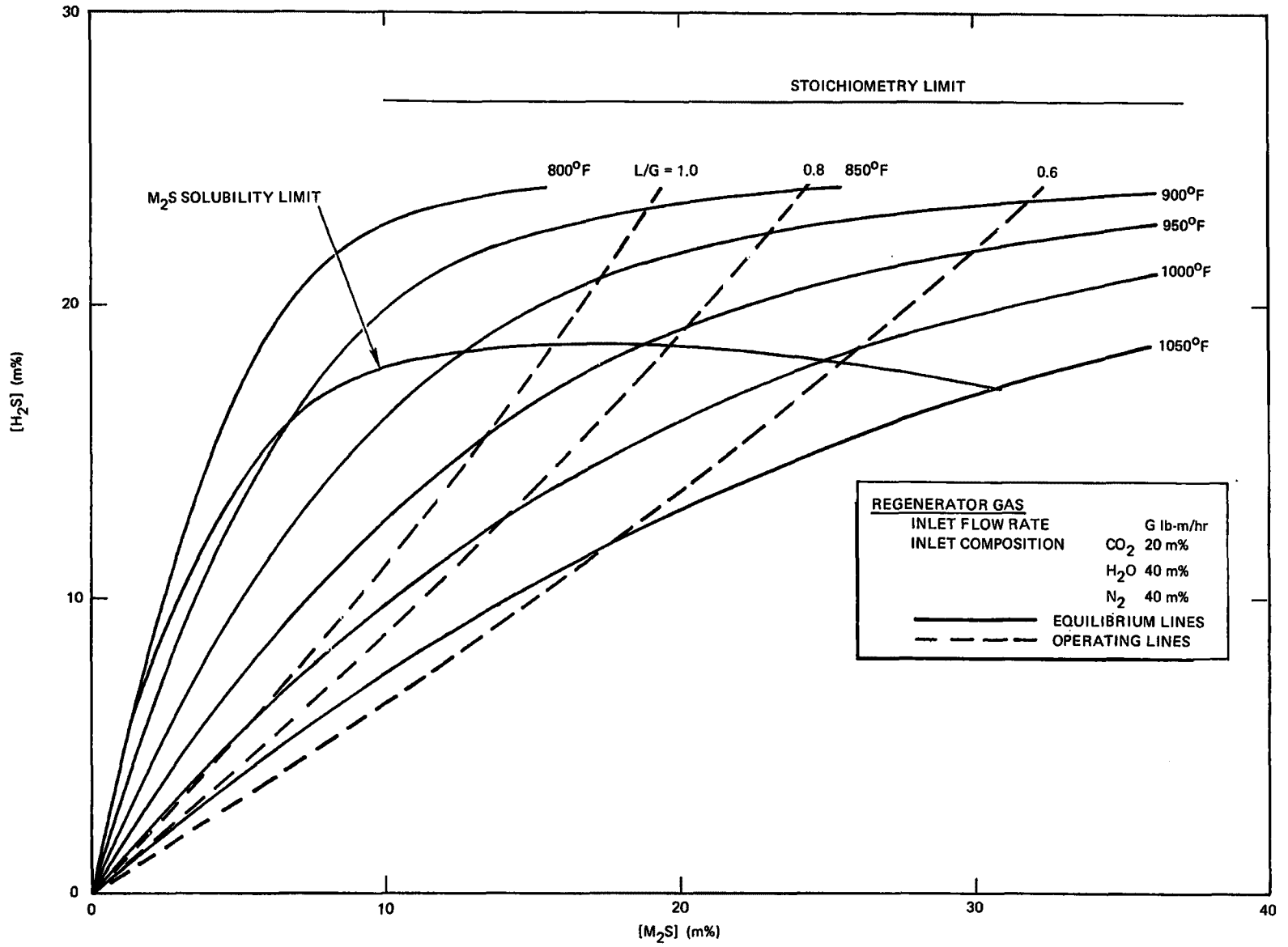

Figure 7. Molten Carbonate Regenerator Equilibria (E)

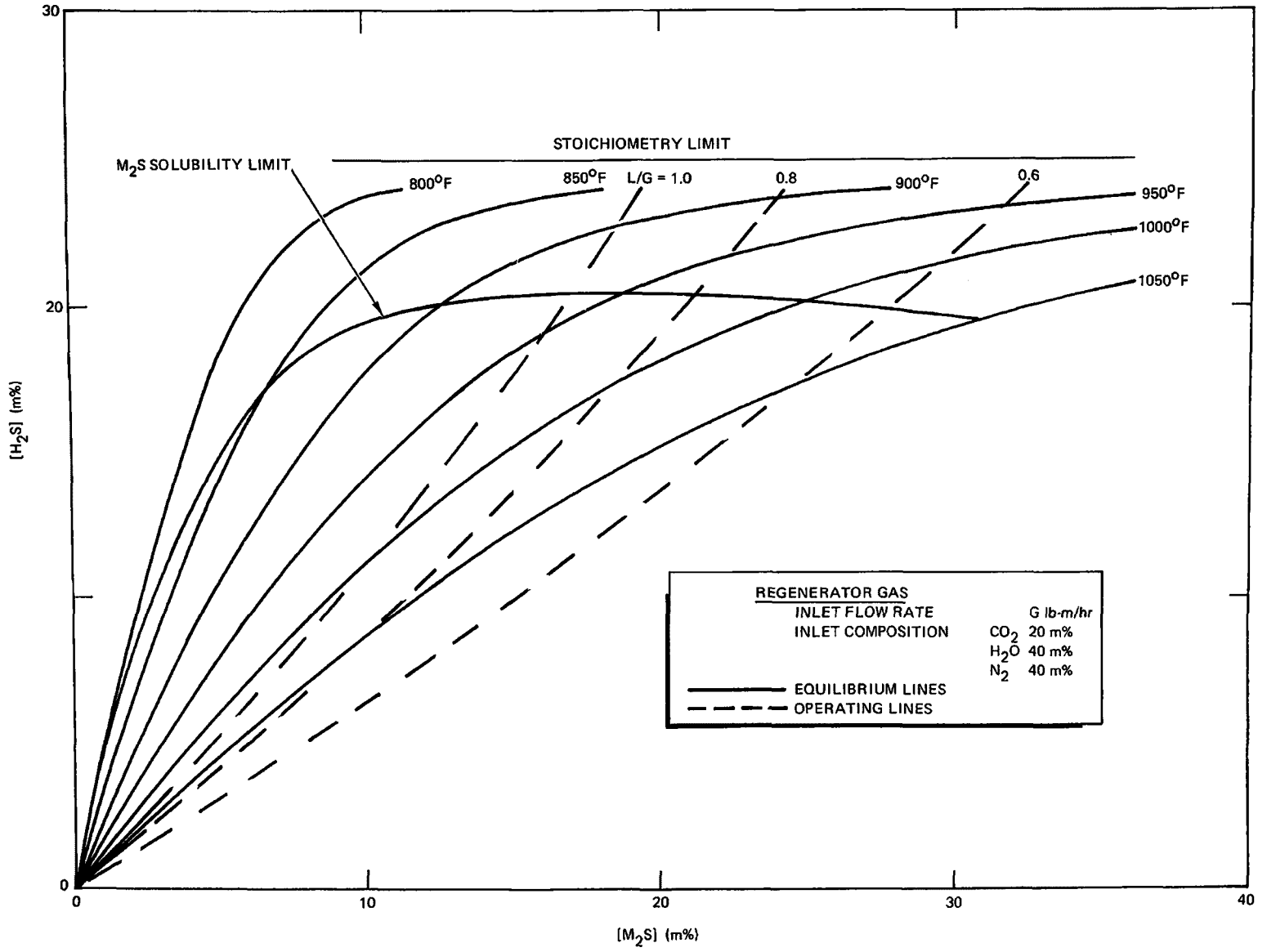

Figure 8. Molten Carbonate Regenerator Equilibria (E, 2 Atmospheres)

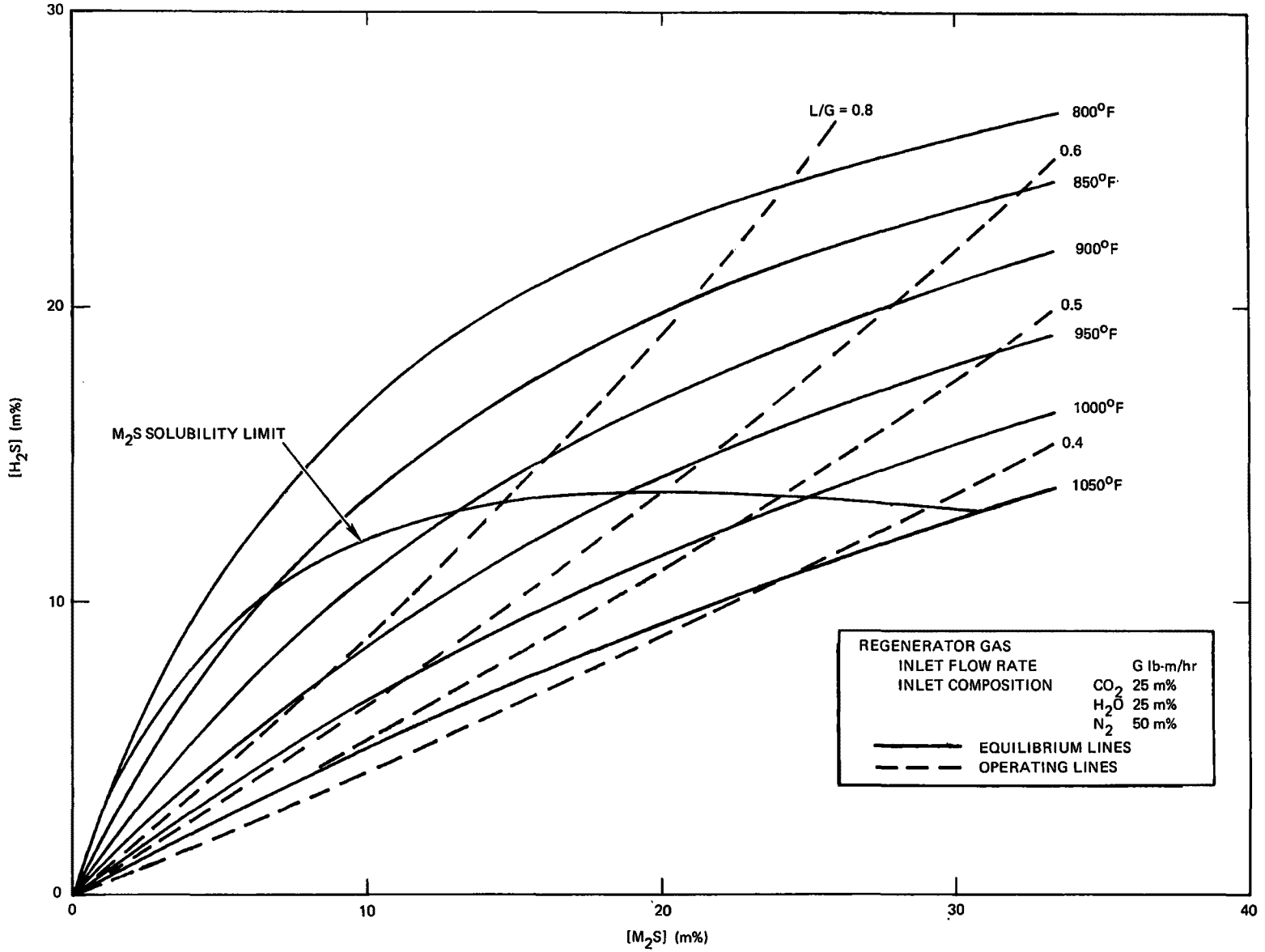

Figure 9. Molten Carbonate Regenerator Equilibria (F)

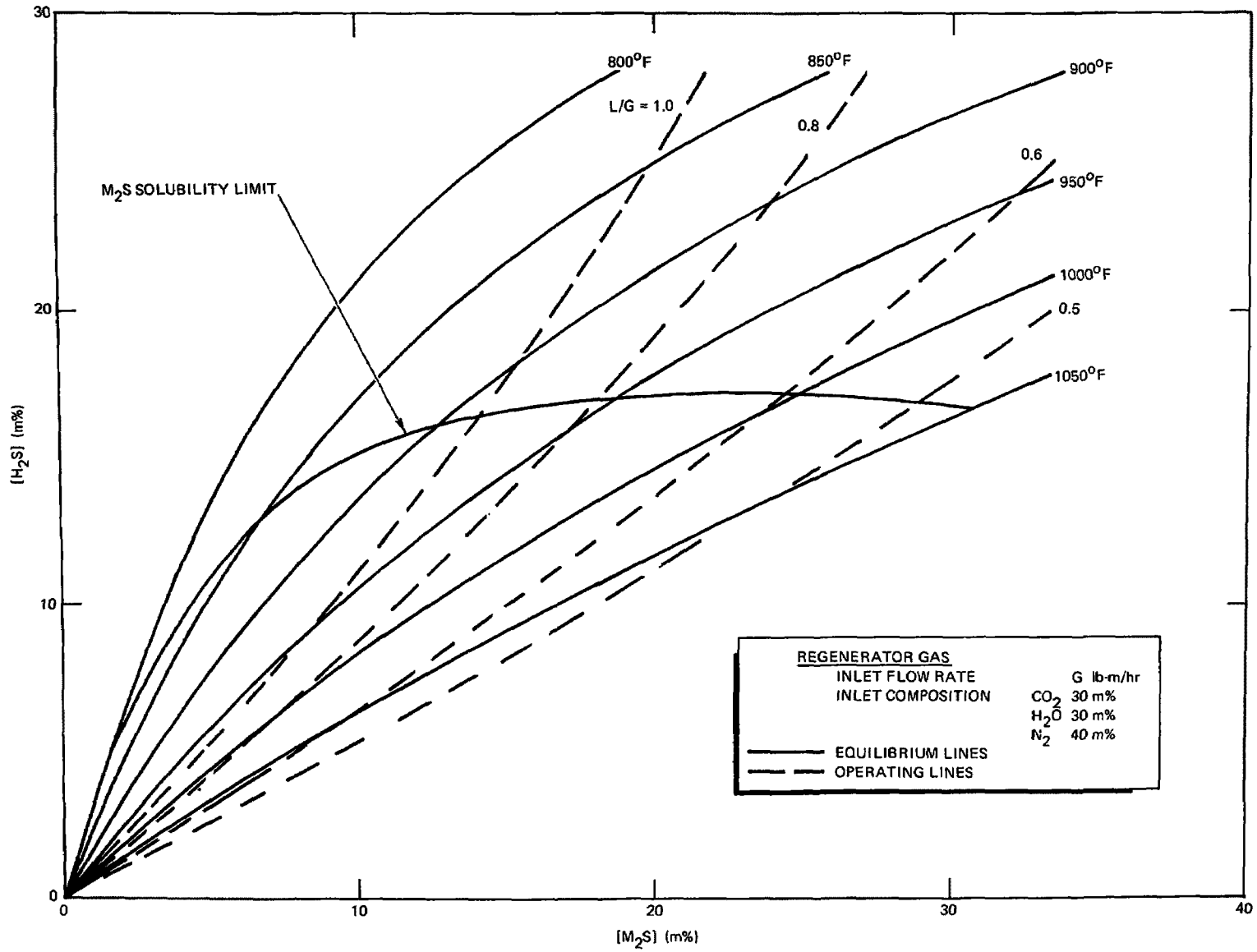

Figure 10. Molten Carbonate Regenerator Equilibria (G)

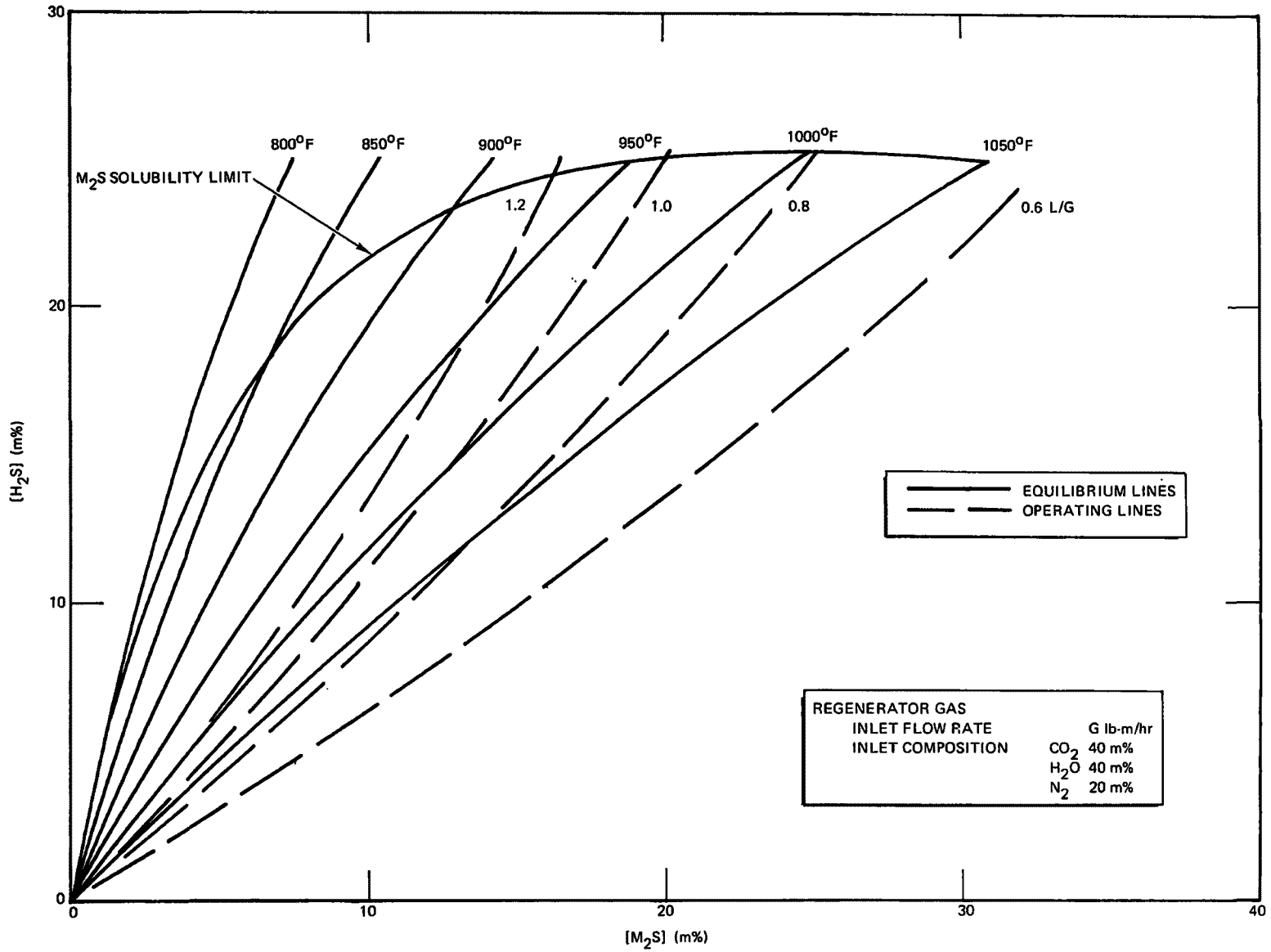

Figure 11. Molten Carbonate Regenerator Equilibria (H)

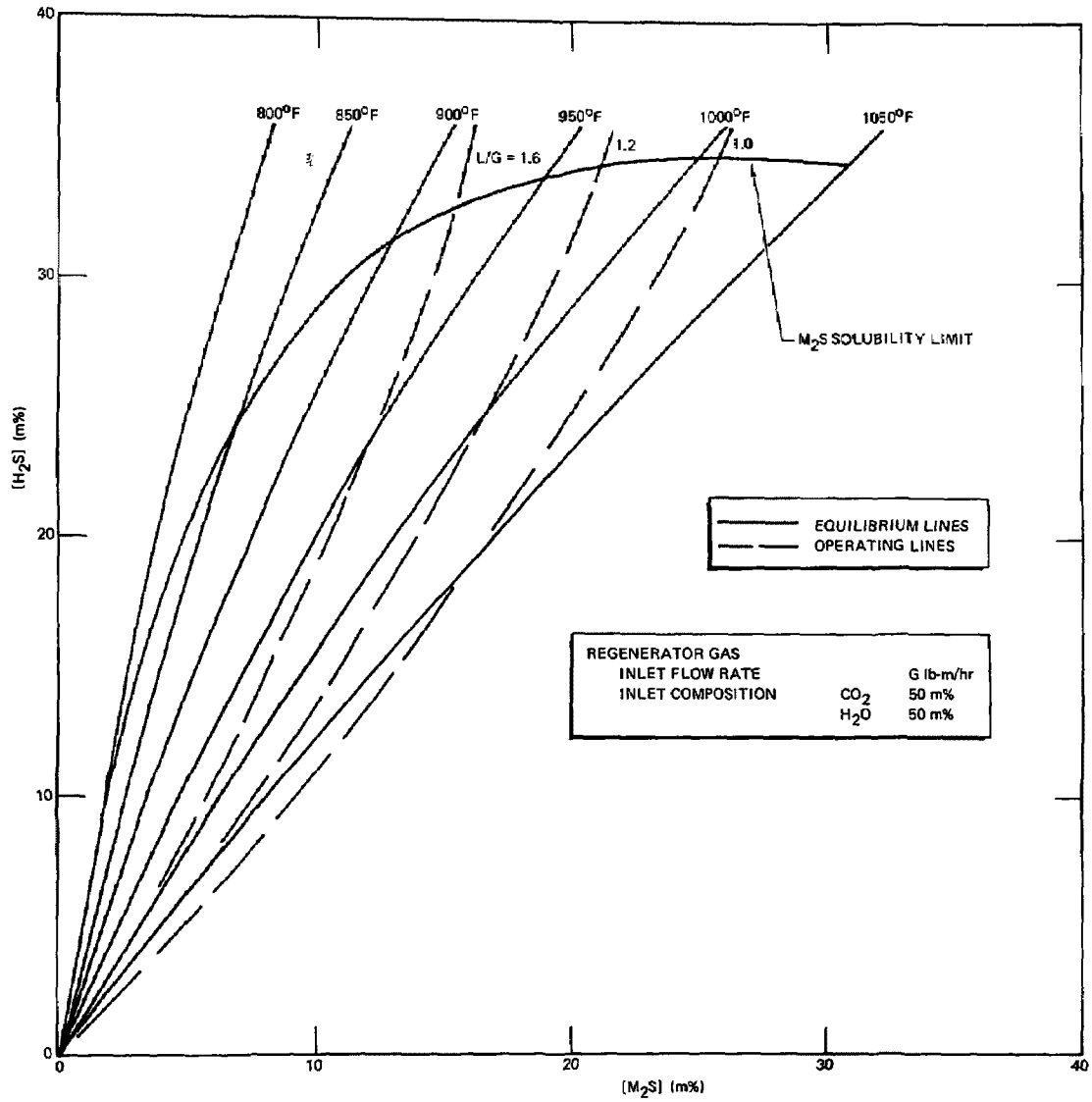

Figure 12. Molten Carbonate Regenerator Equilibria (I)

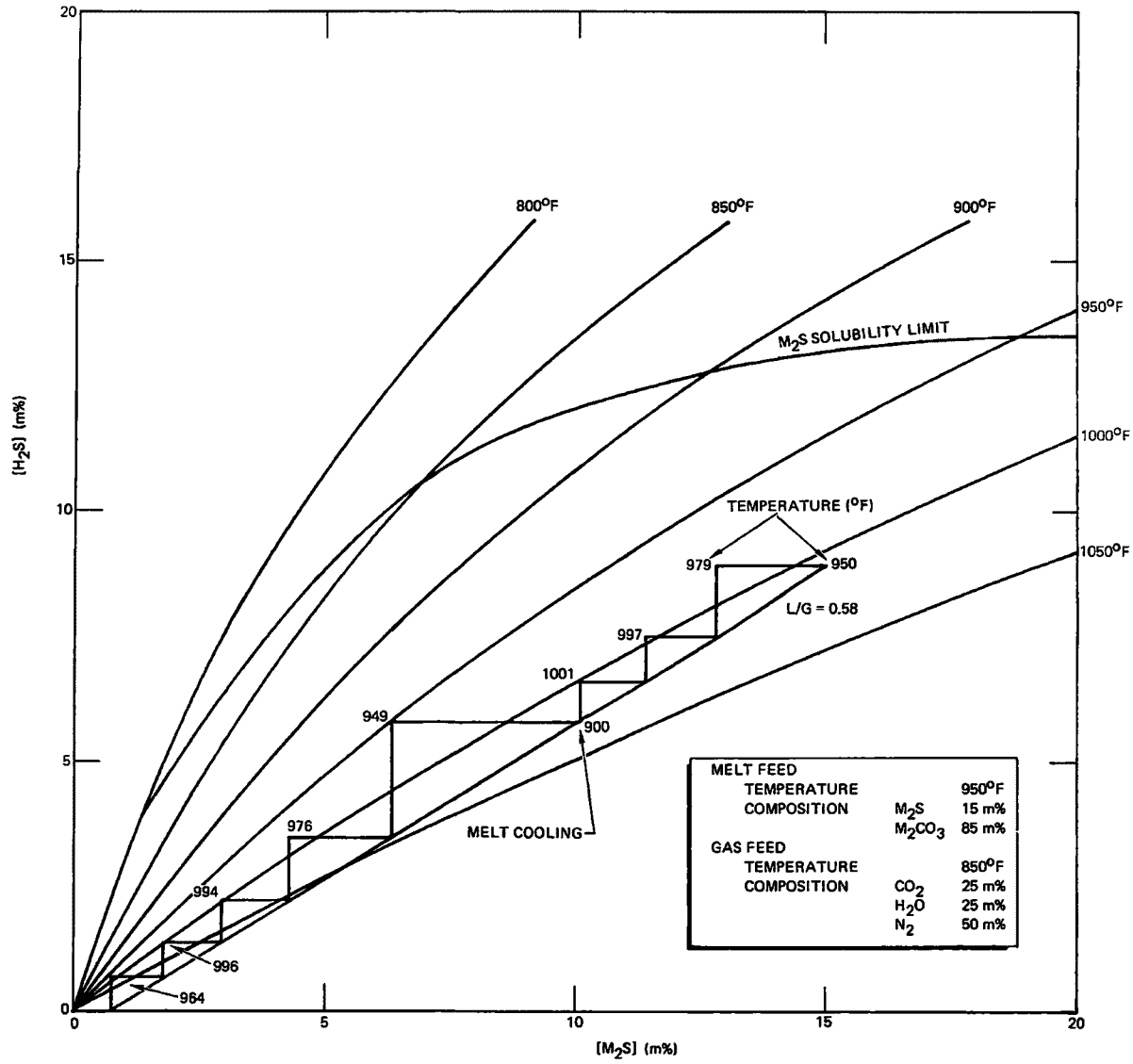

Figure 13. Theoretical Plate Diagram for Molten Carbonate Regenerator (F, 1 Atmosphere)

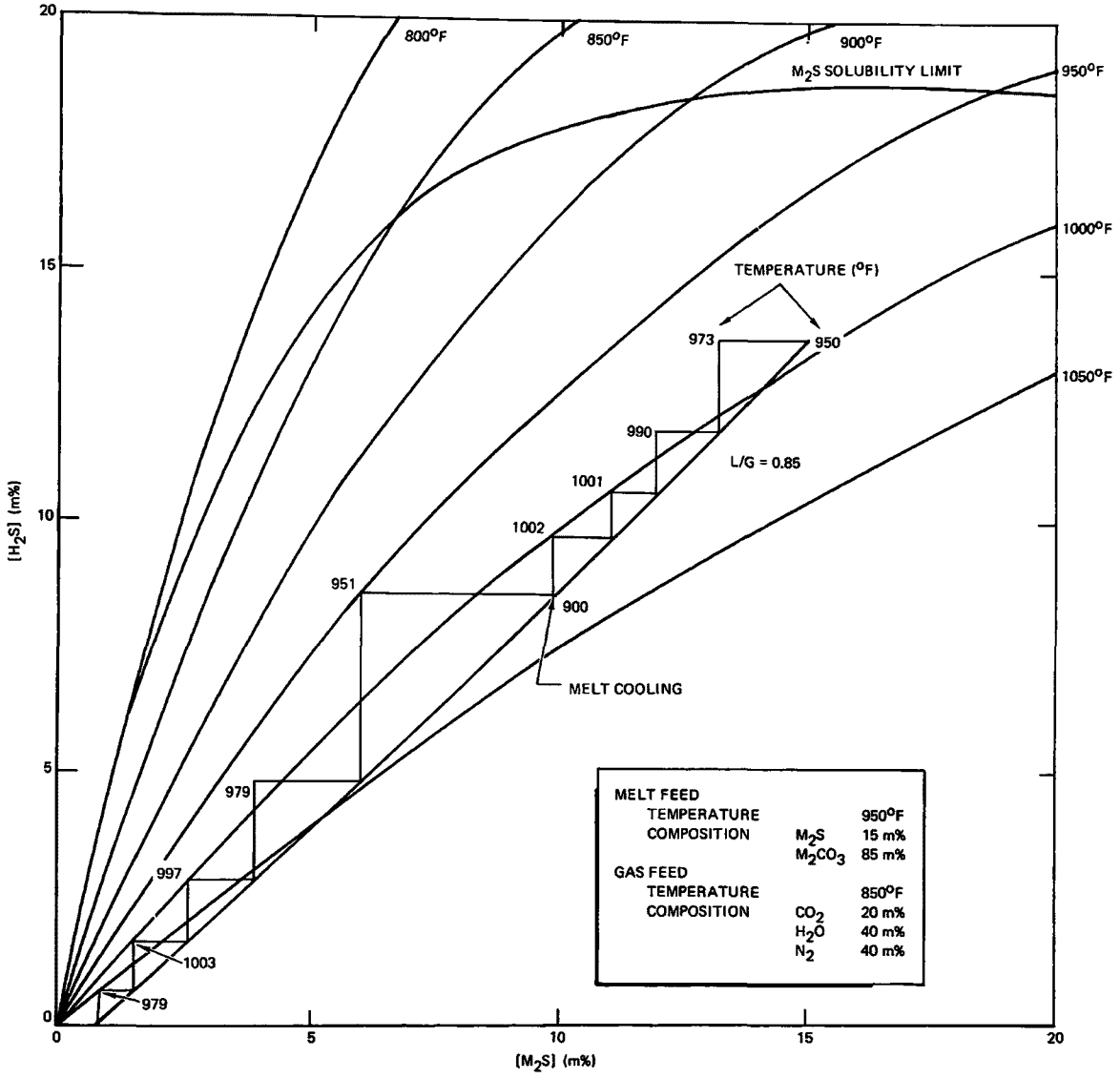

Figure 14. Theoretical Plate Diagram for Molten Carbonate Regenerator (E, 1 Atmosphere)

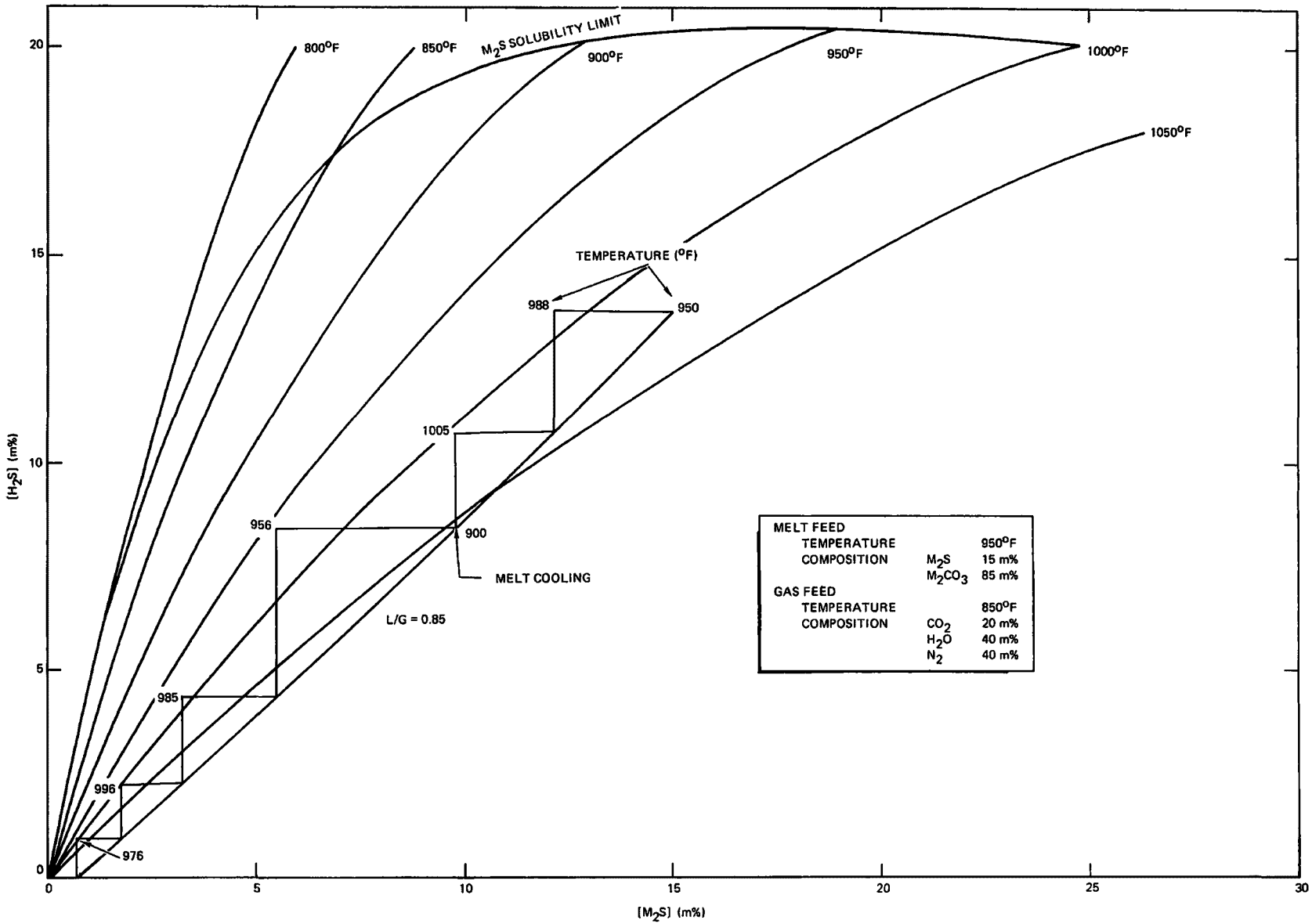

Figure 15. Theoretical Plate Diagram for Molten Carbonate Regenerator (E, 2 Atmospheres)

applicable equilibrium line. In a simplified manner it was assumed that for each percent of sulfide regenerated in the melt 46,400 x 0.01 = 464 Btu/lb mole of heat would be generated on a plate, which with an approximate specific heat of the melt of 41.4 Btu/lb mole ^{o}F, would raise the temperature of the melt by about 11^{o}F. In actuality the melt would receive heat not only from the chemical reaction on the plate but also from the sensible heat brought by the hotter gas rising from the plate below. A value of 13^{o}F was estimated for the temperature rise of the melt per percent of the melt regenerated to take into account this sensible heat of the gas. Exceptions were made for the plate from which the melt was taken to the intercooler and the two bottom plates to take into account the effect of the colder gas rising to these plates. More detailed heat balances were performed for these plates (the regenerator feed gas was assumed to be introduced at a temperature of 850^{o}F).

Additional calculational background and data are presented in Section VI.

V. DISCUSSION

Figures 3 through 12 show that for a given regenerator feed gas composition at a given total operating pressure the flatness of the M_2S solubility limit curve for concentrations of M_2S above a relatively low value (generally less than 10 mole %) prevents improvement of the H_2S concentration ideally achievable in the product gas by means of an increase in the M_2S concentration in the melt. Increasing the M_2S concentration in the melt only raises the required operating temperature in the regenerator without any H_2S concentration increase in the product gas. It does, however, decrease the melt flow requirements through the overall SO_2 removal system and the preheating requirements in the reducer.

Figure 2, and Figures 3 through 12 show that on the basis of the assumed sulfide solubility data, operation of the regenerator at various temperature ranges would impose the following constraints on the M_2S concentrations in the regenerator feed melt (the subscript F here again applies to the feed):

860 to 900°F	$[M_2S]_F \leq 6$ mole %
900 to 950°F	$[M_2S]_F \leq 11$ mole %
950 to 1000°F	$[M_2S]_F \leq 17$ mole %
1000 to 1050°F	$[M_2S]_F \leq 22$ mole %

These could be raised somewhat if one were willing to use several stages of melt intercooling, rather than a single stage, or cooling of the melt directly on each individual plate. A feed melt temperature of 950°F and M_2S concentration of 15 mole % were arbitrarily selected in this study to allow operation of the regenerator within the 950 to 1000°F temperature range of present day materials compatibility technology.

As stated previously the stoichiometric limitation on the maximum H_2S concentration achievable in the product gas is equal to the lesser of $[CO_2]/(1-[CO_2])$ or $[H_2O]/(1-[H_2O])$ in the feed gas. This value could be achieved only in equilibrium with a melt with an M_2S concentration of unity. Concentrations actually achievable are generally limited by the approach to the pinch point between the operating line and the equilibrium line at the maximum allowable operating temperature. For equal concentrations of CO_2 and H_2O in the regenerator feed gas (i.e., as in Figures 3, 5, 6, 9, 10, 11, and 12) they are roughly estimated at

$[CO_2]_F = [H_2O]_F = 10$ mole %	$[H_2S] \leq 3$ mole %
$[CO_2]_F = [H_2O]_F = 15$ mole %	$[H_2S] \leq 6$ mole %
$[CO_2]_F = [H_2O]_F = 20$ mole %	$[H_2S] \leq 8$ mole %
$[CO_2]_F = [H_2O]_F = 25$ mole %	$[H_2S] \leq 10$ mole %
$[CO_2]_F = [H_2O]_F = 30$ mole %	$[H_2S] \leq 13$ mole %
$[CO_2]_F = [H_2O]_F = 40$ mole %	$[H_2S] \leq 19$ mole %
$[CO_2]_F = [H_2O]_F = 50$ mole %	$[H_2S] \leq 26$ mole %

It is to be noted that to be suitable for economic recovery of sulfur through a Claus-type recovery process the product gas should have an H_2S concentration of at least 10 mole %. For lower concentrations a Stretford-type process[2] may well prove to be more economical.

The off-gas from a fluid coke molten carbonate reducer may contain up to about 67 mole % of CO_2, yielding a 40% CO_2 - 40% H_2O mixture. This should be adequate for regeneration. An even better source would be a pure CO_2 generator, but this would add the requirement for an additional major piece of equipment to the molten carbonate SO_2 removal system. While pure CO_2 is normally not available at a molten carbonate SO_2 removal plant, considerable quantities of excess steam are produced in such a plant. Since the thermodynamic equilibrium relationship, equation (2) above, is such that the effect of steam concentration on the achievable H_2S concentration is much more important than that of CO_2 concentration, it seems obvious that an appreciable improvement should be achieved through the addition of excess steam to a CO_2 containing regeneration feed gas.

Doubling the amount of steam in an originally 25 mole % CO_2, 25 mole % H_2O (composition F) gas increases its H_2O concentration to 40 mole % while its CO_2 concentration is decreased to 20 mole % (composition E). The net effect is shown in Figure 7. The H_2S concentration achievable in the product gas is raised from approximately 10 mole % to approximately 15 mole %, a more than adequate value for the economic recovery of sulfur through a Claus-type process (though the gas may have to be dried prior to or during its treatment in the Claus plant). A regeneration feed gas with a composition of 20 mole % CO_2, 40 mole % H_2O and 40 mole % N_2 is easily obtainable in a molten carbonate SO_2 recovery plant through addition of by-product steam to reducer off-gas.

Figure 4 shows a comparable situation with a low CO_2 content regeneration feed gas. The 10 mole % CO_2, 25 mole % H_2O, 65 mole % N_2 (composition B) gas is representative of a gas obtainable from the combustion of natural gas (the actual CO_2 concentration in such a combustion flue gas would be about 8.8 mole %). The maximum achievable H_2S concentration in the product gas is less than 7 mole %. This is probably inadequate for a Claus process recovery plant, but should be suitable for the Stretford process.

Figure 8 shows the effect of increasing the total pressure in conjunction with the use of the composition E regeneration feed gas. An increase from one to two atmospheres increases the maximum achievable H_2S concentration in the product gas from about 15 mole % to about 17 mole %. Such operation would, however, imply appreciably pressurized operation of the reducer, which might not be technically feasible or economically practical.

Figures 13 and 14 show typical McCabe-Thiele theoretical plate diagrams for operation with a regeneration feed gas obtained from the reducer off-gas through the addition of steam to form the 1:1 CO_2 H_2O and 1:2 CO_2-H_2O gas compositions previously used (F and E). Figure 15 applies to the composition E feed gas at a pressure of two atmospheres. M_2S concentration in the feed melt was 15 mole %. Feed melt and feed gas temperatures were 950 and 850°F, respectively. A single stage of melt cooling was provided. The results can be summarized as follows:

Feed Gas Composition	Operating Conditions: Pressure (atm)	Operating Conditions: Temp (°F)	L/G	Regeneration Effectiveness (%)	H_2S Product Conc. (%)	No. of Theoretic Plates
CO_2 25 mole % H_2O 25 mole % N_2 50 mole %	1	950-1000	0.58	95	8.9	8
CO_2 20 mole % H_2O 40 mole % N_2 40 mole %	1	950-1000	0.85	95	13.7	9
CO_2 20 mole % H_2O 40 mole % N_2 40 mole %	2	950-1000	0.85	95	13.7	6

It can be seen that 95% regeneration can be achieved with a reasonable number of theoretical plates. The H_2S concentration in the product gas is completely adequate for economic recovery of sulfur through a Claus-type process.

In the 2 atmosphere process case a still higher concentration of H_2S (about 16 mole %) could be achieved in the product gas but at the expense of an increase in the number of theoretical plates required.

As a last item, it is important to emphasize that this whole analysis has been based on a rather limited amount of analytical data. Especially with respect to the M_2S solubility data in the carbonate melt there are indications that intermediate compounds formed in the regeneration process, such as the thiocarbonate M_2CO_2S, are considerably more soluble in the melt than the sulfide itself. How much this can be taken advantage of in the process remains in question. It is expected that the results are conservative, however, since any decrease in initial freezing point temperature below that assumed will make the regeneration easier.

VI. BACKGROUND DATA

A. EQUILIBRIUM CONSTANTS

$$K_1 = 1.90 \times 10^{-6}\, e^{50,400/RT} \qquad K_2 = 1.24 \times 10^{-3}\, e^{27,720/RT}$$

Temperature (°F)	K_1	K_2
800	1051	79.8
850	487	52.3
900	239	35.4
950	123	24.6
1000	66.6	17.5
1050	37.5	12.76
1100	21.9	9.49
1200	8.22	5.54
1300	3.45	3.44
1400	1.59	2.24

B. M_2S SOLUBILITY IN CARBONATE MELTS

Melt Composition (mole %)				Liquidus Point (°F)
M_2S	M_2CO_3	M_2SO_4	M_2SO_3	
-	100.00	-	-	751
	98.5	1.5	-	754
1.5	75.2	10.1	13.2	802
17.2	81.4	1.4	-	937
31.8	66.9	1.3	-	1059
31.8*	66.9	1.3		769

*Treated with CO_2 at 1112°F (600°C)

Data from Figure 2

Temperature (°F)	M_2S Solubility (mole %)
800	1.4
850	6.8
900	12.7
950	18.8
1000	24.8
1050	30.8

C. SOLUTION OF EQUILIBRIUM EQUATION

1. Determination of $[M_2S]$ as a function of $[H_2S]$

As described in the text of the Appendix:

$$[M_2S] = \frac{1-[I]}{1+\gamma} \qquad (6)$$

with [I] being neglected for purposes of this calculation, and

$$\gamma = K_1 \frac{\alpha \beta / [H_2S]}{\frac{1}{\pi} + K_2 \alpha} \tag{3}$$

Since use of a large computer was not available, the numerical calculations were carried out on the Commodore Electronic Desk Top Calculator Model AL 1000 using the following programs:

(a) Calculation of α

Memories: I 1
III $[H_2S]$
IV $[CO_2]_F$

Program: 427352.795324252
*432639537.

(b) Calculation of $\alpha \beta / [H_2S]$

Memories: I 1
III $[H_2S]$
IV $[H_2O]_F$

Program: 427352.795324252
*4326395386.39637.
6. → α

(c) Calculation of $[M_2S]$

Note that both previous sets of calculations were purely stoichiometric and therefore independent of temperature and pressure. It is only in this calculation that the effects of temperature and pressure are introduced.

Memories: I 1
III K_1
IV K_2

Program: 87326.252.6.953863
*24252.49537.
Start program with o
6. → $1/\pi$
6. → $\alpha \beta / [H_2S]$

2. Alternate Determination of $[H_2S]$ as a Function of $[M_2S]$

Equation (2) can be solved for $[H_2S]$. Define:

$$a = \frac{[CO_2]_F}{1 \quad [CO_2]_F} \qquad b = \frac{[H_2O]_F}{1 \quad [H_2O]_F} \tag{9}$$

$$c = \frac{K_2}{K_1} (1+b) \frac{[M_2CO_3]}{[M_2S]} \tag{10}$$

$$d = \frac{a + b + c\left(a + \frac{1+a}{K_2 \pi}\right)}{2(1+c)} \tag{11}$$

Equation (2) is then rewritten in the quadratic form:

$$[H_2S]^2 - 2d[H_2S] + \frac{ab}{1+c} = 0 \tag{12}$$

which yields:

$$[H_2S] = d\left[1 - \sqrt{1 - \frac{ab}{d^2(1+c)}}\right] \tag{13}$$

D. EQUATION OF OPERATING LINE

Let $[M_2S] = x$

$[H_2S] = y$

From the stoichiometry of equation (1), the gas flow rate G_n leaving plate n can be expressed as follows:

$$G_n = \frac{G}{1 + y_n} \tag{14}$$

where G is the feed gas flow rate.

Since the regenerator feed gas does not contain any H_2S, a sulfide mass balance below plate (n - 1) from the top of the regenerator can be written as follows:

$$G_n y_n = L\left\{x_{n-1} - (1-\eta)x_F\right\}$$

where η = efficiency of regeneration and $x_F = [M_2S]_F$ in the feed melt.

$$\therefore\ G\frac{y_n}{1+y_n} = L\left\{x_{n-1} \quad (1-\eta)x_F\right\} \tag{15}$$

$$y_n = \frac{L/G\left\{x_{n-1} - (1-\eta)x_F\right\}}{1 - L/G\left\{x_{n-1} \quad (1 \quad \eta)x_F\right\}} \tag{16}$$

$$[H_2S] = \frac{L/G\left\{[M_2S] \quad (1 \quad \eta)[M_2S]_F\right\}}{1 - L/G\left\{[M_2S] - (1-\eta)[M_2S]\right\}} \tag{8}$$

It is to be noted that in the molten carbonate SO_2 removal process using a fluid coke reduction system the amount of regeneration gas available from the reducer is limited, so that the ratio L/G has a definite lower boundary.

If the total amount of sulfur processed by the system is S lb-mole/hr:

$$L = \sim \frac{S}{[M_2S]} \qquad \therefore\ \frac{L}{G} > \sim \frac{1}{12\,[M_2S]} \tag{17}$$

$$G <\sim 12\,S$$

Therefore if: $[M_2S] = 10\%\ \frac{L}{G} > 0.83$

$= 15\%\ \frac{L}{G} > 0.56$

$= 20\%\ \frac{L}{G} > 0.42$

E. HEAT BALANCE DATA

Specific heat of melt at 950°F:

$$C_L = 28.41 + 16.56 \times 10^{-3} \frac{1410}{1.8} = 41.4 \text{ Btu/lb mole } ^\circ\text{F}$$

Specific heat of regeneration gases at 900°F:

CO_2	12.3 Btu/lb-mole °F
H_2O	9.0 Btu/lb-mole °F
N_2	7.6 Btu/lb-mole °F
H_2S	10.2 Btu/lb-mole °F

which yields for typical gas compositions:

C_G = 9.1 Btu/°F per lb-mole of feed gas

C_G = 8.8 Btu/°F per lb-mole of product gas

For regeneration of 1 mole % of the melt the heat of reaction amounts to:

46,400 x 0.01 = 464 Btu/lb-mole of melt

which would correspond to a (464/41.4) = 11.2°F temperature rise if all this heat were to go into the melt.

For most plates in the regenerator the gas rising from the plate below is hotter than the liquid on the plate and therefore adds heat to the melt. Checking a few actual heat balances indicated that the sensible heat thus added might amount to about 20% of the heat of reaction. A constant value of 13°F per percent of the melt regenerated was therefore used for the temperature rise on a plate not affected by incoming colder regeneration gas.

An approximate heat balance was carried out for the plate above that onto which the cooled liquid from the intercooler was returned.

For the bottom two plates, plates (n-1) and n, the following heat balance equations were obtained (neglecting the change in gas flow rate):

$$t_n - t_G = \frac{m\left(t_{n-2} \quad t_G\right) + \frac{C_G}{C_L}\,\Delta H\,\Delta R_n + \frac{L}{G}\,\Delta H\left(\Delta R_n + \Delta R_{n-1}\right)}{m + pC_G} \tag{18}$$

$$t_{n-1} - t_n = \frac{C_G\left(t_{n-2} - t_G\right) + \frac{C_G}{C_L}\,\Delta H\,\Delta R_{n-1} \quad \frac{L}{G}\,\Delta H\,\Delta R_n}{m + pC_G} \tag{19}$$

with t_G = regeneration feed gas temperature

t_n = temperature on plate n

t_{n-1} = temperature on plate n-1

t_{n-2} = temperature on plate n-2

ΔH = heat of regeneration, Btu/lb-mole

ΔR_n = fraction of melt regenerated on plate n

ΔR_{n-1} = fraction of melt regenerated on plate n-1

$m = \frac{L}{G} C_L$

$p = 1 + \frac{C_G}{m}$

REFERENCES

1. AI-70-29, "Development of a Molten Carbonate Process for Removal of Sulfur Dioxide from Power Plant Stack Gases - Progress Report No. 3, October 28, 1968 to July 31, 1969," pp 41-43

2. The Stretford Process. The North Western Gas Goard (U.K.), October, 1967